Characterisation of the eukaryotic initiation factor 2α kinases of *Plasmodium falciparum*

Clare Fennell
BSc (Hons), MRes

Submitted in fulfilment of the requirements for the
Degree of Doctor of Philosophy

Division of Infection and Immunity
Institute of Biomedical and Life Sciences
University of Glasgow

September 2008

Abstract

Malaria remains a devastating disease with respect to both mortality and the constraints it places on the economic development of the countries in which it is endemic. Our laboratory is seeking new antimalarial targets, by characterising the protein kinases of the most lethal human malaria parasite, *Plasmodium falciparum*. As central components of many diverse signalling pathways, protein kinases are crucial for the control of proliferation and differentiation in other eukaryotes; we hypothesise that they play similar roles in *P. falciparum*. The life cycle of *P. falciparum* is complex, consisting of a series of tightly controlled stages of division and differentiation. In the related apicomplexan parasite *Toxoplasma gondii,* stress stimuli have been implicated in an important differentiation step, from rapidly dividing tachyzoites, to quiescent bradyzoites (which enable immune evasion). Evidence suggests that stress may also contribute to an essential differentiation stage, gametocytogenesis, in *P. falciparum*. In yeast and metazoans, part of the stress response is mediated through phosphorylation of eukaryotic initiation factor 2α (eIF2α), which results in selective translation of mRNAs encoding stress response proteins. Post-transcriptional control of gene expression is suspected to play an important role in *P. falciparum*. Importantly, the Goldberg laboratory recently demonstrated that similarly, in *P. falciparum* the eIF2α orthologue is phosphorylated in response to starvation.

Here we identify the *P. falciparum* orthologue of the translation initiation factor eIF2α and provide bioinformatic evidence for the presence of three eIF2α kinases in *P. falciparum*; PfeIK1, PfeIK2 and PfPK4, only one of which (PfPK4) has been described previously (Mohrle et al., 1997). We show that one of the novel eIF2α kinases, PfeIK1, is able to phosphorylate *P. falciparum* eIF2α *in vitro*. In addition, initial experiments support previous observations that PfPK4 is indeed an active protein kinase (Mohrle et al., 1997). We present evidence that PfPK4 is essential for asexual growth, which precludes straightforward reverse genetics studies aiming to determine its possible role in gametocytogenesis. In contrast, transgenic parasites allowed us to show that neither PfeIK1 nor PfeIK2 are required for asexual growth, or sexual development of the parasite in the mosquito vector. However, preliminary evidence (requiring confirmation) may indicate that parasites lacking PfeIK1

over-express PfPK4, which would suggest that PfeIK1 may play an important function in the parasite. This study strongly suggests that a mechanism for versatile regulation of translation by several kinases with a similar catalytic domain, but distinct regulatory domains, is conserved in *P. falciparum*.

Table of contents

Abstract 2
Table of contents 4
List of Figures 9
List of Tables 11
Acknowledgements 12
Author's declaration 13
Definitions 14
1 Introduction 17
1.1 Malaria 17
1.2 Plasmodium falciparum 18
1.3 Life cycle of malaria parasites 20
1.3.1 Gametocytogenesis 21
1.4 Available chemotherapies/global antimalarial strategy 22
1.5 Protein kinases 23
1.5.1 Kinases as drug targets 24
1.6 Kinases in *P. falciparum* 25
1.7 Gene regulation in *P. falciparum* 27
1.8 Stress responses 28
1.8.1 Stress Activated Protein Kinases 29
1.8.2 eIF2α pathway 29
1.8.3 eIF2α kinases, mechanisms & activation 32
1.8.3.1 Domain structure 32
1.8.3.2 Activation mechanism 33
1.8.3.3 Substrate recognition and phosphorylation by eIF2α kinases 35
1.8.4 Effects of phosphorylation of eIF2α 35
1.8.5 Feedback to regulate phosphorylation of eIF2α 36
1.8.6 eIF2α kinases in protozoan parasites 36
1.9 Rationale for investigation of eIF2α kinases in *P. falciparum* and aims of this project 37
2 Materials and Methods 39
2.1 Biological and chemical reagents 39
2.2 Bioinformatics 39
2.2.1 PfeIF2α 39

2.2.2 *P. falciparum* eIF2α kinases 39
2.3 Methods in molecular biology 40
2.3.1 Polymerase chain reaction (PCR) 40
2.3.1.1 Takara 40
2.3.1.2 Phusion 41
2.3.1.3 Expand High Fidelity PCR system 41
2.3.2 Reverse transcriptase PCR (RT-PCR) 42
2.3.3 Gene cloning techniques 43
2.3.3.1 pGEM-T easy cloning of PCR products 43
2.3.3.2 Sub-cloning into destination vectors 44
2.3.4 *E. coli* transformation 45
2.3.5 Preparation of competent cells 45
2.3.6 Isolation of plasmid DNA from *E. coli* 45
2.3.7 Restriction endonuclease digestion 46
2.3.8 Determining DNA and RNA concentration 46
2.3.9 DNA Sequencing 46
2.3.10 Agarose gel electrophoresis 47
2.3.11 Southern Blotting 47
2.4 Methods in Biochemistry 48
2.4.1 Sodium dodecyl sulphate polyacrylamide gel electrophesis (SDS-PAGE) 48
2.4.2 Coomassie blue staining of polyacrylamide gels 49
2.4.3 Western blotting 49
2.4.4 Determining protein concentration 50
2.4.5 Generation of polyclonal antibodies 50
2.4.6 Expression of recombinant proteins 50
2.4.7 Purification of tagged recombinant proteins 51
2.4.7.1 GST tag 51
2.4.7.2 His tag 51
2.4.8 Immunoprecipitation 52
2.4.9 Kinase assay 52
2.5 P. falciparum culture 53
2.5.1 Asexual stage culture 53
2.5.2 Synchronisation of parasite culture 53
2.5.3 Preparation of gametocytes 53
2.5.4 Mosquito infection 54

2.5.5 Preparation of stabilates 54
2.5.6 Thawing of stabilates 54
2.5.7 Isolation of parasites from infected erythrocytes 55
2.5.8 Extraction of parasite genomic DNA 55
2.5.9 Extraction of parasite RNA 56
2.5.10 Protein preparation from parasites 56
2.5.11 Transfection 56
2.5.12 Cloning of parasites by limiting dilution 57
2.5.12.1 *Plasmodium* lactate dehydrogenase assay 58
2.5.13 Parasite growth rate analysis, by flow cytometry 58
3 Eukaryotic initiation factor 2α kinases in *P. falciparum*: bioinformatic and biochemical characterisation 59
3.1 Identification of *P. falciparum* eukaryotic initiation factor 2α 59
3.2 Identification of eIF2α kinases in *P. falciparum* 60
3.2.1 *In silico* analysis 60
3.2.1.1 PfeIK1 66
3.2.1.2 PfeIK2 68
3.2.1.3 PfPK4 69
3.2.2 Life cycle stage specific expression of PfeIF2α kinases 70
3.3 Cloning and expression of *P. falciparum* eIF2α 73
3.3.1 Cloning of PfeIF2α 73
3.3.2 Expression of Recombinant PfeIF2α 74
3.4 Cloning, expression and characterisation of the *P. falciparum* eIF2α kinases. 76
3.4.1 PfeIK1 76
3.4.1.1 Cloning of the PfeIK1 catalytic domain 76
3.4.1.2 Expression of recombinant PfeIK1 77
3.4.1.3 PfeIK1 is an active kinase able to phosphorylate PfeIF2α *in vitro* 79
3.4.2 PfeIK2 81
3.4.2.1 Verification of *pfeik2* gene structure 81
3.4.2.2 Cloning of the PfeIK2 catalytic domain 83
3.4.2.3 Expression of recombinant PfeIK2 84
3.4.2.4 Initial activity assay of recombinant GST-PfeIK2 86
3.4.3 PfPK4 86
3.4.3.1 Cloning of PfPK4 catalytic domain 86

3.4.3.2 Expression of recombinant PfPK4 87
3.4.3.3 PfPK4 activity 88
3.5 Perspectives and Discussion 90
3.5.1 Identification of PfeIF2α and its kinases 90
3.5.2 Characterisation of PfeIF2α and its kinases 92
3.6 Summary 93
4 Reverse genetics of eIF2α kinases in *P. falciparum* 95
4.1 Construction of gene disruption and tagging plasmids 95
4.2 PfeIK1 101
4.2.1 PfeIK1 is not required for asexual growth 101
4.2.2 PfeIK1 is not required for gametocytogenesis 104
4.2.3 PfeIK1 is not required for infection of mosquitoes or progression to sporozoites 105
4.2.4 Expression levels of remaining PfeIF2α kinases in pfeik1^{-} parasites. 108
4.3 PfeIK2 109
4.3.1 PfeIK2 is not required for asexual growth 109
4.3.2 PfeIK2 is not required for gametocytogenesis 111
4.3.3 PfeIK2 is not required for infection of mosquitoes or progression to sporozoites 112
4.4 PfPK4 114
4.4.1 PfPK4 is essential for asexual growth 114
4.5 Discussion and Perspectives 119
4.5.1 PfeIK1 119
4.5.2 PfeIK2 119
4.5.3 PfPK4 120
4.5.4 Expression levels of remaining PfeIF2α kinases, following disruption of one of the three genes. 121
4.6 Summary 121
5 Discussion and conclusions 123
5.1 Identification of PfeIF2α and its kinases 123
5.2 Investigation of the role of PfeIF2α kinases 124
5.2.1 Activation stimuli 124
5.2.1.1 Starvation 125
5.2.1.2 Oxidative stress 125
5.2.1.3 Heat shock 126

5.2.2 Complementation of yeast mutants 126
5.2.3 Effect of phosphorylation of PfeIF2α on translation? 127
5.3 Perspectives 128
5.3.1 Phosphoregulation is a two way process 128
5.3.2 Gametocytogenesis; a stress induced response? 129
5.3.3 Relative importance of translation control in *P. falciparum* 130
5.3.4 Search for new therapeutic targets 131
6 Appendix 133
6.1 Biological and chemical reagents 133
6.1.1 Oligonucleotide primers 134
6.1.2 Bacterial strains 138
6.1.3 *P. falciparum* strain 138
6.1.4 Mosquitoes 139
6.1.5 Antibodies 139
6.2 Buffers, solutions and media 140
6.2.1 General Buffers 140
6.2.2 DNA analysis 140
6.2.3 Protein analysis 141
6.2.4 Bacterial culture 142
6.2.5 *P. falciparum* culture 143
6.2.6 Mosquito breeding 144
6.3 Submitted manuscript 144
References 145

List of Figures

Figure 1-1: Maps to illustrate the coincidence of the world malaria burden and poverty. 18
Figure 1-2: Illustration of *P. falciparum* merozoites. 19
Figure 1-3: Illustration of the *P. falciparum* life cycle. 21
Figure 1-4: Schematic to show the conserved subdomains of protein kinases. (Adapted from Hanks 2003 (Hanks, 2003)). 24
Figure 1-5: Integration of stress responses by phosphorylation of eIF2α. 30
Figure 1-6: Schematic of the domain structures of the eIF2a kinases. 33
Figure 2-1: Map of the cloning vector, pGEM-T Easy. 44
Figure 3-1: Alignment of eIF2α sequences. 59
Figure 3-2: Phylogenetic tree showing the clustering of eIF2α kinases. 61
Figure 3-3: Sequence alignment of eIF2α kinases. 65
Figure 3-4: Structure of PKR-eIF2α complex. 65
Figure 3-5: Phylogenetic tree illustrating eIF2α kinases in diverse species. 67
Figure 3-6: Schematic of protein domains of human, *P. falciparum*, and *T. gondii* eIF2α kinases. 68
Figure 3-7: Expression data for the PfeIKs taken from PlasmoDB (Le Roch et al., 2003). 71
Figure 3-8: Expression of PfPK4. 72
Figure 3-9: Map of the expression vector for PfeIF2α. 74
Figure 3-10: Purification of GST-PfeIF2α. 75
Figure 3-11: Western blot analysis of purification of wild type GST-PfeIF2α. 75
Figure 3-12: Map of the expression vector for GST-PfeIK1. 77
Figure 3-13: Purification of GST-PfeIK1. 78
Figure 3-14: Purification of GST-PfeIK1. 78
Figure 3-15: PfeIK1 phosphorylates non-physiological substrates. 80
Figure 3-16: GST-PfeIK1 autophosphorylates and phosphorylates wild type PfeIF2α but not the mutant PfeIF2α S59A. 81
Figure 3-17: Verification of the gene structure of *pfeik2*. 82
Figure 3-18: Western blot showing the size and stage specific expression of PfeIK2. 83
Figure 3-19: Map of the expression vector for GST-PfeIK2. 84
Figure 3-20: Expression of GST-PfeIK2 using *E.coli* BL21c+. 85

Figure 3-21: Expression of GST-PfeIK2 using *E. coli* BL21 codon plus. 85
Figure 3-22: Map of the His-PfPK4 expression vector. 87
Figure 3-23: Expression of His-PfPK4. 88
Figure 3-24: PfPK4-HA Kinase assay. 90
Figure 4-1: Schematic showing the single cross-over homologous recombination strategy used for disruption of the PfeIK genes. 96
Figure 4-2: Map of the plasmid used for disruption of *pfeik1*. 96
Figure 4-3: Map of the plasmid used for disruption of *pfeik2*. 97
Figure 4-4: Map of the plasmid used to attempt disruption of *pfpk4*. 98
Figure 4-5: Schematic showing the single cross-over recombination strategy used to tag PfPK4. 99
Figure 4-6: Map of the plasmid used to add a C-terminal double HA tag to PfPK4. 100
Figure 4-7: Map of the plasmid used to add a C-terminal GFP tag to PfPK4. ... 101
Figure 4-8: PCR analysis of two *pfeik1*$^{-}$ clones. 102
Figure 4-9: Schematic for *pfeik1*$^{-}$ Southern blot. 102
Figure 4-10: Southern blot analysis of *pfeik1*$^{-}$ clones. 103
Figure 4-11: Growth of *pfeik1*$^{-}$ parasites. 103
Figure 4-12: Giemsa stained *pfeik1*$^{-}$ gametocytes. 105
Figure 4-13: PCR analysis of *pfeik1*$^{-}$ infected mosquito midguts. 107
Figure 4-14: Western blot showing expression of PfPK4 in *pfeik1*$^{-}$ parasites. .. 108
Figure 4-15: PCR analysis of *pfeik2*$^{-}$ clones. 109
Figure 4-16: Schematic for *pfeik2*$^{-}$ Southern blot. 110
Figure 4-17: Southern blot analysis of *pfeik2*$^{-}$ clones. 110
Figure 4-18: Giemsa stained *pfeik2*$^{-}$ gametocytes. 111
Figure 4-19: PCR analysis of attempted disruption of *pfpk4*. 115
Figure 4-20: Schematic of expected fragments on Southern blot analysis of *pfpk4*. 116
Figure 4-21: Southern blot analysis of attempted *pfpk4* disruption. 116
Figure 4-22: PCR analysis of integration of *pfpk4* 3' tags. 117
Figure 4-23: Schematic of expected sizes for Southern blot analysis of *pfpk4* 3' tags. 118
Figure 4-24: Southern blot analysis of *pfpk4* 3' tag populations. 118

List of Tables

Table 4-1: Mosquito infection with *pfeik1*$^{-}$ parasites. 106
Table 4-2: Mosquito infection with *pfeik2*$^{-}$ parasites. 113
Table 6-1: Supppliers of biological and chemical reagents. 134
Table 6-2: Oligonucleotide primers. 138
Table 6-3: Primary antibodies. 139
Table 6-4: Secondary antibodies. 139
Table 6-5: General buffer composition. 140
Table 6-6: Composition of buffers used for DNA analysis. 140
Table 6-7: Composition of buffers used for protein analyses, including recombinant protein preparation. 142
Table 6-8: Buffers, medium and antibiotics used for bacterial preparation and culture. 143
Table 6-9: Composition of solutions used for *P. falciparum* culture. 144
Table 6-10: Solution for mosquitoes. 144

Acknowledgements

The relentless energy and enthusiasm of my supervisor Prof. Christian Doerig is an inspiration; his encouragement and conviction have been invaluable. Dr Luc Reininger has also been a great support, for discussion, critical reading, and sharing his bench with a smile! The Doerig team as a whole, including Dr Helen Taylor, has always been a friendly and supportive environment, which I have found very encouraging.

I am grateful to Dr Lisa Ranford-Cartwright, without whom it would have been impossible to carry out mosquito experiments. It was a pleasure to work with Lisa (informative and helpful on every aspect of mosquito work), Liz Peat (who spoke nicely to my parasites), and Georgie Humphreys (who caught mosquitoes and humoured me through dissection).

Jonathan Wilkes has enabled me to complete the bioinformatic analysis in a more sophisticated manner than I would have done if working alone.

In addition to providing interesting data, Prof. Dan Goldberg, Shalon Babbitt and Ilaria Russo have been extremely co-operative and pro-active to collaborate with, as has Dr Rita Tewari. I hope these are examples of international science at its best, and look forward to more such interactions.

I have leant on the unstinting support of Prof. Bill Cushley and Dr Olwyn Byron; kind, helpful and understanding in all circumstances. Their belief in all of us on the Welcome Trust PhD programme has shaped that into another source of strength and support.

Lastly, my boyfriend Sam; he didn't mean to get broken after all, nor enjoyed the process that much, but has been remarkably sage about it all. Now we can move on.

Author's declaration

I hereby declare that I am the sole author of this thesis and performed all of the work presented, with the following exceptions:

Chapter 3

- Multispecies alignments of eIF2α kinases and the phylogenetic tree of all kinase families were completed with Jonathan Wilkes.

Chapter 4

- Ilaria Russo produced the growth curve for *pfeik1*$^{-}$ parasites in the Goldberg lab.

- Lisa Ranford-Cartwright, Georgina Humphries and Liz Peat cultured gametocytes and fed mosquitoes for infection studies.

- Lisa Ranford-Cartwright dissected some mosquitoes for oocysts, and all for sporozoites in the salivary glands.

Definitions

aaRS	Amino-acyl tRNA synthetase
AB	Blood groups A or B
APAD	3-Acetylpyridine adenine dinucleotide
ApiAP2	Apicomplexan AP2 (Apetala2)
Amp	Ampicillin
ADP	Adenosine diphosphate
At	*Arabidopsis thaliana*
ATF4	Activating transcription factor-4
ATP	Adenosine triphosphate
BHH	Benzamidine Hydrochloride Hydrate
BLAST	Basic local alignment search tool
bp	Base pair(s)
BSA	Bovine Serum Albumin
BSD	Blasticidin deaminase
C-terminus	Carboxy-terminus
cDNA	Complementary DNA
CK2	Casein kinase-2
CML	Chronic myelogenous leukaemia
DB	Database
Dd	*Dictyostelium discoydium*
DEPC	Diethylpyrocarbonate
DHFR	Dihydrofolate reductase
DNA	Deoxyribonucleic acid
dNTP	Deoxyribonucleotide triphosphate
DOZI	Development of zygote inhibited
DTT	Dithiothreitol
EB	Elution buffer (for Qiagen DNA kits)
EDTA	Ethylenediaminetetraacetic acid
EGTA	Ethylene glycol-bis(2-aminoethylether)-N,N,N′,N′-tetraacetic acid
eIF	Eukaryotic initiation factor
eIF2α	Eukaryotic initiation factor 2α
eIF2B	Eukaryotic initiation factor 2B
ER	Endoplasmic reticulum
ERD2	Endoplasmic reticulum defective (an ER membrane protein)
ERK	Extracellularly regulated kinase
Exp.	Experiment
GADD34	Growth arrest and DNA damage gene-34
GCN2	General control non-derepressible-2
gDNA	Genomic DNA
GDP	Guanosine diphosphate
GEF	Guanine exchange factor
GFP	Green fluorescent protein
GNP	Gross national product
GST	Glutathione-S-transferase
GTP	Guanosine triphosphate
HA	Hemagglutinin
HEPES	N-(2-Hydroxyethyl)piperazine-N′-(2-ethanesulfonic acid)
HisRS	Histidyl-tRNA-synthetase
HMM	Hidden Markov model
hr	Hour

HRI	Haem-regulated inhibitory kinase
HRP	Horseradish peroxidase
Hs	*Homo sapiens*
Hsc	Heat shock cognate protein
Hsp	Heat shock protein
IgG	Immunoglobulin G
IgY	Immunoglobulin Y
IP	Immunoprecipitate
IPTG	Isopropyl β-D-thiogalactopyranoside
IRES	Internal ribosome entry site
JNK	c-Jun N-terminal kinase
Kan	Kanamycin
kb	kilobase
KD	Kinase domain
kDa	Kilo Dalton
KO	Knock-out
LB	Luria-Bertani medium
LDH	lactate dehydrogenase
M	Molar
Mm	*Mus musculus*
MAPK	Mitogen activated protein kinase
MAPKK	Mitogen activated protein kinase kinase
MBP	Myelin basic protein
MEGA	Molecular evolutionary genetics analysis
MEK	MAP/ERK kinase
MOPS	2-morpholin-4-ylethanesulfonic acid
N-terminus	Amino-terminus
NAD	Nicotinamide adenine dinucleotide
NBT	Nitroblue tetrazolium
ND	Not done
OD	Optical density
ORF	Open reading frame
Os	*Oryza sativa*
PABA	Para-amino benzoic acid
PAGE	Polyacrylamide gel electrophoresis
Pb	*Plasmodium berghei*
PBS	Phosphate buffered saline
PCR	Polymerase chain reaction
PERK	PKR-like endoplasmic reticulum kinase
Pf	*Plasmodium falciparum*
pfmdr1	*Plasmodium falciparum multi-drug resistance protein-1*
PfeIK1	*P. falciparum* eukaryotic initiation factor 2α kinase-1
PfeIK2	*P. falciparum* eukaryotic initiation factor 2α kinase-2
PfPK4	*P. falciparum* protein kinase-4
PKG	Protein kinase G
PKR	Protein kinase RNA
PMSF	Phenylmethanesulfonyl fluoride
PP1	Protein Phosphatase-1
RB/DD	Ribosome binding and dimerization domain
RBM	Roll back malaria
RIPA	Radio immunopreciptation assay buffer
RNA	Ribonucleic acid
Rpm	Revolutions per minute
RT	Room temperature

RT-PCR	Reverse-transcriptase polymerase chain reaction
SAPK	Stress activated protein kinase
Sc	*Saccharomyces cerevisiae*
SDS	Sodium dodecyl sulphate
SDS-PAGE	Sodium dodecyl sulphate-polyacrylamide gel electrophoresis
SSC	Sodium chloride/sodium citrate
STE	Sterile alpha mutant (kinase)
TAE	Tris/Acetate/EDTA
Tb	*Trypanosoma brucei*
TbeIF2K2	*Trypanosoma brucei* eIF2α kinase-2
TEMED	N,N,N′,N′-Tetramethylethylenediamine
TFB1	Transforming buffer 1
TFB2	Transforming buffer 2
Tet	Tetracycline
TgIF2K-A	*Toxoplasma gondii* eIF2α kinase-A
TgIF2K-B	*Toxoplasma gondii* eIF2α kinase-B
TGS	Tris/Glycine/SDS
TM	Transmembrane
tRNA	Transfer RNA
uORF	Upstream open reading frame
UPR	Unfolded protein response
UTR	Untranslated region
UV	Ultraviolet
V	Volt
WHO	World health organisation
WT	Wild-type
X	times

1 Introduction

1.1 Malaria

Malaria remains a devastating disease in most tropical and subtropical regions (Fig. 1-1) (Snow et al., 2005). It is estimated that 40% of the world's population is at risk from malaria, such that every year more than 500 million people become severely ill with the disease resulting in at least 1 million fatalities (WHO, 2007, Snow et al., 2005). In humans, the disease is caused by infection with one of four species of the parasitic protozoan *Plasmodium*; *P. falciparum*, *P. vivax*, *P. malariae,* or *P. ovale.* It has also recently been recognised that *P. knowlesi*, previously thought to infect only non-human primates, can infect and cause disease in humans (Cox-Singh et al., 2008, Luchavez et al., 2008). Infection with malaria parasites results in fever, headache, chills and vomiting, which if not treated promptly and effectively can progress to severe disease that may be fatal. In addition to the threat to health, malaria also has a serious impact on socioeconomic development in endemic countries by impacting on long term demographics and the acquisition of human and physical capital (Sachs and Malaney, 2002). To reduce this to a number, it has been calculated that in the long term, gross national product (GNP) per capita is reduced by more than half in malarious countries, compared to non malarious countries (Sachs and Malaney, 2002, http://www.rollbackmalaria.org/). The emergence and spread of resistance to available antimalarial drugs in the parasite exacerbates the problem, adding urgency to the task of development of novel chemotherapeutic agents (Ridley, 2002b, Ridley, 2002a, Gelb, 2007).

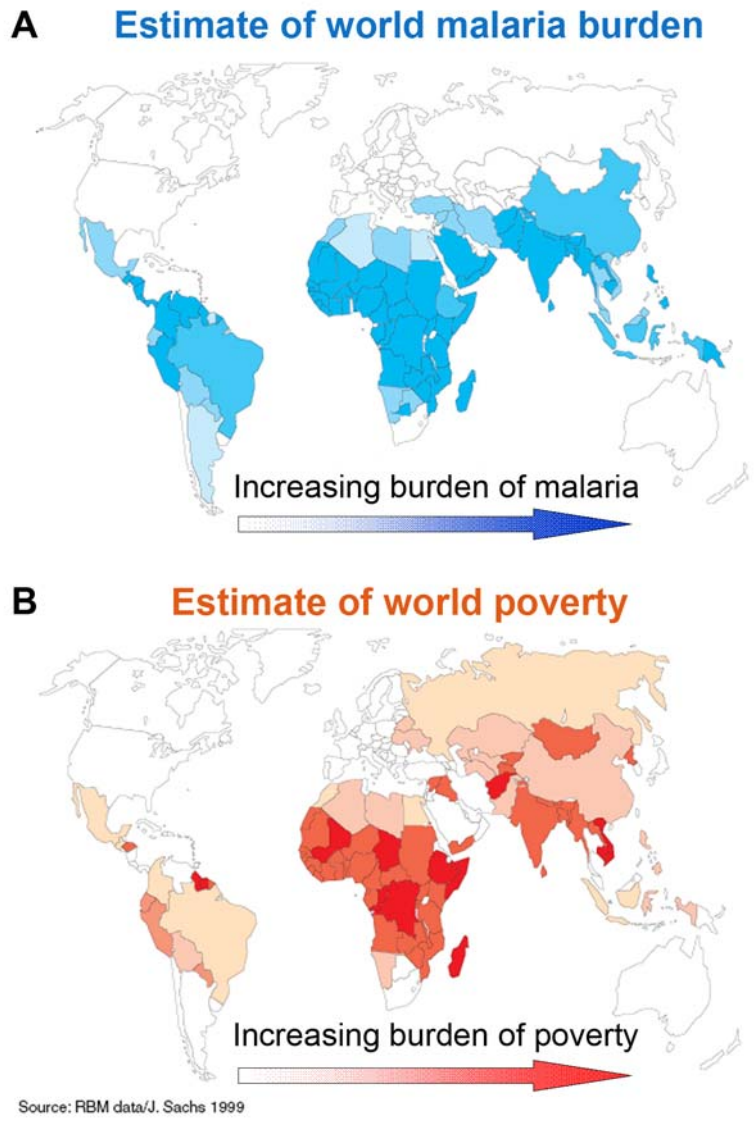

Figure 1-1: Maps to illustrate the coincidence of the world malaria burden and poverty. A: Darker shades of blue indicate greater malaria burden. B: Darker shades of red indicate greater poverty (adapted from Roll Back Malaria fact sheet 10 (http://www.rollbackmalaria.org/)).

1.2 Plasmodium falciparum

P. falciparum is responsible for the majority of lethal cases of malaria (Guerra et al., 2006), although there is increasing concern about the contribution of *P. vivax* to severe malaria (Joshi et al., 2008, Baird, 2007). Fatalities from *P. falciparum* arise as the infection can progress to severe anaemia and central nervous system effects leading to coma and death. *P. falciparum* is the major malaria parasite in sub-Saharan Africa, where greater than 90% of the world's malaria is found (Snow et al., 2005). As a consequence, *P. falciparum* is the most extensively studied of the human malaria parasites. Completion of the *P.*

falciparum genome project in 2002 has transformed research into this parasite (Gardner et al., 2002, Waters, 2008).

Plasmodium is a member of the apicomplexa, all of which are obligate intracellular parasites. Other apicomplexan parasites of medical or agricultural importance include *Toxoplasma gondii*, an opportunistic parasite of immunocompromised individuals; *Theileria* spp, tick borne parasites of cattle in Africa; and *Cryptosporidium*, which is both an animal and opportunistic human parasite. Genome sequences are available for species within each of these genera, which in conjunction with different *in vitro* culture and genetic manipulation possibilities is contributing to advances in our understanding of the apicomplexa as a whole (Abrahamsen et al., 2004, Gajria et al., 2008, Kim and Weiss, 2004). Apicomplexan parasites are distinguished morphologically by the presence of an apical organelle complex for host cell invasion (Fig. 1-2). Apicomplexans have a complex life cycle with multiple developmental stages that occur in diverse tissues, often in more than one host; this probably reflects a series of evolutionary adaptations to optimise the exploitation of hosts (Aravind et al., 2003).

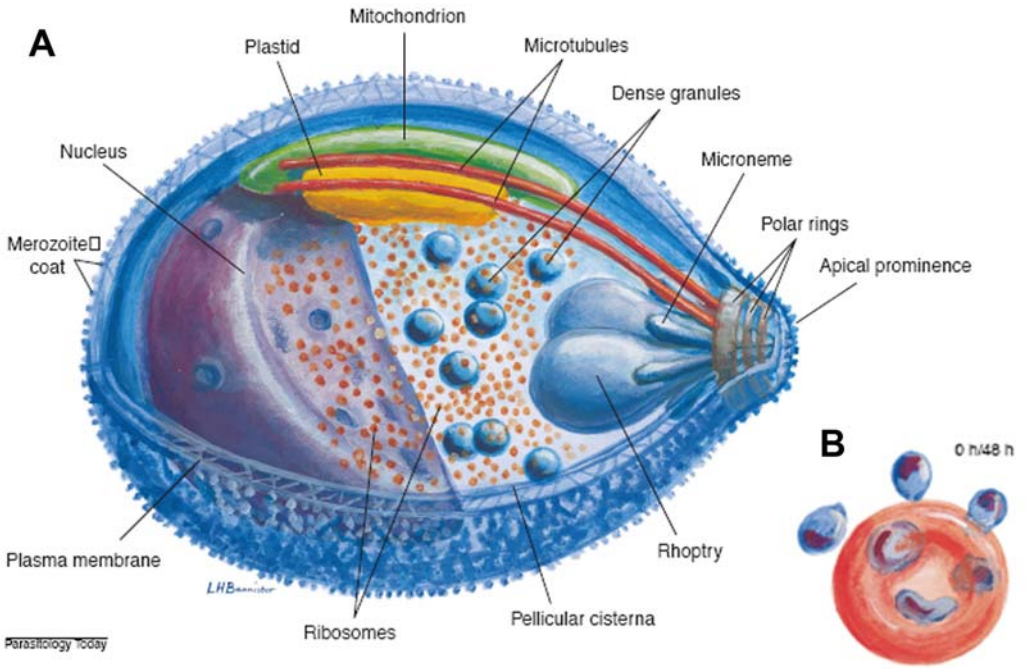

Figure 1-2: Illustration of *P. falciparum* merozoites.

A: Ultrastructure of a merozoite showing the apical organelles (micronemes and rhoptries) used in invasion. B: Shows the relative size of the merozoite and host erythrocyte during invasion. Clockwise, the merozoite orients, anchors and invades, until it is within the erythrocyte inside the parasitophorous vacuole (adapted with permission from Bannister et al. 2000 (Bannister et al., 2000)).

1.3 Life cycle of malaria parasites

Humans are infected following injection of sporozoites into the skin, by the bite of an infected *Anopheles* mosquito (Fig. 1-3). Sporozoites move away from the injection site to reach a capillary, allowing them to travel to the liver where they invade hepatocytes and undergo schizogony to release thousands of merozoites. Merozoites enter the bloodstream where they invade erythrocytes, a cycle that proceeds in a synchronous manner and is responsible for malaria pathogenesis. On entering erythrocytes, a proportion of malaria parasites do not enter schizogony but arrest their cell cycle and differentiate into male or female gametocytes (see 1.3.1). Critically, gametocytes are the only form capable of infecting the mosquito vector, and are therefore required for transmission to the next human host. Ingestion of gametocytes by a female mosquito triggers gametogenesis entailing the release of a single female macrogamete and eight male microgametes. Release of the motile microgametes is termed exflagellation, because male gametes are flagellated. Fusion of the male and female gametes forms the zygote, the only short-lived, diploid stage of the lifecycle. Further development produces a motile ookinete, in which meiosis occurs and which migrates through the mosquito midgut wall to establish an oocyst on the hemocoel side of the midgut. Successive rounds of division and differentiation within the oocysts produce mature sporozoites that spread throughout the mosquito. On reaching the salivary glands the sporozoites are ready to commence the next cycle of infection on the mosquitoes next blood meal.

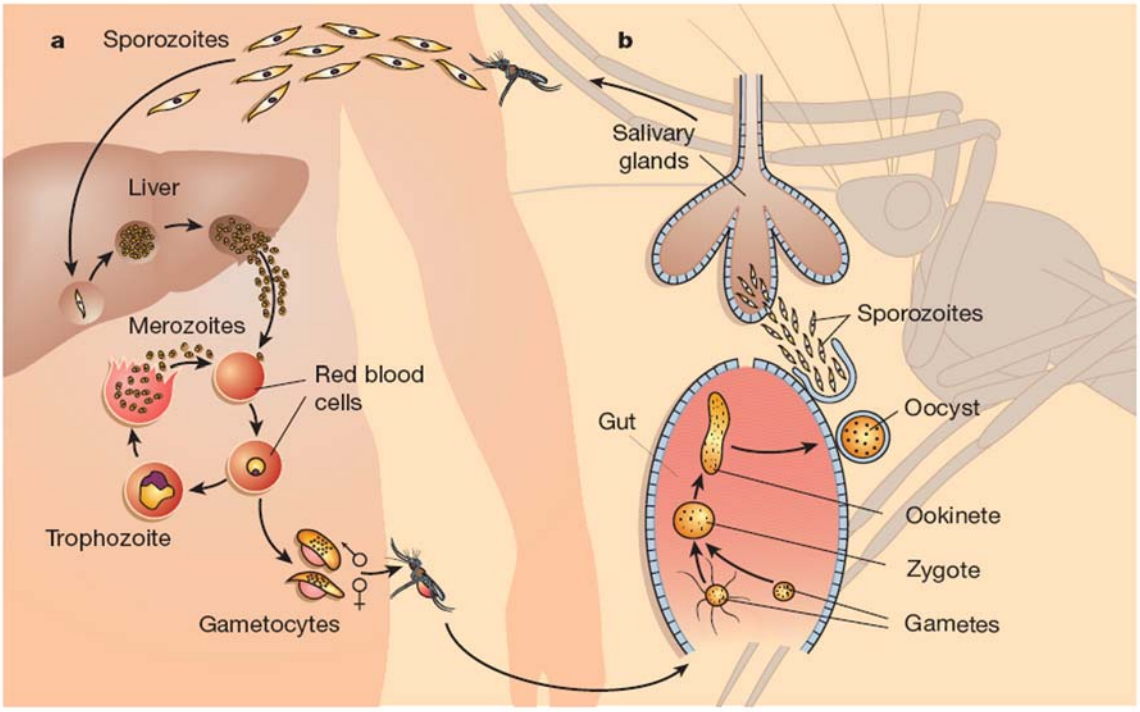

Figure 1-3: Illustration of the *P. falciparum* life cycle.
A: Sporozoites from the bite of an infected Anopheles mosquito are carried to the liver where they invade hepatocytes. After many rounds of division merozoites are released which invade erythrocytes starting the indefinite asexual cycle that gives rise to disease symptoms. Some asexual parasites cease division and differentiate to gametocytes. B: Injestion of gametocytes by a mosquito allows the parasite to complete the life cycle; gametogenesis and fertilization form an ookinete which is able to infect the mosquito mid gut wall. Sporozoites form inside the oocysts, and on maturation reach the salivary glands in preparation for transmission to the next human host (adapted from with permission from Wirth, Nature 2002 **(Wirth, 2002)**).

1.3.1 Gametocytogenesis

As described above sexual differentiation or gametocytogenesis is essential for the transmission of *P. falciparum*, and other *Plasmodia* from one vertebrate host to the next. The molecular mechanisms responsible for sexual differentiation (gametocytogenesis) are not understood (Silvestrini et al., 2005, Alano, 2007). However, various studies indicate that in *P. falciparum* the rate of switching from asexual replication to gametocytogenesis varies between parasite isolates, between cloned lines derived from a single isolate (Graves et al., 1984), and importantly is not constant within a cloned line but is sensitive to environmental conditions (Carter and Miller, 1979). To this end, it has been observed that diverse manipulations of the *in vitro* culture environment, particularly those

that have an adverse effect on asexual replication, increase the rate of gametocytogenesis. These include the presence of erythrocyte lysate (Schneweis et al., 1991), host immune sera and lymphocytes (Schneweis et al., 1991, Smalley and Brown, 1981), the antimalarial, chloroquine (Buckling et al., 1997), and a high asexual parasite density (Bruce et al., 1990). The typically female biased sex ratio of gametocytes in *Plasmodium* is also variable (Alano, 2007).

Commitment to gametocytogenesis occurs at an unidentified time during the asexual cycle, such that a schizont contains either merozoites that will continue the asexual cycle, or that will develop into gametocytes (Bruce et al., 1990). Furthermore, the sex of the gametocytes arising from the same schizont is also previously determined (Silvestrini et al., 2005, Smith et al., 2000). That rates of gametocytogenesis are responsive to environmental change suggests that a stress response mechanism may be involved. Of interest is the observation that in *T. gondii* the switch from rapidly dividing tachyzoites to differentiation to quiescent bradyzoites is a stress-induced response (Weiss and Kim, 2000).

1.4 Available chemotherapies/global antimalarial strategy

The current increase in the world malaria burden is due to a number of factors; particularly the emergence and spread of drug resistance in the parasite, the resistance to insecticides in the mosquito vector , and the breakdown of health infrastructure in many endemic areas (Greenwood and Mutabingwa, 2002, Ridley, 2002b, Ridley, 2002a, Walther and Walther, 2007). This has been recognised in naming malaria as one of the WHO's high priority diseases and in public-private partnership initiatives such as the Medicines for Malaria Venture. Development of antimalarials is particularly challenging due to the circumstances in which they are primarily used, which demand compounds that are both very safe and very cheap. Complexity is added by the benefit of using drugs in combination to minimise the development of resistance (Gelb, 2007).

Antimalarials may target parasites during the asexual cycle, thereby reducing the disease burden. Compounds could also be developed aimed at interfering

with gametocytogenesis, which would therefore act as transmission blocking agents. Transmission blocking agents would represent a useful tool to limit the escape of drug-resistant genotypes selected during schizogony in the human host. Strategies to limit the spread of resistance to available drugs are of paramount importance in the context of frequent sub-curative drug treatment, resulting in selection of drug resistant parasites and therefore increased probability of their transmission (Mackinnon and Read, 2004). Considerable effort continues to be put into development of a vaccine, but to date nothing has progressed beyond mixed results in clinical trials (Matuschewski and Mueller, 2007). Insecticide treated nets and indoor residual spraying are also powerful tools with which limit contact between humans and mosquitoes that deserve further investigation and investment (reviewed (Walther and Walther, 2007)).

1.5 Protein kinases

Since the discovery of protein kinases (Edwin G Krebs & Edmond H Fisher, Nobel Prize 1992) reversible phosphorylation has been established as major mechanism of eukaryotic cellular regulation, with central roles in proliferation, differentiation and metabolism (Hanks, 2003). Protein kinases have a conserved catalytic domain, possession of which forms them into one of the largest superfamiles of homologous genes and proteins (Hanks and Hunter, 1995). The protein kinase superfamily divides into two major groups; the protein-serine/threonine kinases and the protein-tyrosine kinases (Taylor et al., 1995, Johnson et al., 1998). The kinase catalytic domain comprises twelve conserved subdomains that result in the proteins folding into a characteristic bi-lobed structure, as revealed by the now numerous solved 3-D structures (Dar et al., 2005, Taylor et al., 1992, Merckx et al., 2008). Conservation of the catalytic domain maintains three key aspects of the kinase reaction: i) binding and orientation of the phosphate donor, ATP (or GTP); ii) binding and orientation of the protein (or peptide) substrate; and iii) transfer of the terminal phosphate from ATP (or GTP) to the acceptor (Ser, Thr, or Tyr) of the protein substrate (Fig. 1-4) (Hanks and Hunter, 1995). Of particular importance for catalytic function are the invariant lysine in subdomain II, which is involved in the

anchoring and orienting ATP, and the invariant aspartate in subdomain VIB that mediates phosphotransfer (Hanks, 2003, Niedner et al., 2006).

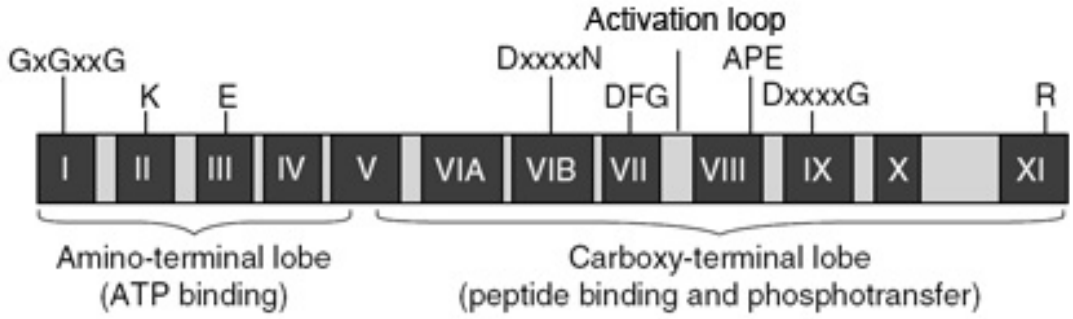

Figure 1-4: Schematic to show the conserved subdomains of protein kinases. (Adapted from Hanks 2003 (Hanks, 2003)).

1.5.1 Kinases as drug targets

The human genome encodes 518 kinase genes that are subdivided into 20 families on the basis of structural relatedness. Classical protein kinases account for 478 of these genes, of which 388 are serine/threonine kinases, 90 are tyrosine kinases and the remaining 50 lack a functional catalytic site and are therefore termed pseudokinases (Manning et al., 2002, Boudeau et al., 2006). The large number of kinases and their roles in cellular processes means that their disregulation is associated with diverse diseases, including rheumatoid arthritis, cardiovascular disorders, immunodeficiency and cancer (Cohen, 2002). In the case of cancer, approximately half of the 100 identified oncogenes encode kinases, while the other half either activate kinases, or are phosphorylated by kinases. In the light of this, the development of kinases as drug targets is no surprise (Giamas et al., 2007).

The first kinase inhibitor tested in clinical trials (imatinab mesylate/Gleevec®) has proved a highly successful anticancer drug for patients with chronic myelogenous leukaemia (CML). Gleevec inhibits the Abelson cytoplasmic tyrosine kinase that is constitutively active in most patients with CML (Giamas et

al., 2007). Gleevec has also been found to inhibit additional kinases and is also used in the treatment of gastrointestinal stromal tumours. This raises an interesting point concerning the development of compounds that inhibit more than a single enzyme, which may help to overcome the fact that cells may use more than one overlapping signalling pathway to reach the same outcome. There are now more than 60 kinase-targeted drugs in clinical development, and many more in the pre-clinical stages. Further, kinases are second only to G-protein coupled receptors with respect to the number of screening targets in use by the pharmaceutical industry to identify new molecules (Weinmann and Metternich, 2005).

The conservation of the structure of the kinase domain, where ATP is bound in the cleft between the two lobes of the catalytic domain might suggest that searching for selective competitive ATP-inhibitors would be an impossible task. Remarkably, the minor differences between kinases result in sufficient differences in the 3-D structure to result in changed hydrogen bonding capacities and hydrophobic interactions, causing differences in affinity (Giamas et al., 2007, Fischer, 2004). However, other inhibition paradigms are being developed such as allosteric inhibition to change the conformation, preventing substrate binding, or direct competition with the kinase substrate. These new strategies may facilitate new therapeutic opportunities and also limit off-target side effects, where specific inhibition is desirable (Bogoyevitch and Fairlie, 2007).

1.6 Kinases in *P. falciparum*

Plasmodium and other parasitic protists such as *Toxoplasma* and the trypanosomatids including *Trypanosoma* and *Leishmania*, belong to taxonomic groups that are phylogenetically hugely distant from the Opisthokonta branch, which includes animals and fungi (Baldauf, 2003). Completion of the *P. falciparum* genome project (Gardner et al., 2002) allowed two independent analyses of the complete complement of *Plasmodium* kinases, or kinome (Ward et al., 2004, Anamika et al., 2005). The studies were essentially in agreement, and identified substantial differences between the plasmodium and mammalian kinomes, reflecting their evolutionary distance. Divergence was identified at

the levels of i) the composition of the kinome, ii) the organisation of signalling pathways, and iii) the properties of individual enzyme orthologues, when they can be identified (Doerig, 2004b, Doerig et al., 2005, Doerig and Meijer, 2007). Concerning the composition of the kinome, members of most groups of eukaryotic kinases could be identified, with the exception of the tyrosine kinases and STEs (which are part of the mitogen activated protein (MAP) kinase pathway). On the other hand, many 'orphan' kinases were identified that do not cluster with any of the identified mammalian or yeast kinase families. Intermediate to these extreme examples are a number of genes that clearly cluster with a defined kinase family, but branch off at the base of the cluster, such that assignment of orthology to a specific mammalian enzyme is impossible; these kinases are referred to as semi-orphans (Ward et al., 2004). At the level of signalling cascades a notable example is the lack of a classical three-tier MAP kinase pathway (Dorin et al., 2005). *P. falciparum* has two atypical MAPKs but the absence of MAPKKs indicates that their activation is through other as yet uncharacterised mechanisms. Finally, with regard to divergence at the individual enzyme level, even clear orthologues display significant differences, such as the presence of large insertions/extensions, or variant regulatory sites (Doerig and Meijer, 2007). Illustrations of such differences are a MAPK lacking the usual TxY motif (Dorin et al., 1999) and a PKG (protein kinase G) homologue with an atypical regulatory region (Deng et al., 2003).

Data is accumulating that many members of the *Plasmodium* kinome are essential for schizogony, (Dorin-Semblat et al., 2007) (Doerig lab, in prep.) and therefore represent potential targets for curative drugs. Kinases demonstrated to have an essential role in the sexual development of the parasite represent potential transmission-blocking targets (Reininger et al., 2005). The emerging differences between parasite protein kinases and their host homologues is supportive of the idea of specific targeting of the former (Doerig, 2004a, Doerig, 2004b, Doerig and Meijer, 2007, Leroy and Doerig, 2008).

1.7 Gene regulation in *P. falciparum*

Completion of the *P. falciparum* genome sequence, in conjunction with that of the rodent malaria *P. yoelii* in 2002, and more recently *P. berghei*, and *P. chabaudi* has opened a new level of investigation into all aspects of *Plasmodium* biology, including gene regulation (Gardner et al., 2002, Carlton et al., 2002, Hall et al., 2005). Initially, very few genes could be categorised as transcription factors, although it was acknowledged that this could have been due to difficulties in identification, due to their divergence from known examples, and exacerbated by the A-T richness of the genome (Gardner et al., 2002). Two studies of the *P. falciparum* transcriptome followed shortly after (Le Roch et al., 2003, Bozdech et al., 2003); the more comprehensive data set, composed of 1 hour time points over the 48 hour intra-erythrocytic developmental cycle, demonstrates transcriptional regulation resulting in a continuous cascade of gene expression, unlike anything observed previously in eukaryotic biology (Bozdech et al., 2003). Furthermore, contiguous genes on chromosomes were rarely found to be co-regulated (Bozdech et al., 2003). This transcriptional pattern, which must underlie the complex developmental changes that occur during the parasite life cycle, the use of monocistronic mRNAs, and the conservation of basal eukaryotic transcription factors, inspired a continued search for a more sophisticated transcriptional network. This has been rewarded with the identification of Apicomplexan AP2 (ApiAP2) DNA-binding proteins (Balaji et al., 2005, De Silva et al., 2008). DNA binding specificities for two *P. falciparum* ApiAP2 proteins have been defined and represent sequence motifs found in the 3' region of sets of genes that show coregulation during the asexual cycle (De Silva et al., 2008).

Despite this recent advance a body of evidence supports a significant role for post-transcriptional control in *P. falciparum*. An analysis of the *P. falciparum* genome for transcription-associated proteins revealed only one third of the expected number, for the genome of a free living eukaryote; however, the CCCH-type zinc finger, commonly found in proteins involved in modulating mRNA decay and translation rates is over represented (Coulson et al., 2004). Sequences with homology to deadenylase enzymes that modify translation

initiation and mRNA decay were also identified (Coulson et al., 2004). The pattern of mRNA decay rates across the *P. falciparum* genome contrasts with that observed in other organisms; the half-life of each mRNA is usually precisely related to its physiological role, whereas *P. falciparum* shows a genome-wide decrease in mRNA decay rate through the intra-erythrocytic developmental cycle (Shock et al., 2007). Although sexual differentiation is a special case, several examples exist of transcripts produced in gametocytes, but translated only after gametogenesis has been initiated (Paton et al., 1993, Hall et al., 2005). In *P. berghei* one mechanism of implementing this translational repression has been described; in female gametocytes DOZI (development of zygote inhibited), an RNA helicase, is found in complex with RNAs known to be translated only after fertilisation, including p25 and p28 (Mair et al., 2006). PbDOZI was found to play a critical role in formation of ribonucleoprotein complexes, without which nearly 400 transcripts were degraded instead of stored (Mair et al., 2006).

In spite of recent progress, much remains to be discovered about the regulation of protein levels in *P. falciparum;* much of this regulation may prove to be mediated at the level of translation.

1.8 Stress responses

The ability of a cell to sense and respond appropriately to stress is essential to maintain homeostasis. Diverse factors may be stressful to a cell, including oxidative agents, chemical assault, nutrient deprivation, genetic damage and even the process of differentiation. Response to stress involves induction of programmes of gene expression that enable damage repair, or alternatively induce apoptosis. A significant element of the stress response is mediated by transcriptional change; however, since significant damage could result from mis-translation or aberrant protein folding, stress responses are also mediated through regulation of translation.

1.8.1 Stress Activated Protein Kinases

A large component of the stress response is mediated through a family of proteins termed stress-activated protein kinases (SAPKs). The SAPKs, specifically JNKs and p38 kinases, are subfamilies of mitogen activated (MAP) kinases (see 1.6) that are expressed in essentially all tissues and respond to a variety of stress conditions (Engelberg, 2004). As members of the MAPK family, the SAPKs are at the bottom of three-tier kinase cascades, the downstream targets of which are diverse, but include a range of transcription factors (Engelberg, 2004, Robinson and Cobb, 1997, Davis, 2000, Nebreda and Porras, 2000). This is of interest here for two reasons: firstly with regard to the dearth of *P. falciparum* proteins identified to play a role in transcriptional regulation, and of the conserved sequences on which they might act (for further discussion see 1.7) (Coulson et al., 2004); secondly, both bioinformatic and experimental approaches suggest that classical three-component MAPK signalling pathways do not operate in malaria parasites. Furthermore, although the parasite kinome includes two MAPK homologues, none of these are members of the SAPK subfamily (Dorin et al., 2005).

1.8.2 eIF2α pathway

The SAPKs described above mediate change by regulation of transcription; gene function can also be regulated by modulation of protein synthesis. Initiation, elongation and termination of translation can all be regulated although influencing the earliest stages of the pathway conserves resources most effectively. Phosphorylation of eukaryotic initiation factor-2α (eIF2α) in response to stress is one mechanism of regulating translation initiation. Phosphorylation of eIF2α at residue Ser51 is a well-characterised and conserved mechanism of post-transcriptional control that regulates initiation of translation (Wek et al., 2006, Holcik and Sonenberg, 2005, Proud, 2005, Choi et al., 1992, Murtha-Riel et al., 1993, Colthurst et al., 1987). This mechanism is conserved in the vast majority of eukaryotes. One notable exception is the microsporidium *Encephalitozoon cuniculi*, whose kinome does not include eIF2α kinases (or other stress-response kinases), a probable adaptation to its parasitic lifestyle

(Miranda-Saavedra et al., 2007). In mammalian cells this phosphorylation event is mediated by four distinct protein kinases; general control non-derepressible-2 (GCN2), protein kinase RNA (PKR), haem-regulated inhibitor kinase (HRI), and PKR-like endoplasmic reticulum kinase (PERK), all four of which serve to integrate diverse stress signals into a common pathway (Wek et al., 2006, Holcik and Sonenberg, 2005, Proud, 2005, Chen and London, 1995).

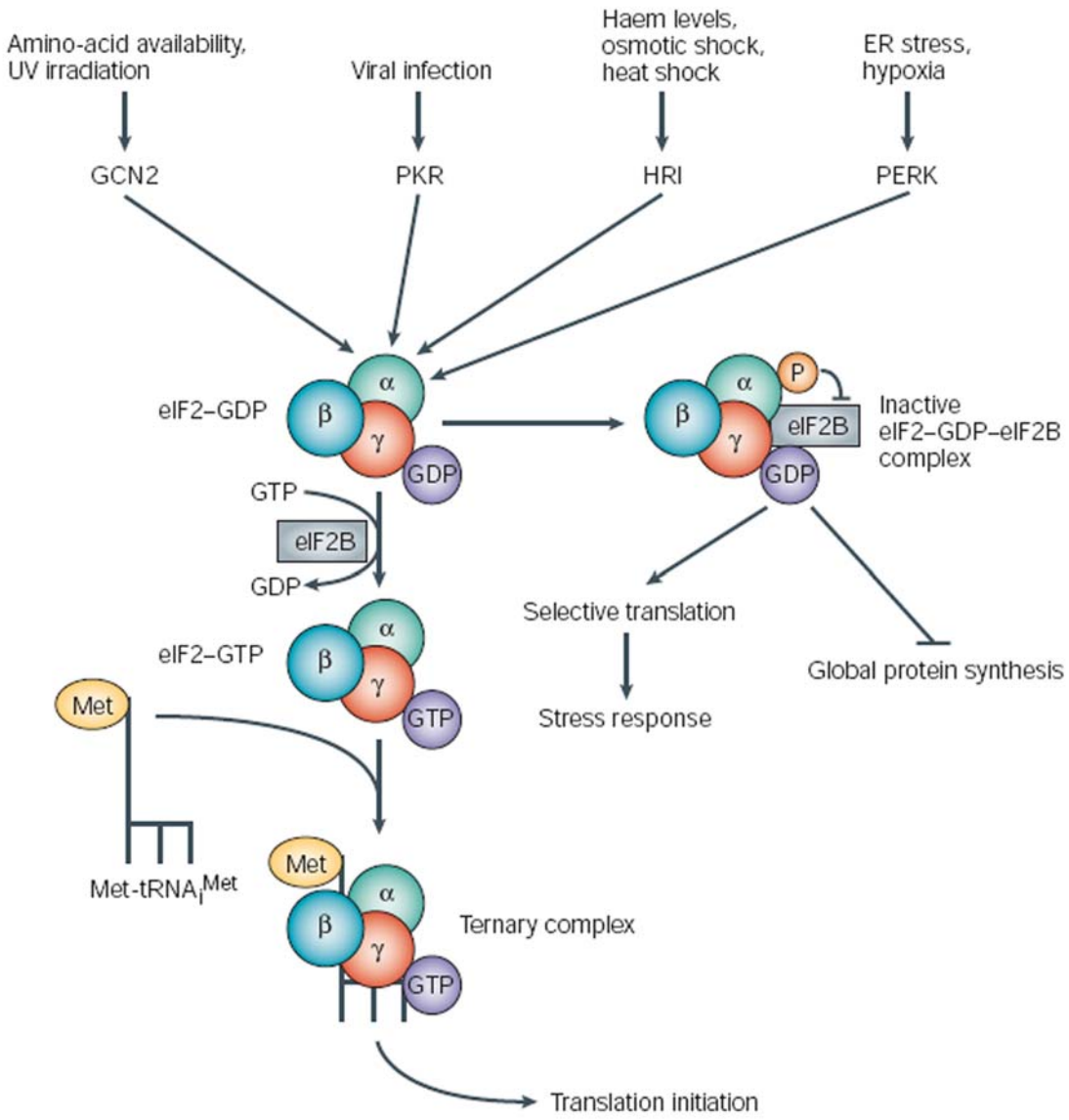

Figure 1-5: Integration of stress responses by phosphorylation of eIF2α.
The eIF2α kinases (GCN2, PKR, HRI, PERK) are activated by diverse stress stimuli to phosphorylate eIF2α. Phosphorylation of eIF2α inhibits the GDP-GTP exchange by reducing the dissociation rate of eIF2B. This reduces the availability of the ternary complex resulting in a decrease in global protein synthesis, and selective translation that mediates the stress response (adapted with permission from Holcik & Sonenberg 2005 (Holcik and Sonenberg, 2005)).

Translation of eukaryotic mRNAs involves the recognition and recruitment of mRNAs by the translation initiation machinery, and the assembly of the 80S ribosome on the mRNA, which is mediated by proteins known as eukaryotic initiation factors (eIFs). Formation of the 43S preinitiation complex depends on binding of the ternary complex that consists of the heterotrimeric G-protein eIF2, methionyl-initiator tRNA (met-tRNAi) and GTP (Fig. 1-5) (Holcik and Sonenberg, 2005, 2000). Initiation of translation and release of the initiation factors involves hydrolysis of GTP to GDP, which leaves an inactive eIF2α-GDP complex. Before further rounds of translation initiation can occur eIF2α must be reactivated by exchange of GDP for GTP by eIF2B (Holcik and Sonenberg, 2005). Presence of a phosphate group on the eIF2α subunit inhibits recycling of inactive eIF2-GDP to active eIF2-GTP by limiting the activity of the guanine nucleotide exchange factor activity of eIF2B (Sudhakar et al., 2000). The consequence of activity of the eIF2α kinases therefore is global translation repression, since initiation complexes cannot form, thus preserving energy and nutrients.

It is interesting to note however, that in spite of the mechanism described above, leading to translational repression, the translation of some mRNAs is enhanced when eIF2α is phosphorylated (Holcik and Sonenberg, 2005, Proud, 2005). The paradigm for such regulation is provided by the mRNA for the yeast protein Gcn4p that has four short upstream open reading frames (uORFs). When the ternary complex (containing the initiator methionine) is plentiful these four uORFs are translated, but ribosomes are likely to fall off the mRNA before reaching the start codon of Gcn4. When the ternary complex is in short supply due to eIF2α phosphorylation some ribosomes are able to move quickly along the mRNA reaching the Gcn4 start codon, some of which will bind a ternary complex, enabling translation initiation. A similar mechanism is believed to operate for mammalian ATF4 (Proud, 2005). An alternative mechanism that operates for other mRNAs and in some instances is regulated by eIF2α phosphorylation, is the use of internal ribosome entry sequences (IRESs), which allow translation initiation independently of the 5'cap and eIF4 complex utilised by most mRNAs (Fernandez et al., 2002).

Signal transduction through the eIF2α pathway is very rapid; phosphorylation and translational repression have been shown to be complete as soon as 30 minutes after exposure to stress (Novoa et al., 2003), whereas in responses by activation of gene expression programs the latency will be measured in hours (Harding et al., 2002). The immediacy of this pathway is important under stress conditions where rapid deployment of appropriate response and use of resources is essential for cell survival.

1.8.3 eIF2α kinases, mechanisms & activation

1.8.3.1 Domain structure

The eIF2α kinases have a homologous catalytic domain that enables them to phosphorylate the same substrate, eIF2α. However, in order to respond to different stimuli they have different regulatory domains (Fig. 1-6) and are located in different subcellular compartments. GCN2 is one of few proteins to possess both a functional and an inactive kinase domain (Boudeau et al., 2006). The degenerate kinase domain lies N-terminal to the functional kinase domain, which is followed by the major motif for activation: the histidyl-tRNA synthetase (HisRS)-like domain (Wek et al., 1989, Wek et al., 1995, Dong et al., 2000). The HisRS domain functions by binding uncharged tRNAs that accumulate during amino acid limitation, leading to activation of the kinase domain (Wek et al., 1995). PKR has an N-terminal double-stranded RNA (dsRNA) binding domain composed of two copies of a dsRNA-binding motif, and a C-terminal kinase domain (Meurs et al., 1990, Dar et al., 2005). HRI has an N-terminal region containing one heme-binding domain, and a second heme-binding domain within an insertion in the kinase domain (Rafie-Kolpin et al., 2000, 2000, Chefalo et al., 1998). Finally, PERK has a single trans-membrane domain and resides in the endoplasmic reticulum (ER); an amino-terminal luminal domain similar to that of the ER-stress-sensing kinase Ire1 monitors the protein folding environment, while the cytoplasmic portion contains the kinase domain where it can interact with the translation initiation machinery (Harding et al., 1999). PERK is involved in the unfolded protein response (UPR); its position in the ER membrane allows this

kinase to have immediate impact on proteins destined for secretion by its proximity to the ribosomes on the rough ER.

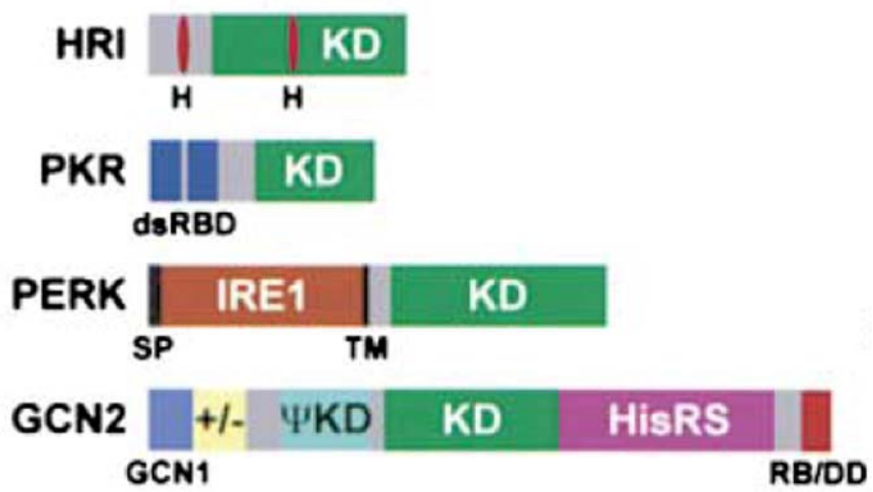

Figure 1-6: Schematic of the domain structures of the eIF2a kinases.
Conserved kinase domains (KD) are depicted in green. The two heme binding sites (H) in HRI are marked in red. The double stranded RNA binding domains (dsRBD) in PKR are shown in blue. The N-terminal half of PERK resembles the corresponding domain of the ER stress-responsive IRE1 kinase. The signal peptide (SP) and transmembrane domain (TM) of PERK are also shown. The regulatory histidyl-tRNA synthetase (hisRS) domain in GCN2 is shown in purple. The locations of the GCN1 binding domain (blue), charged region (+/-) and pseudo-kinase domain (ψKD), as well as the C-terminal ribosome binding, and dimerisation domain (RB/DD) domain in GCN2 are also indicated (adapted from Dever 2002 (Dever, 2002)).

A characteristic of the eIF2α kinases is the presence of insertions within the kinase domain between subdomains IV and V (Figs. 3-5 & 3-6). The length and composition of these inserts is variable and no function has been ascribed to date, apart from HRI where one of the heme binding domains is in this region (Mathews, 2007). The sequence between subdomains VII and VIII, comprising the activation loop may also be extended (Figs. 3-5 & 3-6) (Mathews, 2007).

1.8.3.2 Activation mechanism

Dimerisation and autophosphorylation appear to be an integral part of PERK, HRI and GCN2 kinase function (Bertolotti et al., 2000, Bauer et al., 2001, Qiu et al., 2001, Liu et al., 2000). For example ER stress induces ligand-independent lumenal-domain driven homodimerisation of PERK, following dissociation of the ER chaperone BiP (Bertolotti et al., 2000). PERK subsequently

autophosphorylates, activating the kinase domain (Liu et al., 2000). Evidence suggests HRI is active as an autokinase immediately following synthesis, however additional multiple autophosphorylation events facilitate formation of the stable homodimer capable of eIF2α phosphorylation, that is positively regulated by heme (Bauer et al., 2001, Rafie-Kolpin et al., 2003). In PKR, binding dsRNA initiates dimerization and autophosphorylation on Thr466 within the activation segment of its catalytic domain. This leads to the full catalytic activation of PKR and the selective ability to phosphorylate eIF2α (Ung et al., 2001, Zhang et al., 2001, Nanduri et al., 2000). Dar et al. have shown that in PKR the N-terminal lobe of the catalytic domain mediates dimerization (Dar et al., 2005). The mechanism of dimerization in PKR is found to differ critically from the classical *in trans* activation paradigm of receptor tyrosine kinases (TRK). Such a mechanism is precluded in PKR by the back-to-back arrangement of the kinase domain dimer, so that PKR autophosphorylation must occur *in cis* or through the action of a PKR dimer on other PKR dimers or monomers (Dar et al., 2005).

Conservation of the activation-segment phosphoregulatory site and basic phosphocoordinating residues underlines the importance of activation segment phosphorylation for regulation of the kinase activity of three of the four eIF2α kinases. GCN2 exists as a constitutive dimer, and has therefore potentially lost this requirement (Dar et al., 2005). Similarities between the catalytic domains of the eIF2α kinase family suggest that the mechanisms of catalytic regulation and substrate recognition discerned from the PKR/eIF2α complex are functionally relevant for the eIF2α protein kinase family as a whole.

Mutational analysis of PKR identified residues that activate PKR in the absence of its regulatory domains, and that map to the dimerization surface on the kinase catalytic domain (Dar et al., 2005, Dey et al., 2005). Distinct sites were identified that block autophosphorylation and eIF2α phosphorylation, whilst mutation of PKR Thr466, an autophosphorylation site within the catalytic domain activation segment, impairs eIF2α phosphorylation (Dey et al., 2005). An ordered mechanism of PKR activation was proposed whereby catalytic domain

dimerization triggers Thr446 autophosphorylation and specific eIF2α substrate recognition (Dey et al., 2005).

1.8.3.3 Substrate recognition and phosphorylation by eIF2α kinases

To understand the basis for substrate recognition by PKR and its regulation, Dar et al. (Dar et al., 2005) determined X-ray crystal structures of the catalytic domain of PKR in complex with eIF2α, and were able to show that eIF2α binds to the C-terminal catalytic lobe (Dar et al., 2005). As a result of the potent antiviral role played by PKR, most viruses have evolved mechanisms of circumventing its function, and the study of these mechanisms has been informative in elucidating the normal workings of PKR (Kawagishi-Kobayashi et al., 1997, Dar and Sicheri, 2002). The eIF2α recognition mechanism is fully conserved across eIF2α kinases, with the primary determinants appearing to consist of the unique size and orientation of helix αG, rather than a strict conservation of residues comprising the eIF2α contact surface (Dar et al., 2005) (see below, section 3.2.1, for a full discussion of the structure). The evidence presented suggests that the higher-order substrate recognition mechanism employed by PKR is restricted to eIF2α recognition, however the possibility of alternate substrate targeting mechanisms are not ruled out (Dar et al., 2005).

1.8.4 Effects of phosphorylation of eIF2α

eIF2 has a much higher affinity for GDP than GTP so the guanine-nucleotide exchange factor (GEF) eIF2B is required to return eIF2 to a GTP bound state. Phosphorylation of eIF2α on Ser51 converts eIF2 from a substrate to a competitive inhibitor of eIF2B, effectively sequestering eIF2 in an inactive state. This results in a reduction in the availability of the ternary complex and therefore decreases translation of most mRNAs, by reducing initiation. Paradoxically, as mentioned above, phosphorylation of eIF2α increases the translation of certain specific mRNAs, which encode proteins involved in the response to the stress, and recovery of translation (Dever, 2002).

1.8.5 Feedback to regulate phosphorylation of eIF2α.

Since the consequence of eIF2α phosphorylation is repression of translation, a cell cannot function under these conditions indefinitely; furthermore, long-term adaptation to stress conditions requires synthesis of new proteins. It must therefore be possible to terminate the activities of the eIF2α kinases and remove the phosphates they add when a cell is no longer under stress, whilst retaining the capacity to respond appropriately for the duration of exposure to stressful stimuli (Rutkowski and Kaufman, 2004). Some mRNAs may have features that protect them from translational repression, such as the ATF4 mRNA, the translation of which is actually induced by global translational repression due to its 5' uORF structure (Proud, 2005). However, translation of most mRNAs, including important ER chaperones (such as BiP) that are ultimately required for the stress response, requires relief from the repressed state. It is established that translational repression in response to both ER stress and exposure to arsenite is transient, and that expression of stress-induced mRNAs and their encoded proteins coincides with a phase of translational recovery (Brostrom et al., 1989). Protein phosphatase 1 (PP1) has been shown to dephosphorylate eIF2α *in vitro* and *in vivo* (Redpath and Proud, 1990, Novoa et al., 2001, He et al., 1997). Evidence suggests growth arrest and DNA damage gene 34 (GADD34), a stress-inducible regulatory subunit of a holophosphatase complex that includes PP1 as a catalytic subunit, plays a key role in the recovery process (Novoa et al., 2003). GADD34 requires activation of PERK for its upregulation, and its expression is probably controlled by ATF4 (Rutkowski and Kaufman, 2004). There is also evidence to suggest that PP1 activity may be negatively regulated by the redox state *in vivo*, such that under conditions of oxidative stress, PP1 activity is inhibited, increasing the levels of phosphorylated eIF2α (O'Loghlen et al., 2003).

1.8.6 eIF2α kinases in protozoan parasites

T. gondii switches from the rapidly dividing tachyzoite form to differentiate to quiescent bradyzoites under stress conditions (Weiss and Kim, 2000); it was

therefore hypothesised that phosphorylation of eIF2α could play a role in this process. An eIF2α kinase (TgIF2K-A) and orthologue of the initiation factor (TgIF2α) were identified (Sullivan et al., 2004). It was shown that TgIF2K-A phosphorylates the regulatory serine of yeast eIF2α *in vitro* and *in vivo*, and can modulate translation when expressed in the yeast model system (Sullivan et al., 2004). Finally, treating tachyzoites with heat shock, or alkaline stress, conditions which are known to induce differentiation to bradyzoites, resulted in increased phosphorylation of TgeIF2α (Sullivan et al., 2004). A family of three potential eIF2α kinases has also been identified in Trypanosoma brucei (Moraes et al., 2007). TbeIF2K2 was found to be active *in vitro* and able to phosphorylate the unusual eIF2α found in *T. brucei*. TbeIF2K2 is a transmembrane glycoprotein that localises mostly to the flagellar pocket, suggesting a role in sensing protein or nutrient transport which is likely to be critical to an organism that relies on post-transcriptional control of gene expression to respond to different environmental conditions. An eIF2α kinase (PfPK4) was previously identified in *P. falciparum,* initial characterisation showed PfPK4 possesses kinase activity and is expressed throughout the asexual cycle (Mohrle et al., 1997).

1.9 Rationale for investigation of eIF2α kinases in *P. falciparum* and aims of this project

As has been described above, the molecular mechanisms of a stress response in *P. falciparum*, and in particular those regulating the switch from asexual multiplication to differentiation into gametocytes are not understood (Dyer and Day, 2000). Notably, the related apicomplexan parasite *T. gondii* has been shown to phosphosphorylate TgeIF2α in response to various stress stimuli, concomitant with differentiation to bradyzoites (Sullivan et al., 2004, Narasimhan et al., 2008). In contrast, the microsporidium *E. cuniculi*, does not encode any eIF2α kinases (or other stress-response kinases), which may be an adaptation to its parasitic lifestyle (Miranda-Saavedra et al., 2007). It is therefore of interest to investigate the extent to which malaria parasites may rely on eIF2α phosphorylation for stress-response and/or life cycle progression.

The analysis of the *P. falciparum* kinome published by this laboratory (Ward et al., 2004), in conjunction with experimental approaches (Dorin et al., 2005, Dorin et al., 1999), shows that the parasite does not possess SAPK homologues. Additionally MEK1/2 and ERK/ERK2 orthologues, which mediate mating type differentiation in yeast are not present in the *P. falciparum* kinome (Barr et al., 1996). In contrast, the *P. falciparum* kinome contains three kinases that cluster with eIF2α kinases on phylogenetic trees (Ward et al., 2004). This is consistent with the evidence supporting a significant role for post-transcriptional regulation of stress response in *Plasmodium*, compared to yeast or mammalian cells (Coulson et al., 2004, Wirth, 2002, Bozdech et al., 2003).

The aims of this project are as follows:

- To express the three eIF2α kinase-related enzymes and the *P. falciparum* eIF2α orthologue in bacteria, and determine if the latter is a substrate for the protein kinases.

- To determine the function of the PfeIF2α kinase-related enzymes in parasite development.

2 Materials and Methods

2.1 Biological and chemical reagents

Details of biological and chemical reagents and their suppliers, including oligonucleotide primers and antibodies, are provided in the appendix (6.1), followed by details the composition of buffers, solutions and media (6.2).

2.2 Bioinformatics

2.2.1 PfeIF2α

BLASTP searches of the *Plasmodium* genome database PlasmoDB (Bahl et al., 2003) using metazoan eIF2α sequences were used to identify PF07_0117, which was then confirmed by reciprocal analysis. Alignment of these sequences was performed using ClustalW (Thompson et al., 1994). Microarray data for gene expression (Le Roch et al., 2003) were taken from PlasmoDB (Bahl et al., 2003).

2.2.2 P. falciparum *eIF2α kinases*

Catalytic domains of the putative PfeIF2α kinases, defined by the alignment of *P. falciparum* kinases (Ward et al., 2004) were used to identify their closest human and *P. berghei* orthologues by BLASTP analysis. These sequences were aligned either against a profile generated from our previous *P. falciparum* kinome analysis (for the alignment of sequences from all families of kinases) (Ward et al., 2004), or against the PKinase profile from Pfam (for the multi-species alignment of eIF2α kinase sequences) using the HMMER package (Finn et al., 2006). To analyse the relationships between sequences in the alignments, gaps and positions with a low quality of alignment were removed. For the analysis of sequences from all families of kinases alternate phylogenies generated with the neighbour joining method were visualised using NeighbourNet implemented on SplitsTree version 4 (Huson and Bryant, 2006). To analyse the relationships between diverse eIF2α kinases, the MEGA analysis

package (Kumar et al., 2004) was used to generate a neighbour joining tree. Microarray data for gene expression (Le Roch et al., 2003) were taken from PlasmoDB (Bahl et al., 2003). Information on additional domains to the protein kinase domains was also taken from PlasmoDB (Bahl et al., 2003).

2.3 Methods in molecular biology

2.3.1 Polymerase chain reaction (PCR)

Plasmodium genes were amplified from either cDNA or gDNA using the following PCR systems.

2.3.1.1 Takara

Reactions using the Takara Ex Taq polymerase contain 0.6 units Ex Taq, 1X Ex Taq buffer (2mM $MgCl_2$), dNTPs (200μM each), 10-100ng template, 1μM each oligonucleotide in a final volume of 25μl. PCR conditions were as follows:

Initial denaturation: 3 minutes, 94°C

30 - 32 cycles of:

Denaturation: 30 seconds, 94°C

Annealing: 30-45 seconds, 45-55°C

Elongation: 1minute per kb to be amplified, 60 or 68°C

Final elongation: 60 or 68°C, 10 minutes

For addition of adenine overhangs for pGEM-T cloning of PCR products obtained with a proof-reading polymerase (which does not add adenine overhangs), Ex Taq buffer, dNTPs and Ex Taq polymerase (concentrations as above) were added to a purified PCR product, and incubated at 68°C for 10 minutes.

2.3.1.2 Phusion

Where a proof reading polymerase was required, the Phusion polymerase (Finnzymes) was used. Reactions contained 1X Phusion High Fidelity buffer, 200μM each dNTP, 0.5μM each oligonucleotide, 10-100ng template DNA, 0.5U Phusion polymerase in a final volume of 25μl. PCR conditions were as follows:

Initial denaturation: 3minutes, 98°C

30 cycles of:

Denaturation: 10 seconds 98°C

Annealing: 30 seconds, 50 - 55°C

Extension: 30 seconds per kb to be amplified, 68°C

Final extension: 10 minutes, 68°C

2.3.1.3 Expand High Fidelity PCR system

The Expand High Fidelity PCR kit (Roche) provided an alternative proof-reading system; it was set up in two master mixes. The first mix contained 200μM each, dNTPs, 300nM each oligonucleotide, 10 - 100ng gDNA template in 12.5μl. The second mix contained 1X reaction buffer, $MgCl_2$ 1.5 - 4mM, Expand High Fidelity enzyme mix, 1.3 units in 12.5μl. 12.5μl of each mix were then combined to produce a complete reaction mix in 25μl. The $MgCl_2$ concentration was increased where necessary to increase the yield, although at the expense of some fidelity. The enzyme mix contained a Taq DNA polymerase and a Tgo DNA polymerase with proofreading activity. PCR was carried out as follows:

Initial denaturation: 2 mins 94°C

Followed by 10 cycles of:

Denaturation: 30 seconds, 94°C

Annealing: 30 seconds, 55°C

Elongation: 1minute/kb to be amplified, 68°C

20 cycles of

Denaturation: 30 seconds, 94°C

Annealing: 30 seconds, 55°C

Elongation: 1 minute/kb to be amplified + additional 5 seconds for elongation at each subsequent cycle, 68°C

Final elongation: 10 minutes, 68°C

2.3.2 Reverse transcriptase PCR (RT-PCR)

cDNA was prepared immediately after isolation of parasite RNA (2.5.9), using the SuperScript First -Strand Synthesis System (Invitrogen) as follows. cDNA was prepared from total RNA and primed using random hexamers. RNA samples were treated with DNase I (Invitrogen), prior to RT-PCR by incubating 1μg RNA sample, 1μl 10X DNase I reaction buffer, 1μl DNase I, Diethylpyrocarbonate (DEPC)-treated H_2O to 10μl at room temperature (RT), 15 minutes. DNase I was inactivated by addition of 1μl 25mM EDTA, 65°C, 10 minutes. RNA/primer mixes contained up to 5μg total RNA, 50 ng random hexamers, 1mM dNTP and DEPC treated water to 10μl and were denatured at 65°C, 10 minutes. Reaction mixes contained 2μl 10X Reverse Transcriptase buffer, 4μl, 25mM $MgCl_2$, 0.1M DTT, 1μl RNaseOUT Recombinant Ribonuclease Inhibitor per reaction. Annealing was by addition of 9μl reaction mix to each RNA/primer mix, incubation 25°C, 2 minutes, followed by 1μl (50 units) of SuperScript II Reverse Transcriptase (except the no Reverse Transcriptase control) and incubation 25°C, 10 minutes. Reactions were incubated at 42°C, 50 minutes for cDNA synthesis and terminated

at 70°C, 15 minutes. To improve sensitivity of subsequent PCR reactions RNA was removed from the cDNA:RNA hybrid molecules by addition of 1μl RNase H to each reaction, 37°C, 20 minutes. cDNA was either stored at -20°C, or used immediately for PCR (2.3.1).

2.3.3 Gene cloning techniques

PCR products were either cloned directly into pGEM-T easy, using the adenine overhangs produced by the Taq (Takara) and High Fidelity (Roche) polymerases, or were digested using restriction sites in the oligonucleotide primers for direct insertion into vectors that had been digested to produce complementary sticky ends.

2.3.3.1 pGEM-T easy cloning of PCR products

PCR products carrying adenine overhangs at their 3' ends were cloned into the pGEM-T easy vector (Fig. 2-1) (Promega), following manufacturer's instructions.

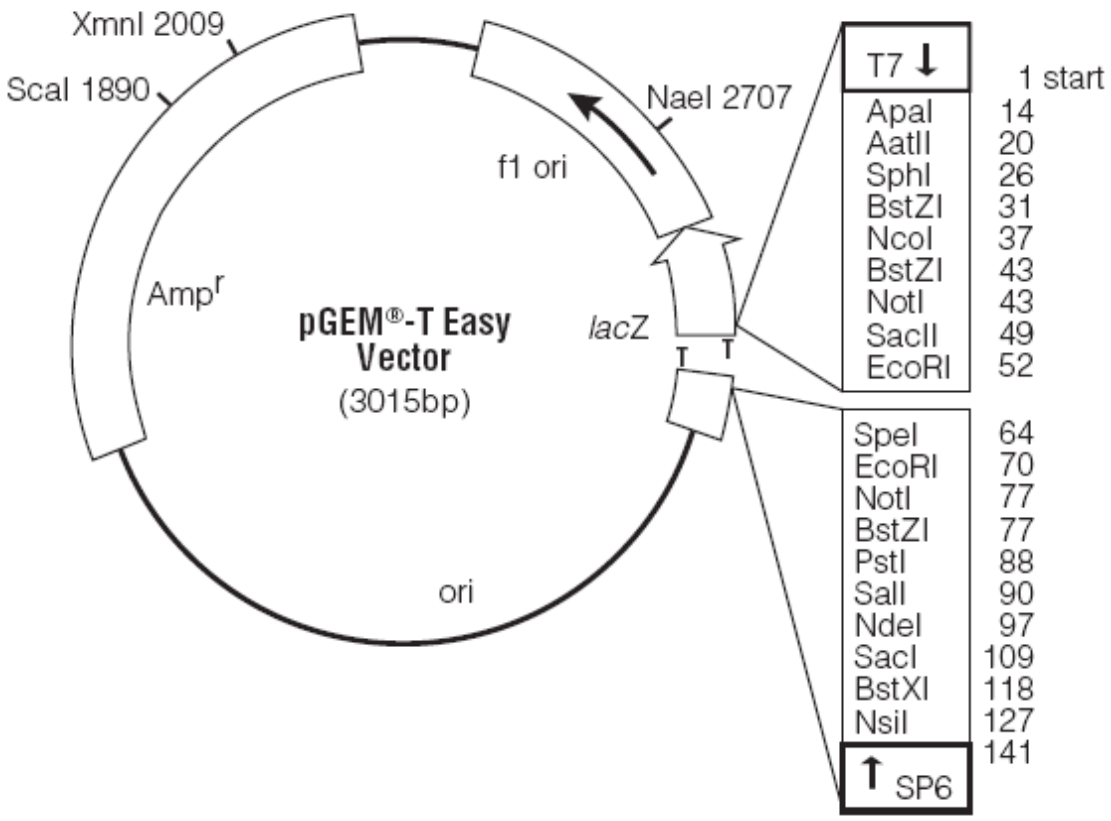

Figure 2-1: Map of the cloning vector, pGEM-T Easy.

2.3.3.2 Sub-cloning into destination vectors

Inserts of verified pGEM T-easy clones were subcloned into the appropriate destination vector. The inserts were removed from pGEM-T by digestion with the appropriate restriction endonucleases (2.3.7). The destination plasmid was linearised using either the same restriction enzymes, or with enzymes to generate complementary sticky ends. Both digests were separated by agarose gel electrophoresis, the fragments of interest excised from the gel and purified using the Qiagen Gel Extraction kit, according to manufacturer's instructions. DNA was eluted in 30μl EB buffer.

The insert and destination vector were ligated using T4 DNA ligase (Invitrogen). Molar ratios of vector to insert ranged from 3:1 - 1:3 and ligated either at RT for 1-3 hours, or overnight at 16°C. 5μl of the ligation reaction was transformed

into thermocompetant *E. coli* XL-10 gold and plated on LB plates containing the appropriate antibiotics. Single colonies were analysed by PCR screening followed by DNA miniprep (2.3.6) and restriction endonuclease digestion (2.3.7). Plasmids containing an insert of the correct size were verified by DNA sequencing.

2.3.4 **E. coli *transformation***

5μl of a ligation reaction or 1μg of plasmid miniprep were transformed into thermocompetant *E. coli* by incubating for 5 minutes on ice, 30-42 seconds at 42°C, followed by 2 minutes on ice. Cells were mixed with an equal volume of 2YT medium and plated into LB agar plates containing the appropriate antibiotic.

2.3.5 Preparation of competent cells

Thermocompetant *E. coli* were prepared using the modified Rubidium Chloride method. A single colony of the required strain was inoculated into 5ml LB medium and grown overnight at 37°C, shaking (200rpm). Overnight cultures were diluted 1:100 and grown at 37°C, shaking, to OD_{600} 0.4 - 0.6. Cells were pelleted by centrifugation at 4500 g, 4°C, 5 minutes, resuspended in 0.4 original culture volume of ice cold TFB1 and incubated on ice for 5 minutes. Cells were centrifuged as before, gently resuspended in 0.04X the original culture volume of ice cold TFB2 and incubated on ice for 15 - 60 minutes. Aliquots of 100μl were prepared, frozen on dry ice and stored at -80°C.

2.3.6 Isolation of plasmid DNA from **E. coli**

Plasmid DNA was isolated from *E. coli* in two different ways, depending on the amount of DNA required.

For small scale isolations the Qiaprep Spin Miniprep kit (Qiagen) was used. A single colony was inoculated into 5ml LB medium containing the appropriate antibiotic and grown overnight, 37°C, shaking (200 rpm). Cells were pelleted by

centrifugation at 2300g, 5 minutes and plasmid DNA extracted according to manufacturers instructions. DNA was eluted in 30μl EB and stored for further analysis.

Relatively large amounts of plasmid DNA were required for transfection of *P. falciparum*; In this case the PlasmidMaxi kit (Qiagen) was used. A 5ml culture was grown for 8 hours by inoculation of a single colony to LB medium containing the appropriate antibiotic. This culture was diluted 1:100 to 250ml LB medium, plus antibiotic and grown overnight at 37°C, shaking (200 rpm). Cells were collected by centrifugation at 3800g, 4°C for 20 minutes and DNA isolated according to manufacturers' instructions. DNA was eluted in 150μl H_2O under sterile conditions and concentration assessed by spectrophotometric analysis (2.3.8).

2.3.7 Restriction endonuclease digestion

Plasmid DNA was routinely analysed by digestion with restriction endonucleases. Typically, reactions contained 2μl plasmid DNA, 8 units of restriction enzyme and 2μl of the appropriate 10X buffer in a total volume of 20μl, and were incubated at 37°C for > 1 hour. 10μl of the reaction was mixed with DNA loading buffer and separated by agarose gel electrophoresis.

2.3.8 Determining DNA and RNA concentration

The concentration of nucleic acid solutions was assessed by measuring the A_{260} in a spectrophotometer. An absorbance of 1 corresponded to 50μg/ml of DNA, or 40 μg/ml of RNA. The ratio of A_{260}/A_{280} was used to assess the purity of the samples; for DNA the further the value from 1.8, the greater the level of impurities, likewise for RNA where a pure sample has a ratio of 2.0.

2.3.9 DNA Sequencing

DNA was sequenced by The Sequencing Service, University of Dundee (www.dnaseq.co.uk), using Applied Biosystems Big-Dye version 3.1 chemistry on

an Applied Biosystems model 3730 automated capillary DNA sequencer. Sequencing reactions required 200 - 300ng plasmid DNA and 3.2 pmoles sequencing primer per reaction.

2.3.10 Agarose gel electrophoresis

DNA was analysed on 0.8 - 1% agarose gels, prepared in 1X TAE at 110V for > 30 minutes. DNA was visualized by exposure to UV light following incorporation of Ethidium bromide into the gel. When bands were to be excised for purification and cloning, SybrSafe was used instead of Ethidium bromide.

2.3.11 Southern Blotting

2μg *P. falciparum* gDNA were digested overnight with the appropriate restriction endonucleases. Digested DNA was separated on 0.8% agarose gels, 80V 15 minutes followed by 23 - 30V, 16 - 24 hours. Gels were incubated in depurination solution for 10 minutes, rocking, room temperature (RT) and washed briefly in dH_2O. Next, gels were incubated in denaturation solution for 25 minutes, rocking, RT, and washed as before. Finally gels were incubated in neutralization solution for 30 minutes, rocking, RT and washed. DNA was transferred to N^+ Hybond membrane by capillarity, in 10X SSC overnight. The blot was constructed by layering three pieces of filter paper (whose ends are immersed in 10X SSC), the gel, Hybond N+ membrane (cut to fit the gel), three further pieces of filter paper, a thick pad of absorbent paper towels, and finally a weight. The filter paper and membrane were previously soaked in 10X SSC. After transfer membranes were washed in 2X SSC for 5 minutes, RT and air dried on Whatman paper. DNA was crosslinked to the membrane using UV light.

To analyse the Southern blot the Gene Images AlkPhos Direct Labelling and Detection System were used (GE Healthcare). The probe was labelled with a thermostable alkaline phosphatase enzyme according to manufacturers' instructions as follows. 10μl DNA (gel purified PCR product at 5 - 10ng/μl) was denatured at 100°C for 5 minutes, cooled immediately on ice and collected by a brief spin. 10μl reaction buffer, 2μl labelling reagent, and 10μl of the

crosslinker working solution were added sequentially, mixing gently after each addition. The reaction was incubated at 37°C for 30 minutes; labelled probes were used immediately or stored at -20°C with 50% glycerol (v/v).

The membrane was blocked in pre-warmed hybridization solution at 55°C for > 2 hours, rotating. The probe (prepared as above) was added to the hybridization solution and hybridized overnight at 55°C - 60°C (as determined for the probe used), rotating. After hybridisation, the membrane was washed twice with primary wash at 55°C, >15 minutes each, and twice with secondary wash at RT, >5 minutes each. Detection was with the CDP-*Star* chemiluminescent detection reagent, which uses the probe bound alkaline phosphatase to catalyze the decomposition of a substrate in a light-producing reaction. Membranes were incubated with CDP-*Star* reagent RT for 5 minutes and exposed to autoradiography film ~1hour, RT.

2.4 Methods in Biochemistry

2.4.1 Sodium dodecyl sulphate polyacrylamide gel electrophesis (SDS-PAGE)

Proteins were separated by polyacrylamide gel electrophoresis (PAGE) as described by Laemmli (1970). Gels were prepared with between 6% and 15% acrylamide according to the molecular weight of the protein of interest (low percentage acrylamide for high molecular weight proteins and *vice versa*). Gels were composed of a mixture of dH2O, 30% acrylamide mix (Biorad), 1.5M Tris (pH 8.8), 10% SDS, 10% ammonium persulphate and were polymerized by addition of TEMED; proportions for the appropriate percentage gel are as described by Sambrook & Russell (Sambrook). Stacking gel consists of the same mixture, apart from the Tris, which is 1.0M (pH 6.8); proportions required for 5% gel are described by Sambrook & Russell (Sambrook).

Protein samples were prepared by addition of 4X Laemmli buffer and denatured at 100°C for 5 minutes. Samples were loaded and separated in TGS at 80V for 10 minutes, followed by 180-200V until the required separation was achieved

(approximately 45 minutes). Gels were then stained with Coomassie blue (2.4.2) or analysed by western blot.

2.4.2 Coomassie blue staining of polyacrylamide gels

Gels were removed from the casting plates and immersed in Coomassie stain for at least 15 minutes (rocking) at room temperature, after which the stain was replaced with destain solution for 2 or more hours, until the background staining was removed.

2.4.3 Western blotting

Proteins separated by SDS-PAGE were transferred to a nitrocellulose membrane using the Biorad Criterion wet transfer system. Gels were assembled in a stack composed of sponge, two layers of filter paper, the gel, the membrane, two further layers of filter paper and lastly a sponge. Before assembling, all components were immersed in the appropriate transfer buffer and care was taken to exclude air bubbles. Transfer was carried out on ice, at 30V overnight for high molecular weight proteins, or 100V for one hour for low molecular weight proteins. After transfer was complete, gels were stained with Coomassie (2.4.2) to assess transfer efficiency. Membranes were blocked in 5% (w/v) non-fat milk in PBS for at least 30 minutes, RT (or 4^{o}C overnight). Primary antibodies were diluted in 5% milk in PBS (according to Table 5-3, appendix) and incubated for at least 1 hour, RT (or 4^{o}C overnight). Membranes were then washed three times for at least 10 minutes with PBS containing 0.05% Tween20. Secondary antibodies conjugated to HRP, (specific for the animal in which the primary antibody was raised) were diluted in 5% milk (according to Table 6-4, appendix) and incubated with the membrane for at least 45 minutes, RT. Three further PBS/Tween20 washes were carried out (as before) before detection. Equal volumes of the two detection reagents (enhanced luminol reagent and oxidizing reagent) were mixed and added to the membrane. The reaction catalysed by the HRP produced light at 482nm, (by oxidative degradation of luminol) which was detected on autoradiography film (Kodak).

2.4.4 Determining protein concentration

The concentration of protein solutions (parasite extract or recombinant protein) was determined by the Bradford assay. The absorbance of a protein solution mixed with Bradford reagent (Biorad) was measured at 595 nm and the protein concentration determined by comparison to a reference curve of BSA of known concentration.

2.4.5 Generation of polyclonal antibodies

Specific peptides were selected in collaboration with Biogenes, to maximize immunogenicity whilst minimizing cross reactivity with other *P. falciparum* proteins. The peptides were synthesized and used to immunise rabbits according to their standard protocol. Resulting sera and immunopurified IgGs were tested on parasite extract and recombinant protein, (where available).

2.4.6 Expression of recombinant proteins

The appropriate *E. coli* strain was transformed with the expression vector for the protein in question. A single colony was used to inoculate a 10ml overnight culture in LB medium containing the appropriate antibiotic. For IPTG induction, the overnight culture was then diluted 1/100 into LB medium containing antibiotic and grown at 37°C, shaking (200 rpm) until OD_{600} 0.5 - 0.6 when the temperature was reduced to the temperature to be used for expression (15 - 30°C). Expression was induced by addition of IPTG to the appropriate concentration once the bacteria reached an OD_{600} of 0.6 - 0.8. Autoinduction has been reported to yield several fold more target protein than standard IPTG induction (Studier, 2005). Overnight cultures were diluted 1/100 into autoinduction medium (Table 6-8, appendix), containing antibiotic and grown at 15 or 30°C for 24 or 48 hours. After the appropriate induction time had elapsed, cells were collected by centrifugation at 3800g, 4°C for 30 minutes, the supernatant discarded and the pellets stored at -20°C until use.

2.4.7 Purification of tagged recombinant proteins

2.4.7.1 GST tag

Bacterial pellets were thawed on ice in lysis buffer 1 (Table 6-7, appendix) (1ml per 50ml bacterial culture) containing 1mg/ml lysozyme, and DNase (2 units per 50ml bacterial culture), and resuspended by pipetting and vortexing intermittently over a 30 minute period. Cells were disrupted by sonication at 20% amplitude (Bioblock Scientific, Vibracell 72405), 15 seconds on, 15 seconds off, on ice, until the viscosity was reduced. The disrupted bacteria were centrifuged at 11,000g, 4°C for 30 minutes, and the resulting supernatant used for purification of soluble proteins. Prior to use, glutathione-agarose beads were hydrated in lysis buffer 1 for at least 1 hour, and washed 4 times in the same buffer, by centrifugation at 60g, 1 minute. The cleared lysate was then incubated with the prepared beads (100μl of a 50% slurry, per 50 ml bacterial culture) and fresh PMSF to 1mM, 4°C, rotating, 1 ½ - 2 hours. Beads were recovered by centrifugation as before, and washed four times with cold lysis buffer 1, containing fresh PMSF (1ml buffer per 50ml bacterial culture), and once with elution buffer without glutathione (Tris 50mM, pH 8, NaCl 75mM). Bound proteins were then eluted by rotation at 4°C, 20 minutes in elution buffer containing 15mM reduced glutathione (100μl per 50 ml culture)(Sigma), and the supernatant recovered by centrifugation as before. Protein concentration was measured (2.4.4) for immediate use in kinase assays

2.4.7.2 His tag

Purification of His tag proteins followed the method described for GST-tagged proteins, section 2.4.7.1, except i) lysis buffer 2 (Table 6-7, appendix) replaced lysis buffer 1, ii) nickel-agarose beads replaced glutathione-agarose beads, (80μl of 50% bead slurry per 50ml bacterial culture), iii) after binding of proteins to the beads two washes were performed with lysis buffer 2, containing 10mM imidazole, followed by two washes containing 40mM imidazole, iv) finally, beads were washed once in elution buffer (50mM Tris-HCl, pH 8, 400mM NaCl) before elution in elution buffer containing 400mM imidazole.

2.4.8 Immunoprecipitation

Parasites pellets prepared by saponin lysis (2.5.7) were lysed in ice cold RIPA buffer (Table 6-7, appendix) (150μl buffer per ~ 100μl parasite pellet), by sonicating for 3 seconds at 20% amplitude (Bioblock Scientific, Vibracell 72405). Lysates were cleared by centrifugation at 11,000g, 4°C for 30 minutes. Protein concentration of the resulting supernatant was measured with the Bradford assay (2.4.4) and adjusted to 1mg/ml. Parasite proteins were bound to the specific antibody by incubation with 1.5μg antibody per 100μg parasite protein, on ice for 2 hours. During this time protein A -Sepharose beads (GE Healthcare) were washed four times in RIPA buffer. The target protein-antibody complexes were then bound to the washed beads (10μl 50% bead slurry, per 100μg parasite protein) by rotation at 4°C for 1 ½ hours. Beads were washed three times in ice cold RIPA buffer by centrifuging at 1000g for 15 seconds at 4°C, and then once with RIPA buffer containing 0.1% SDS. At this stage, for western blot analysis the beads were resuspended in Laemmli buffer, or, for kinase assay, beads were washed once more in kinase buffer (Table 6-7, appendix), before resuspension in 20μl kinase buffer for assay in the standard reaction mix (2.4.9).

2.4.9 Kinase assay

Kinase reactions (30μl) were carried out in a standard kinase buffer (Table 6-7, appendix) using <1μg recombinant kinase, or the immunoprecipitate from 100μg parasite proteins, and <10μg recombinant or artificial substrate (α-casein, β-casein, myelin basic protein (MBP) or histone H1). Reactions were allowed to proceed for 30 minutes at 30°C and were stopped by addition of reducing Laemmli buffer, 3 minutes at 100°C. Phosphorylation of kinase substrates was assessed by autoradiography of dried SDS-PAGE gels.

2.5 *P. falciparum* culture

2.5.1 Asexual stage culture

P falciparum clone 3D7 was cultured as previously described (Trager and Jensen, 1976), (Lin et al., 1996). In brief, asexual cultures were maintained in complete RPMI 1640 at a haematocrit of 5%. Cultures were maintained at 37°C, under an atmosphere of 5% CO_2, 1% O_2, 96% N_2. The parasitaemia (percentage of infected erythrocytes) was kept between 0.5% and 10%; medium was changed every other day at low parasitaemias (<4%) (Kim et al., 2007), or every day at higher parasitaemias. Parasitaemia was determined by counting the infected erythrocytes in Giemsa stained blood smears. Smears were fixed in ethanol for > 30 seconds followed by staining with Giemsa diluted 1/10 in Giemsa buffer for 10 -20 minutes. Stained blood smears were analysed by light microscopy.

2.5.2 Synchronisation of parasite culture

Parasites were synchronized using sorbitol according to Lambros and Vanderberg (Lambros and Vanderberg, 1979). Cultures containing a high proportion of ring stage parasites were used for synchronization. The culture was centrifuged at 680g for 2 minutes, RT and the supernatant discarded. The pellet was resuspended in 10 pellet volumes of 5% sorbitol, incubated for 10 minutes at RT and centrifuged as before, and sorbitol discarded. The pellet was washed by resuspending in 10 pellet volumes of warm complete medium and centrifuging. Finally the pellet was resuspended in the appropriate volume of warm RPMI complete medium and cultured as described above (2.5.1). If necessary the process was repeated after 48 hours at the next ring stage of the cycle.

2.5.3 Preparation of gametocytes

Gametocyte cultures were set up at 0.5 - 0.7% parasitaemia in 6% haematocrit, in an initial volume of 15ml, to give 25ml final volume in 75cm^2 flasks. Cultures were maintained as normal for 4-5 days until 8-10% parasitaemia was reached and parasites appeared stressed, (judged by the presence of mis-shaped ring

stage parasites) after which the volume was increased to 25ml and medium changed daily until day 15 after set up, when mature gametocytes were present.

2.5.4 Mosquito infection

Feeding of gametocytes to mosquitoes was carried out by the Ranford-Cartwright lab, as described previously (Carter et al., 1993). Briefly, a mixture of day 14 and day 17 gametocytes was resuspended in fresh blood (and heat inactivated serum) to give a final packed cell volume of 40%. The mixture was fed to 5-7 day old mosquitoes that had not previously fed on blood, and had not been given glucose overnight to encourage a good blood meal to be taken. After the feed, the mosquitoes were maintained at 26^{o}C, and supplied with ample glucose/PABA solution (Table 6-10, appendix). Mosquitoes were dissected and midguts examined for oocysts 10 days post feeding, and salivary glands for sporozoites 16 days post feeding. The significance of infection prevalence variation between comparable clones, or between oocyst and sporozoite positive mosquitoes was assessed using Fisher's exact test.

2.5.5 Preparation of stabilates

Frozen parasite stabilates were prepared using 3-5ml cultures containing >2% ring stage parasites. Erythrocytes were pelleted by centrifugation at 850g, RT, 5 minutes and supernatant discarded. The pellet was resuspended in an equal volume of deep-freeze solution, transferred to a cryovial (0.5ml maximum per tube) and stored in liquid nitrogen.

2.5.6 Thawing of stabilates

Stabilates were removed from liquid nitrogen and thawed at room temperature before transferring to a 15ml tube, measuring the volume of blood. 0.2 volumes of solution A (Table 6-9, appendix) were added dropwise, mixing constantly, then allowed to stand for 3 minutes. 10 volumes of solution B (Table 6-9, appendix) were added, dropwise and mixed well by pipetting. Cells were pelleted by centrifugation at 850g, RT for 5 minutes and the supernatant

discarded. Cells were resuspended by dropwise addition of the same volume of solution C (Table 6-9, appendix) as solution B, and mixed well. Cells were centrifuged as before, supernatant discarded and resuspended in 3ml warm (37°C) RPMI 1640 complete medium, adding fresh erythrocytes to obtain a haematocrit of 5%. Once cultures reached >2% parasitaemia they were diluted to 5ml, and the appropriate drug selection applied.

2.5.7 Isolation of parasites from infected erythrocytes

Parasite harvest was by saponin lysis (Umlas and Fallon, 1971); erythrocytes were pelleted by centrifugation at 1300g, RT for 2 minutes and washed once in one culture volume of cold PBS, centrifugation 1300g, 4°C for 2 minutes. Cells were lysed on ice, by repeated pipetting in 1/3 culture volume cold saponin (0.15% (w/v) in PBS). After lysis PBS was added to a total of 2 culture volumes and parasites recovered by centrifugation 5500g, 5 minutes, 4°C. After two further PBS washes, discarding the final wash, pellets were stored at –80°C.

2.5.8 Extraction of parasite genomic DNA

After saponin lysis the parasite pellets were resuspended in approximately 5 pellet volume proteinase K (150μg/ml)/SDS (2%) and incubated at 55°C for 2 - 12 hours. DNA was extracted by addition of an equal volume of Phenol: Chloroform: Isoamyl alcohol (25:24:1) saturated with 10mM Tris, pH 8, 1mM EDTA (Sigma). Tubes were inverted repeatedly to mix gently and centrifuged at 16,000g, RT for 5 minutes. The top aqueous layer was transferred to a new tube leaving protein at interface; an equal volume of Phenol: Chloroform: Isoamyl alcohol was added, inverted to mix and centrifuged as before. Phenol extraction was repeated twice more. After the final aqueous layer was removed to a new tube 0.1 volume of 3M sodium acetate (pH 5.2) was added and DNA precipitated in 2 - 4 volumes of ethanol, -20°C, >30 minutes. DNA was obtained by centrifugation at 16000g for 15 minutes, and discarding the supernatant. Pellets were dried briefly and resuspended in dH_2O.

2.5.9 Extraction of parasite RNA

After saponin lysis parasite pellets were resuspended in 10 pellet volumes Trizol and stored at -80°C until use. The Trizol/parasite suspension was thawed on ice, 2 pellet volumes of RNase free Phenol:Chloroform: Isoamylalcohol (25:24:1) were added, shaken for 15 seconds and incubated, RT for 3minutes. The mixture was centrifuged 9000g, 4°C, 30 minutes and the aqueous layer removed to a fresh tube. Isopropanol was added at a ratio of 6:5 (supernatant: isopropanol) and incubated on ice for > 2 hours. RNA was pelleted by centrifugation at 12000g, 4°C for 30 minutes and the supernatant discarded. Pellets were washed by adding 500μl cold 75% ethanol (in DEPC treated water) and centrifuging 12000g, 4°C for 5 minutes before drying with tubes inverted for 5 minutes. RNA was resuspended in 20μl dH_20 and incubated at 60°C, 10 minutes and placed on ice. Concentration was assessed by measuring the absorbance, as described (2.3.8).

2.5.10 Protein preparation from parasites

Where a total protein mixture was required parasite pellets were lysed directly by addition of Laemmli buffer and boiled, 100°C for 5 minutes. In some instances, for western blot analysis, parasite pellets were resuspended in parasite solubilisation buffer (Table 6-7, appendix), before adding Laemmli buffer, and proceeding as before. To prepare parasite protein extracts for immunoprecipitation, parasite pellets were resuspended in ice cold RIPA buffer (Table 6-7, appendix, 200μl per 25ml parasite culture at 6-10% parasitaemia) and sonicated at 20% amplitude (Bioblock Scientific, Vibracell 72405), for 3 seconds. The resulting lysate was cleared by centrifugation at 11,000g, 4°C for 30 minutes, and protein content quantified as described (2.4.4).

2.5.11 Transfection

The method of transfecting erythrocytes infected with ring stage parasites, at a parasitemia of 4 - 6% was used (Crabb and Cowman, 1996). For each transfection, a 3ml culture was pelleted by centrifugation at 1000g, RT for 4

minutes, and washed by resuspending in 3ml cytomix buffer (Table 6-9, appendix) and centrifuged as before. 100μg of plasmid DNA was suspended in 100μl cytomix buffer and used to resuspend the washed parasite pellet, further cytomix buffer was added to a total volume of 400μl. This mixture was electroporated in a cold 2mm cuvette, 310V, 950μF (time constant ~10ms for good transfection efficiency). The mixture was transferred to a culture flask by mixing with 2ml RPMI 1640 complete medium; a further 3ml fresh uninfected erythrocytes, RPMI mix (4% haematocrit) was added. Medium was changed 3-4 hours after transfection, and the following day with complete medium. From the second day post transfection media containing the selection drug (Blasticidin 2.5μg/ml) was used. 0.1ml fresh erythrocytes were added once per week, until parasites were detectable on Giemsa stained slides, usually ~21 days post transfection, after which cultures were maintained as normal for asexual parasites (2.5.1).

2.5.12 Cloning of parasites by limiting dilution

Parasites were cloned as previously described (Kirkman et al., 1996). Briefly, the erythrocyte number of a culture containing 3% parasitized erythrocytes was determined and diluted in RPMI 1640 complete medium so that 10ml contained 10^6 cells. Three tubes of 15ml medium were prepared at 1% haematocrit, to these, 6.25, 12.5 and 25μl of the 10ml containing 10^6 cells were added. Each mixture was transferred to one third of a 96 well plate, 200μl per well, to give 36 wells with a probability of 0.25, 0.5 or 1 parasite per well, respectively. After 5-6 days the medium was changed. After another 5-6 days the medium was changed using medium containing 1% erythrocytes and the selection drug. Around day 15 the plates were monitored by both the lactate dehyrogenase assay (2.5.12.1), and careful blood smears to ascertain which wells contained parasites. Positive wells were transferred to 12 well plates, (2ml culture, 5% haematocrit) and monitored by blood smear until appropriate to transfer to 5ml cultures and cultured for further analysis.

2.5.12.1 *Plasmodium* lactate dehydrogenase assay

Plasmodium LDH (pLDH) can be distinguished from human LDH by its ability to use the 3-acetyl pyridine analog of NAD (APAD+) in the conversion of lactate to pyruvate. pLDH activity can be measured in lysed blood samples of 0.2-10% parasitemia. A mix was prepared of 100μl Malstat reagent, 10μl Diaphorase (1mg/ml) and 10μl NBT per well, to which 20μl culture suspension was added. Plates were incubated at RT for 20 minutes and monitored by eye for colour change; wells containing parasites change to purple (Makler and Hinrichs, 1993, Makler et al., 1993).

2.5.13 Parasite growth rate analysis, by flow cytometry

Parasite growth rate analysis was carried out in the Goldberg lab by flow cytometry (Liu et al., 2005), using a protocol adapted from Barkan Ginsburg et al. 2000 (Barkan et al., 2000). In brief, samples of asynchronous parasite cultures were acquired every 30 minutes for ~4days and fixed in 0.05% glutaraldehyde in PBS and stored at 4°C. The DNA content of the cells was measured by permeabilizing with 0.25% Triton X-100 in PBS for 5 minutes at room temperature followed by staining with 5μg/ml propidium iodide (Molecular Probes, Eugene, USA). The cells were then diluted 10-fold in PBS and analyzed using an Epics XL-MCL flow cytometer (Beckman). $1x10^5$ erythrocytes were counted in triplicate for each sample. Data were analyzed using FlowJo software (Treestar Inc., Ashland, USA).

3 Eukaryotic initiation factor 2α kinases in *P. falciparum*: bioinformatic and biochemical characterisation

3.1 Identification of *P. falciparum* eukaryotic initiation factor 2α

BLASTP searches of PlasmoDB using metazoan eIF2α sequences were used to identify PF07_0117 as the *P. falciparum* orthologue, which was confirmed by reciprocal analysis. The alignment of *P. falciparum* eIF2α with sequences from *T. gondii,* human and rice is shown in Figure 3-1. Overall, the *P. falciparum* sequence shares ~70%, ~ 50%, ~ 40% and ~28% identity with those of *T. gondii, Homo sapiens* and *Oryza sativa* (rice) and *E. cuniculi*, respectively. Importantly, the serine residue (Ser 51 in the human orthologue) that is targeted for phosphorylation by eIF2a kinases is conserved in all species. Furthermore, eIF2α contacts the kinase through a large number of residues that interact with the surface of the kinase domain. These residues are also conserved in most species, as are the residues that protect the regulatory serine from the activity of other kinases (Dar et al., 2005); interestingly, several of these are not conserved in the *E. cuniculi* orthologue, which is consistent with the absence of eIF2α kinases in this organism (Miranda-Saavedra et al., 2007).

```
Pf    MEGMILMSELSKRRFRSVNKLIRVGRHEVVLVLRVDSQKGYIDLSKRRVSPKDIIKCEEK   108
Tg    MEGMILMSELSKRRFRSVNKLIRVGRHEVVMVLRVDPKKGYIDLSKRRVSPEDIVKCEEK   120
Mm    IEGMILLSELSRRRIRSINKLIRIGRNECVVVIRVDKEKGYIDLSKRRVSPEEAIKCEDK   100
Hs    IEGMILLSELSRRRIRSINKLIRIGRNECVVVIRVDKEKGYIDLSKRRVSPEEAIKCEDK   100
Os    IEGMILYSELSRRRIRSIPSLIKVGRQEPAVVLRVDHDKGYIDLSKRRVSHHDRRTCEDR   102
Ec    LEGLVLLGELSKRRVRSIQQVTKVGNIEICNVLKVDEGRGYIDLSMSKVTENEKSECRET   101
      :**::*  ***:** **:  : ::*  *   *::**  :****** :*:  :   * :
```

Figure 3-1: Alignment of eIF2α sequences.
Sequences surrounding the conserved regulatory serine are shown (*P. falciparum* numbering: M49 - K108). The black highlighted residue marks the serine that when phosphorylated exerts the regulatory effect on translation. Blue highlights indicate residues involved in contacting the kinase domain; pink highlights indicate conserved residues that protect the phosphorylation site from the activity of other kinases. Asterisks (*****) indicate the residue is identical in all sequences, colons (**:**) indicate conservation of residue properties. Pf; *P. falciparum*, Tg; *T. gondii*; Mm; *Mus musculus*, Hs; *Homo sapiens*, Os; *Oryza sativa*, Ec; Encephalitozoon cuniculi.

3.2 Identification of eIF2α kinases in *P. falciparum*

3.2.1 In silico *analysis*

The phylogenetic analysis of the full complement of *P. falciparum* kinases published by this laboratory in 2004 (Ward et al., 2004) identified a distinct cluster of three sequences, PF14_0423, PFA0380w and PFF1370w, the latter of which (called PfPK4) had previously been characterised as encoding an eIF2α kinase (Mohrle et al., 1997). Reciprocal BLASTP analysis using the putative catalytic domains as queries confirms the relatedness of these three genes with the eIF2α kinase family (not shown). In order to identify kinase families in phylogenetic clusters, the Ward *et al*. analysis contained a number of human kinase sequences in addition to the *P. falciparum* sequences; however, these did not include any human eIF2α kinases. With help from Jon Wilkes, the bioinformatician at the Wellcome Centre for Molecular Parasitology, I therefore sought to extend this analysis by using a Hidden Markov Model to align the three putative PfeIF2α kinases with the four human eIF2α kinases; sequences from other kinase families were included as outgroups. The resulting alignment was used to generate a phylogenetic tree (Fig. 3-2), which clearly shows that the three *P. falciparum* genes do indeed cluster with sequences of the eIF2α kinase family, as opposed to other families.

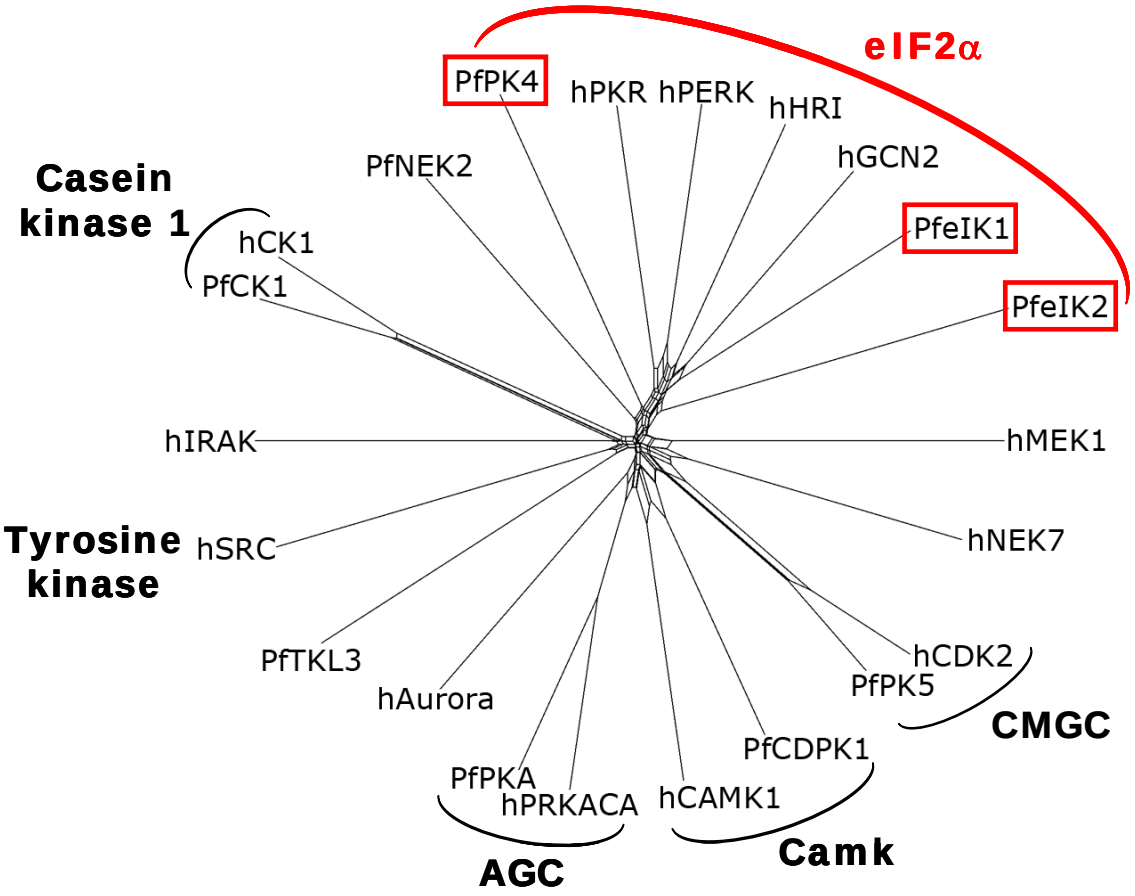

Figure 3-2: Phylogenetic tree showing the clustering of eIF2α kinases.
Sequences were selected from across the kinase superfamily to investigate whether the proposed *P. falciparum* eIF2α kinases cluster with other members of the eIF2α kinase family. Sequences were aligned using the HMMER package against a profile generated from our previous kinome analysis (Ward et al., 2004). After removal of gaps and positions with a low qualify of alignment, alternate phylogenies generated with the neighbour joining method were visualised using NeighbourNet implemented on SplitsTree version 4 (Huson and Bryant, 2006). The three *P. falciparum* sequences are boxed in red, brackets indicate kinase families.

To more closely investigate the relationship between the three PfeIF2α kinases and other members of the family, I selected sequences of eIF2α kinase catalytic domains from diverse species, and aligned them against the Pfam protein kinase domain (Pfam entry PF00069) using the HMMER package; human aurora kinase and CDK2 were included as outgroups (Fig. 3-3). The crystal structures of PKR in complex with eIF2α and of GCN2 have been solved, revealing that helix α-G is longer, and in an abnormal position in eIF2α kinases, when compared to other kinases (Dar et al., 2005) (Padyana et al., 2005, Mathews, 2007). By comparison to the structure-based alignment produced by Dar et al. 2005, Figure 3-3 suggests that the PfeIF2α kinases, and indeed all other eIF2α kinases considered

here, share the non-canonical α-G helix that is critical for the binding of eIF2α, illustrated in Figure 3-4. The conserved Thr and Glu at the N-terminus of helix α-G (Fig. 3-3) were found to interact with each other to stabilise the structure of this helix (Dar et al., 2005). All eIF2α kinases are required to interact with eIF2α; conservation of the size and position of helix α-G in the eIF2α kinases is consistent with such an interaction as this helix is responsible for both positioning the phosphoacceptor Ser51 towards the catalytic cleft of the kinase, and allowing the interaction to proceed without distortion of other regions of either the kinase or eIF2α (Dar et al., 2005).

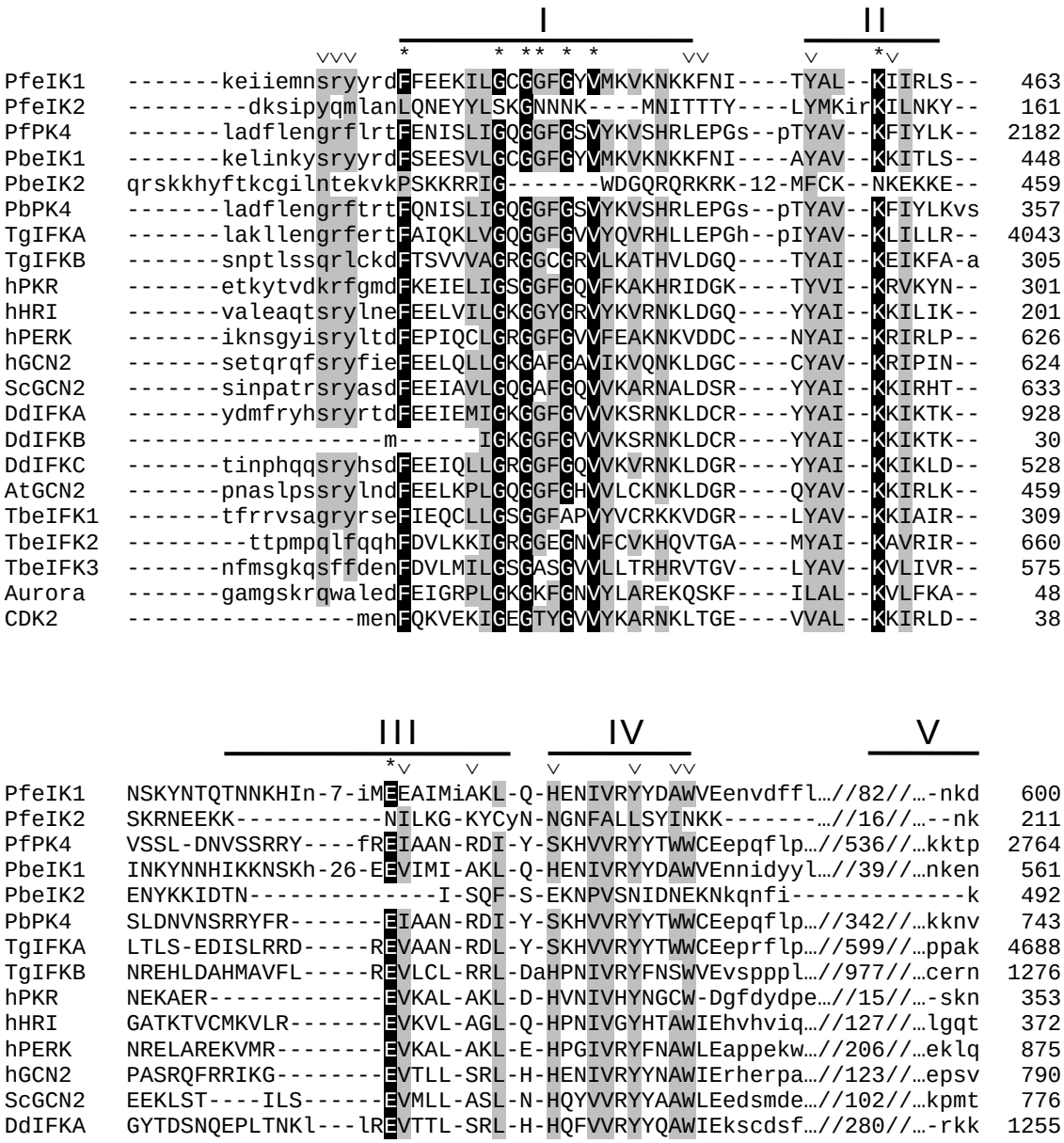

```
DdIFKB   GYTDSNQEPLTNKl---lREVTTL-SRL-H-HQFVVRYYQAWIEkscdsf…//277//…srkk   355
DdIFKC   SNQSLNRRILR--------EVITL-SRL-H-HQHVVRYYQAWIEsaesls…//194//…knik   765
AtGCN2   DKEIPVNSRIVR-------EVATL-SRL-Q-HQHVVRYYQAWFEtgvvdpa…//26//…-eqd   529
TbeIFK1  KNEAEK---ALR-------EVQSL-AAL-S-HKHIVRYYDAWIEpgcddel…//82//…mhsh   433
TbeIFK2  EEDKQRCVR---------EAILH-SSL-D-NPNVVRYFYSWIEniarsia…//29//…vssa   731
TbeIFK3  DKFAETAVMQ--------EVRLH-AVL-H-NEHIVRYYTCWSEmitpar…//103//…erss   720
Aurora   QLEKAGVEHQLRR------EVEIQ-SHL-R-HPNILRLYGYFHD------------------    83
CDK2     TETEGVPSTAIR-------EISLL-KEL-N-HPNIVKLLDVIHT------------------    72
```

hinge

V

```
PfeIK1   pnvnDKYLY-ILMEYCPGK-----TLREAID----------------------CGFIcR--N   633
PfeIK2   etkyKFNLY-IRMEYCKS------TLENYIN--------------------TRENM-----N   241
PfPK4    vpefSIVLL-LQMELCKGY-----TLRKWLDr--------stRsdkplhfTYSDKKM-----N  2808
PbeIK1   ikinEKYLY-ILMEYCPGK-----TLREAID----------------------CGFIyK--N   593
PbeIK2   nkkyKFNLY-IRMEYCKD------TIENYIN--------------------RRTRI-----N   522
PbPK4    gpefSIVLL-LQMEFCKGF-----TLRRWLD-----------R------sSRSDKPLY-F--T   780
TgIFKA   etlyPVVLL-IQMEMCNGV-----TLREWLDrkdrstvamgfV------pSSKNRWH-----S  4734
TgIFKB   qckvAVSLY-IQMEYCGM------SLDEYIA--------------------QTPEV-----D  1306
hPKR     ssrsKTKCLfIQMEFCDKG-----TLEQWIE------------------KRRGEKL-----D   387
hHRI     eaqyHLMLH-IQMQLCEL------SLWDWIVern-----krgRe----yvDESACPY--V--M   415
hPERK    psspKVYLY-IQMQLCRKE-----NLKDWMN--------------------GRCTI-----E   906
hGCN2    tteaVHYLY-IQMEYCEKS-----TLRDTID--------------------QGLYR-----D   821
ScGCN2   avkkKSTLF-IQMEYCENR-----TLYDLIH--------------------SENLNQ-----Q   808
DdIFKA   ppkeTHTLY-IQMEYCSKK-----TLKTLID--------------------NVGGI-----A  1286
DdIFKB   ppkeTHTLY-IQMEYCSKK-----TLKTLID--------------------NVGGI-----A   386
DdIFKC   kstsIPYLY-IQMEYCQK------ILR---------------N------lTETGMNL-----E   795
AtGCN2   nnleSTYLY-IQMEYCPRTLrQVFESY---------------------------NHF-----D   559
TbeIFK1  keeeFSTLY-IQMELCSKH-----SLRHLID-----------Q------cDKEEGSLLtAgnG   473
TbeIFK2  tgapLNVLF-IQMEYFKSG-----TLADHFR--------------------NRNAF-----S   762
TbeIFK3  sileGRVVF-LQLEYYRT------TLAQRLG--------------------SRGSI-----D   750
Aurora   ----ATRVY-LILEYAPLG-----TVY----------------------RELQKLSkF--D   110
CDK2     ----ENKLY-LVFEFLHQDLkKFMDAS-----------------------ALTGI-----P   100
```

catalytic loop

VIA VIB VII

```
PfeIK1   EKL---I-------WELIKQILKGISYIHDMKIMHRDIKPSNIFLQiTDNIL------IAKIG   680
PfeIK2   INR---N-------YEIIQMIILGLYSIHNNNIMHRDLKPSNIFIS-DNNIV--------KIG   285
PfPK4    HPL---E-------FDLFKQLIKGLKDIHATCFIHRDLKPENIFVD-PDTYT-------LKIG  2853
PbeIK1   EKL---I-------WELIKQILKGIYYIHDMKMMHRDIKPSNIFLQiNDDIL------SAKIG   640
PbeIK2   IKR---N-------IEIINMIIMGLNYIHNNNIMHRDLKPSNIFIS-NNDIV--------KIG   566
PbPK4    YGD---KntnhpleFDLFKQLIKGLKDIHSTCFIHRDLKPENIFVD-LDTYI-------LKIG   832
TgIFKA   MEL-----------ELFKQLMKGIRDIHERGIVHRDLKPENIFVD-PDTLV-------LKIV  4777
TgIFKB   PER---N-------EEIVAMIISGLYQCHSAGVMHRDLKPSNIFIDkETGVV--------KIG  1351
hPKR     KVL---A-------LELFEQITKGVDYIHSKKLIHRDLKPSNIFLV-DTKQV--------KIG   431
hHRI     ANV---A-------TKIFQELVEGVFYIHNMGIVHRDLKPRNIFLHgPDQQV--------KIG   460
hPERK    ERErsvC-------LHIFLQIAEAVEFLHSKGLMHRDLKPSNIFFT-MDDVV--------KVG   953
hGCN2    TVR---L-------WRLFREILDGLAYIHEKGMIHRDLKPVNIFLD-SDDHV--------KIG   865
ScGCN2   RDE---Y-------WRLFRQILEALSYIHSQGIIHRDLKPMNIFID-ESRNV--------KIG   852
DdIFKA   EEE---A-------FRLLRQIVEGLNHIHSQQIIHRDLKPANIFID-NEQNV--------KIG  1330
DdIFKB   EEE---A-------FRLLRQIVEGLNHIHSQQIIHRDLKPANIFID-NEQNV--------KIG   430
DdIFKC   DDD---I-------WKLFRQIVEGMAYVHGQGIIHRDLKPSNIFFD-SCGDI--------KIG   839
AtGCN2   KDF---A-------WHLIRQIVEGLAHIHGQGIIHRDFTPNNIFFD-ARNDI--------KIG   603
TbeIFK1  DKV---A-------TKIFRQLLTVVSHFHRQGIVHRDLKPDNILFE-MQSSVSSddvgTIRVA   525
TbeIFK2  RLE---N-------VEHLLQIVRGLRYIHQQDVIHRDLKPTNIFVS-DAGIM--------KIG   806
TbeIFK3  RFE---N-------IIIALQLFAAVRYVHRSGFLHRDVKPPNIFID--YRQV--------RLG   904
Aurora   EQR---T-------ATYITELANALSYCHSKRVIHRDIKPENLLLG-SAGEL--------KIA   154
CDK2     LPL---I-------KSYLFQLLQGLAFCHSHRVLHRDLKPQNLLIN-TEGAI--------KLA   144
```

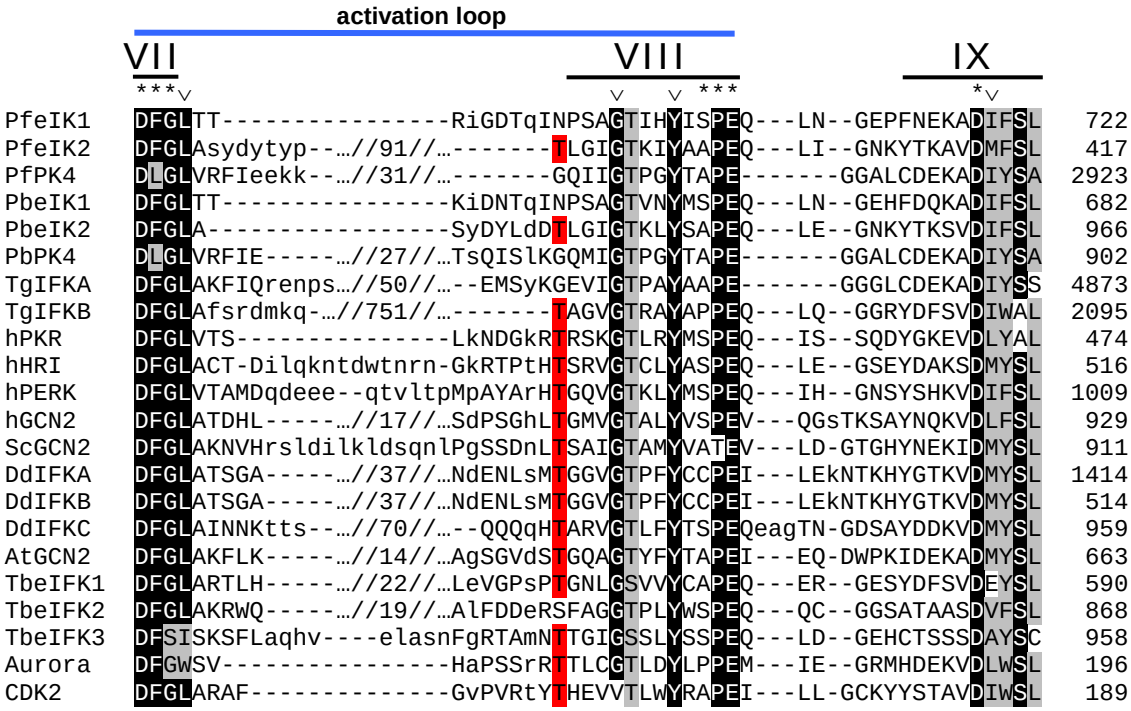
activation loop
VII
VIII
IX
PfeIK1 722
PfeIK2 417
PfPK4 2923
PbeIK1 682
PbeIK2 966
PbPK4 902
TgIFKA 4873
TgIFKB 2095
hPKR 474
hHRI 516
hPERK 1009
hGCN2 929
ScGCN2 911
DdIFKA 1414
DdIFKB 514
DdIFKC 959
AtGCN2 663
TbeIFK1 590
TbeIFK2 868
TbeIFK3 958
Aurora 196
CDK2 189

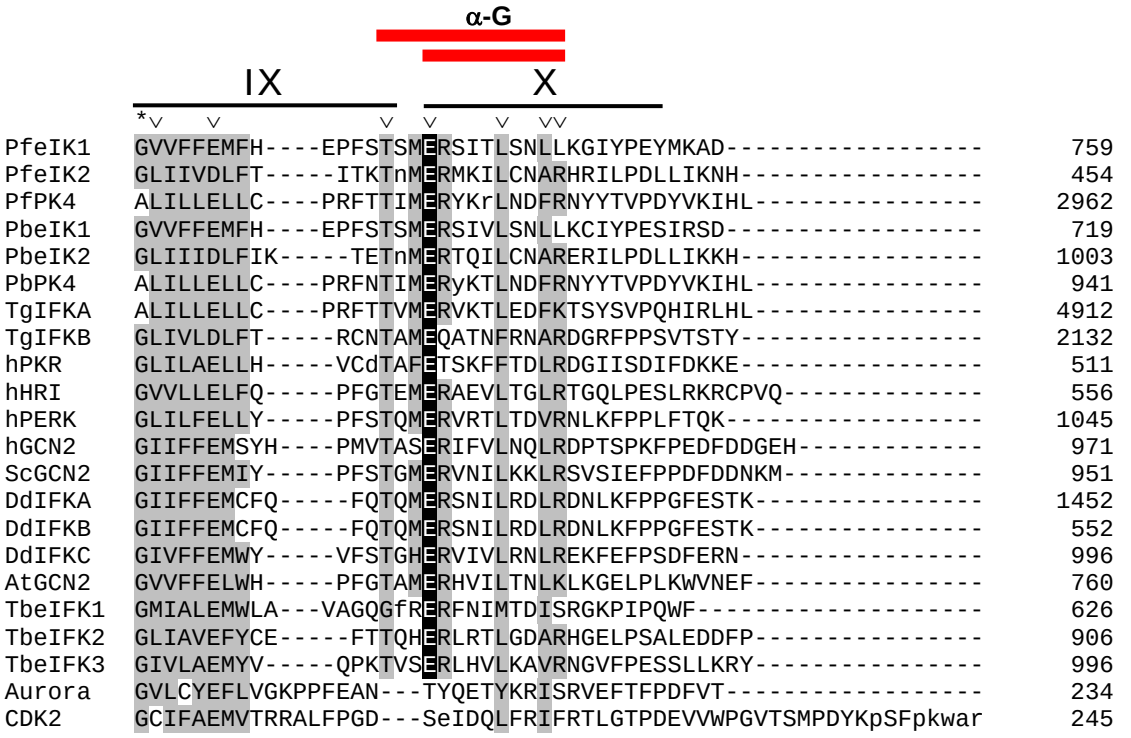
α-G
IX
X
PfeIK1 759
PfeIK2 454
PfPK4 2962
PbeIK1 719
PbeIK2 1003
PbPK4 941
TgIFKA 4912
TgIFKB 2132
hPKR 511
hHRI 556
hPERK 1045
hGCN2 971
ScGCN2 951
DdIFKA 1452
DdIFKB 552
DdIFKC 996
AtGCN2 760
TbeIFK1 626
TbeIFK2 906
TbeIFK3 996
Aurora 234
CDK2 245


XI
PfeIK1 809
PfeIK2 488
PfPK4 3009
PbeIK1 769
PbeIK2 1044
PbPK4 989
TgIFKA 4960

```
TgIFKB    ----------PWVVPFC-RWCLQNDPSKRPTIRQLYQH---ycstgsvfgpktatsrcsas  2179
hPKR      --------------KTLL-QKLLSKKPEDRPNTSEILRT--Ltvwkkspeknerhtc-----   551
hHRI      --------------AKYI-QHLTRRNSSQRPSAIQLLQSELFqnsgnvnltlqmkiieqeke   603
hPERK     ----------YPCEYVMvQDMLSPSPMERP---EAINI--Ienavfedldfpgktvlrqrs  1091
hGCN2     ----------AKQKSVI-SWLLNHDPAKRPTATELLKSELLpppqmeeselhevlhhtltn  1021
ScGCN2    ----------KVEKKII-RLLIDHDPNKRPGARTLLNSGWLpvkhqdevikealkslsnps  1001
DdIFKA    ----------PDQTQII-RSLLSRDPTQRPSTKQLLESGLLpskmeddilkeaiktianpt  1502
DdIFKB    ----------PDQTQII-RSLLSRDPTQRPSTKQLLESGLLpskmeddilkeaiktianpt   602
DdIFKC    ----------HSRQATLI-RMLIDKDPAKRPSAQQLLQSELMppkmedeyiknsirvitnpt  1047
AtGCN2    ----------PEQASLL-RRLMSPSPSDRPSATELLKHAFPprmeselldnilrimqtsed   751
TbeIFK1   -------YAWNPRMAEVI-ASLLERDPGKRRTSEEILNK---adlpgdpadvvealetikrh   677
TbeIFK2   ----------EEAEVF--RQMLGEQPDGRPSVDEVVQK--Lkhivveirsggngsaklgdn   953
TbeIFK3   ----------PELC-VV-QYLTLKDPSHRMSLMDASRA--Lrrtvyrillsffsev-----  1038
Aurora    ----------EGARDLI-SRLLKHNPSQRPMLREVLEH---p------------------   262
CDK2      qdfSkVvPPLDEDGRSLL-SQMLHYDPNKRISAKAALAHPFFqdvtkpvphlrl--------   298
```

Figure 3-3: Sequence alignment of eIF2α kinases.
The sequences of catalytic domains of eIF2α kinases were aligned against the Pfam kinase domain (PF00069) using the HMMER package (J. Wilkes), Aurora kinase and CDK2 were included as outgroups. Residues identical in >90% of the sequences are highlighted in black, residues conserved in >75% of sequences are highlighted in grey, the threonine residue within the activation loop, phosphorylated for activation of PKR is highlighted in red. Positions and lengths of inserts within the kinase domain are indicated by breaks in the sequence marked //-//. Conserved kinase domains are indicated by horizontal black lines numbered with roman numerals. Regions of important function are marked with labeled blue lines. The probable position of helix a-G is indicated in horizontal red bars, the longer one represents eIF2α kinases, and the shorter one canonical Ser/Thr kinases (see text for details). Key residues conserved in all types of kinase are indicated with asterisks (*) while important residues in eIF2α kinases are marked with arrowheads (∨). The alignment was adjusted by hand in domain X, with reference to Dar et al 2005. Pf; *P. falciparum*, Pb; *P. berghei,* Tg; *T. gondii,* h; *Homo sapiens,* Sc; *Saccharomyces cerevisiae,* Dd; *Dictyostelium discoydium*, At; *Arabidopsis thaliana*, Tb; *Trypanosoma brucei*. PlasmoDB IDs: PfeIK1; PF14_0434, PfeIK2; PFA0280w, PfPK4; PFF1370w, PbeIK1; PB000582.03.0, PbeIK2; PB001255, PbPK4; PB000480.02.0. TgIFKA; GI44889870, TgIFKB; GI: 169656460, hPKR; GI4506103, hHRI; GI: 6580979, hPERK; GI: 18203329, hGCN2; GI: 65287717, ScGCN2; GI6320489, AtGCN2; GI: 24940154, hAurora; GI: 37926805, hCDK2; GI1942427. Dictybase IDs: DdIFKA; DDB0185218, DdIFKB; DDB0185219; DdIFKC; DDB0216407; GeneDB IDs: TbeIFK1; Tb11.02.5050, TbeIFK2; Tb927.4.2500, TbeIFK3; Tb927.6.2980.

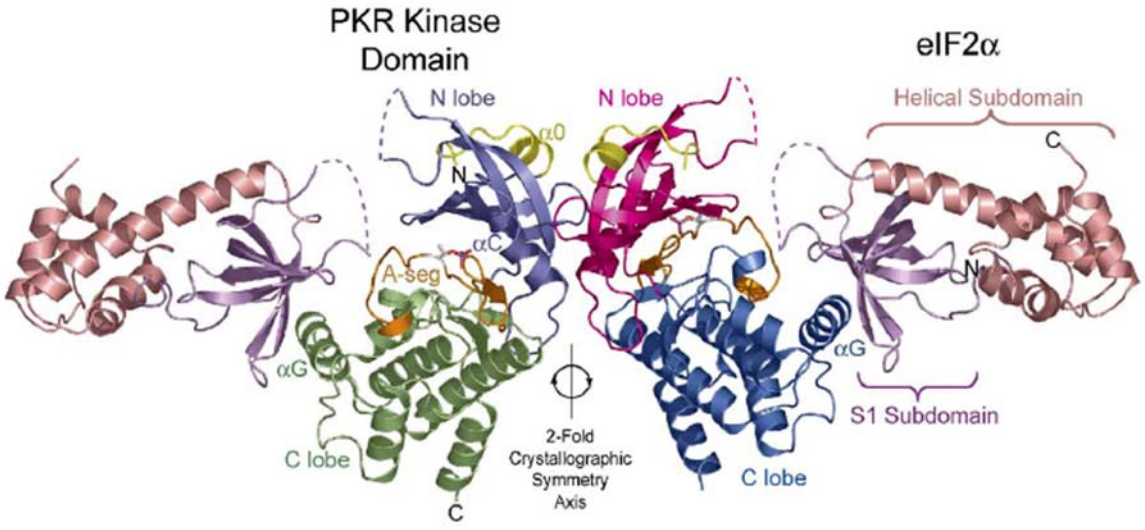

Figure 3-4: Structure of PKR-eIF2α complex.

Ribbons representation of the PKR/eIF2α complex highlighting eIF2α recognition mediated by helix α-G in the C-terminal lobe of PKR and catalytic domain dimerization mediated by the N-terminal lobe of PKR. The N-terminal and C-terminal lobes of PKR are coloured purple and green (left molecule) and red and blue (right molecule), respectively. The activation segment is coloured orange and the phosphor-Thr for activation is shown as ball and stick representation. The region shown with a dashed line in PKR has not been modelled due to disorder and/or deletion; this includes the characteristic kinase insert. The dashed region of eIF2α has not been modeled due to disorder and encompasses the Ser51 acceptor site. (Adapted with permission from Dar et al. (Dar et al., 2005)).

3.2.1.1 PfeIK1

The alignment in Figure 3-3 was used to generate the phylogenetic tree shown in Figure 3-5 which clearly shows a cluster of GCN2 related sequences, including PfeIK1 and its *P. berghei* orthologue. Although these *Plasmodium* sequences diverge at the base of the branch, it nonetheless suggests a possible role for PfeIK1 in response to nutrient levels, a function fulfilled by GCN2 in yeast and mammalian cells. The PF14_0423 (PfeIK1) gene model proposed in PlasmoDB (Bahl et al., 2003) predicts a single intron that falls close to the 5' end of the sequence so that the kinase domain is encoded entirely within the second exon. All the residues that are required for catalytic activity (Hanks, 2003) are present in the PfeIK1 kinase domain (Fig. 1-4), suggesting the gene encodes an active enzyme. The PfeIK1 sequence also shares the feature of insertions within the catalytic domain with other eIF2α kinases (Figs. 3-3 & 3-6) (Mathews, 2007). As described above (1.8.3.1), GCN2 has extensions either side of the kinase domain; such that not only is PfeIK1 most similar to GCN2 in the sequence of its catalytic domain (BLASTP analysis shows 35% identity), but also in overall primary structure (Fig. 3-6). Furthermore the C-terminal extension of PfeIK1 contains an anti-codon binding domain (Superfamily entry SSF52954) as found in amino acyl synthetases, that may mediate binding to uncharged tRNAs, a function that is performed in GCN2 by the HisRS domain present in the C-terminal extension (Fig. 3-6) (Wek et al., 1995). Other functional domains present in the GCN2 extensions (GCN1 binding domain, charged region, pseudo-kinase domain and C-terminal ribosome binding, and dimerization domain (RB/DD), Fig. 3-6) are not recognizable in PfeIK1.

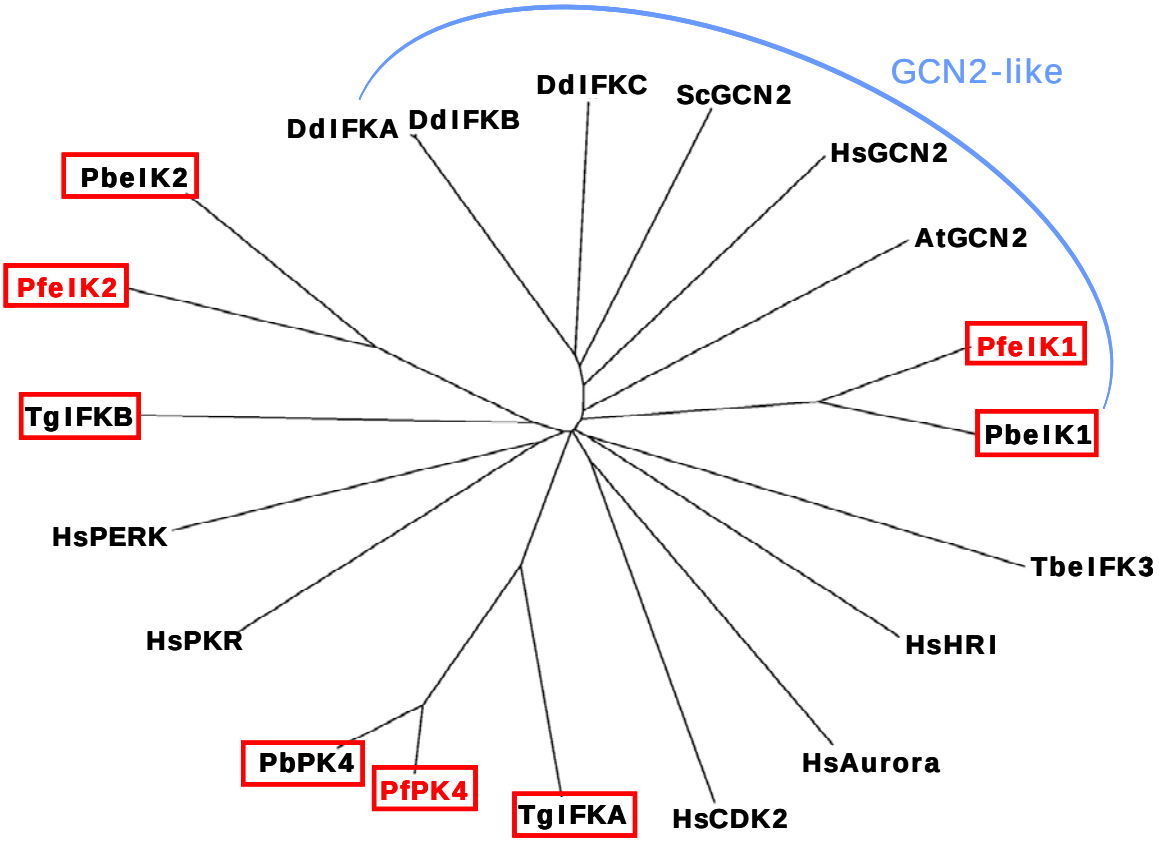

Figure 3-5: Phylogenetic tree illustrating eIF2α kinases in diverse species.
Analysis of the sequence alignment presented in Figure 3-3; the tree was produced from the alignment prior to adjustments made by hand. The three *P. falciparum* sequences investigated here are in red, apicomplexans are boxed in red, and the blue bracket indicates sequences clustering most closely with GCN2. Pf; *P. falciparum*, Pb; *P. berghei,* Tg; *T. gondii,* Dd; *Dictyostelium discoydium*, Sc; *Saccharomyces cerevisiae*, Hs; *Homo sapiens*, At; *Arabidopsis thaliana*, Tb; *Trypanosoma brucei*.

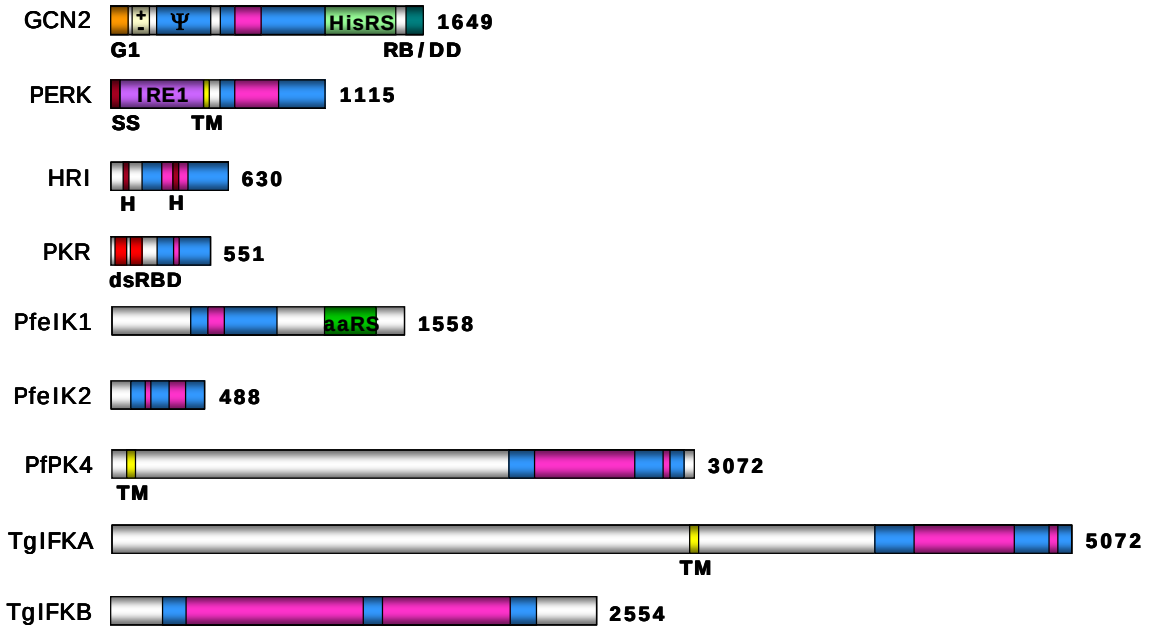

Figure 3-6: Schematic of protein domains of human, *P. falciparum*, and *T. gondii* eIF2α kinases.
Kinase domains are shown in blue, insertions within the kinase domains are shown in pink (characteristic for eIF2α kinases; sizes detailed in Figure3-3). Additional domains are as follows; GCN2: orange; GCN1 binding (G1), cream; charged region (+/-), blue marked (Ψ); pseudo kinase domain, pale green; histidyl tRNA synthetase domain (HisRS), dark green; ribosome binding and dimerization domain (RB/DD). PERK: brown; signal sequence (SS), purple; regulatory domain similar to IRE1 (IRE1), yellow; transmembrane domain (TM). HRI: brown; heme binding (H). PKR: red; RNA binding domains. PfeIK1 contains a putative amino acyl tRNA synthetase domain, green (aaRS), similar to the HisRS domain in GCN2. PfPK4 has a putative transmembrane domain, yellow (TM), as does TgIFKA. White is for regions of unidentified function. The total length of the proteins is given by the number of amino acids, shown at right.

3.2.1.2 PfeIK2

The phylogenetic analysis of eIF2α kinases from diverse species shows PfeIK2 (PFA0380w) clusters with its *P. berghei* orthologue as expected, however there is no clear association with any of the mammalian eIF2α kinases in particular (Fig. 3-5). BLASTP analysis using the kinase domain as a query shows it shares 38% identity with human PKR. Interestingly PfeIK2 is also associated, albeit weakly, with the recently identified TgIFKB, which is suggested to respond to cytoplasmic stresses (Narasimhan et al., 2008). The lack of transmembrane domain or other targeting sequence in PfeIK2 is consistent with a cytoplasmic location (Fig. 3-6). The gene structure of *pfeik2* is discussed in section 3.4.2.1; briefly, the kinase domain is encoded by a single exon. Although the majority of residues required for catalytic activity (Hanks, 2003) are conserved in PfeIK2,

the glycine triad in domain I, required for orientation of the ATP molecule, is not complete (**S**K**G**NN**N**); whether the tertiary structure of PfeIK2 is able to compensate for this to facilitate kinase activity remains unknown. In this context is it interesting to note that the PfPK7 crystal structure reveals that the divergent glycine triad (**N**Q**G**KF**N** in PFPK7) forms the same structure as classical GxGxϕG kinases (where x represents any other amino acid and ϕ a hydrophobic residue), and so allows kinase activity (Merckx et al., 2008). As discussed in section 1.8.3.2 phosphorylation of a conserved threonine residue in domain VIII is part of the activation mechanism of eIF2α kinases. PfeIK2 is the only *P. falciparum* eIF2α kinase in which this threonine residue, and therefore potentially the activation mechanism, is clearly conserved (Fig. 3-3); the functional significance of this remains to be tested.

Although PfeIK2 shares the features of insertions within the catalytic domain with other eIF2α kinases, the sequence of these insertions is not recognizably similar either to other eIF2α kinase inserts, or to other protein motifs. In contrast to human and some other eIF2α kinases that have lengthy extensions containing regulatory domains (1.8.3.1) the N-terminal extension in PfeIK2 is short, with only 118 residues (Fig. 3-6); to date no recognizable motifs have been identified within this region, although this does not exclude the possibility of a regulatory function.

3.2.1.3 PfPK4

The previously published sequence of PfPK4 encodes a predicted 1123 amino acid sequence that encompassed a protein kinase domain (Mohrle et al., 1997). However, the gene prediction algorithms in PlasmoDB propose a 9219 ORF encoding a 3072 amino acid protein that encompasses the previously published sequence. The PfPK4 sequence contains all the residues required for kinase activity, suggesting that the gene encodes an active kinase, consistent with previously published data (Mohrle et al., 1997). PfPK4 also contains inserts within the kinase domain in common with eIF2α kinases; notably, these are very large in comparison to all other eIF2α kinases, except for the *P. berghei* PbPK4

orthologue and the two *T. gondii* sequences TgIFKA and TgIFKB (Fig. 3-6), the former of which clearly clusters with PfPK4 and PbPK4 (Fig. 3-5). However, despite the similarity in size between the inserts in PfPK4, PbPK4 and *T. gondii*, the sequences of the inserts are not conserved.

The phylogenetic analysis presented here confirms previous observations that PfPK4 is most closely related to TgIFKA (Sullivan et al., 2004) (Fig. 3-5), and cannot be assigned orthology to a specific human eIF2α kinase. In spite of this, BLASTP analysis (which is a less sophisticated tool than HMM alignments) using the catalytic domain as the query suggests that PfPK4 is most similar to human PERK, with 29% identical residues. PfPK4 also appears to be more closely related to its *P. berghei* orthologue than PfeIK1 or PfeIK2 (Fig. 3-5), which may be indicative of a role in a conserved function such that greater divergence has not occurred. Despite the lack of sequence similarity between TgIFKA and PERK, evidence has recently been provided that TgIFKA localizes to the ER and shares some regulatory mechanisms with this human ER-stress-responsive kinase (Narasimhan et al., 2008). In TgIFKA, as in PERK the transmembrane domains lie centrally in the protein sequence (Sullivan et al., 2004) (Harding et al., 1999), such that in PERK a domain extends into the lumen of the ER (discussed section 1.8.3.1). Although in PfPK4 the putative transmembrane domain is relatively close to the N-terminus (Fig. 3-6), 108 residues lie to its N-terminus that could enable association with other proteins; it therefore remains an interesting possibility that PfPK4 could perform PERK-like functions in *P. falciparum*.

3.2.2 Life cycle stage specific expression of PfeIF2α kinases

Initial hypotheses about the roles of the PfeIF2α kinases were based on data from the *P. falciparum* genome database, PlasmoDB shown in Figure 3-7. The data are from the Le Roch et al. 2003 microarray study (Le Roch et al., 2003), and suggest PfeIK1 is expressed in merozoites and ring stage parasites. In contrast, PfeIK2 mRNA appears not to be expressed in asexual stages at all, but is found in gametocytes and sporozoites. PfPK4 mRNA is present in all life cycle stages examined, in agreement with previously published data (Mohrle et al., 1997).

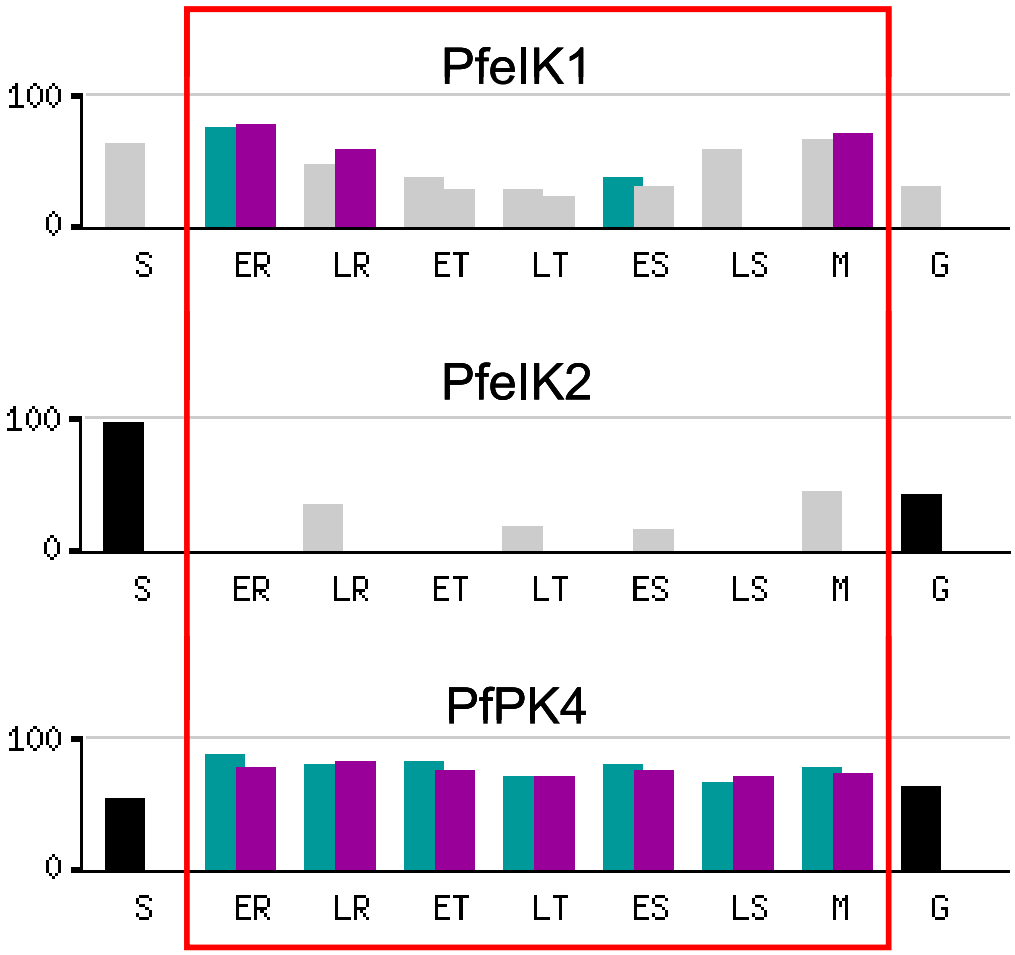

Figure 3-7: Expression data for the PfeIKs taken from PlasmoDB (Le Roch et al., 2003). Y-axis: percentiled gene expression, relative to total gene expression. X-axis: life cycle stage: S= sporozoites, ER = early rings, LR = late rings, ET = early trophozoites, LT = late trophozoites, ES = early schizonts, LS = late schizonts, M = merozoites and G = gametocytes. Purple indicates parasites synchronised using temperature, Green represents parasites synchronised with sorbitol. Black is used for gametocytes and sporozoites where the synchronisation method does not apply, and grey represents data below the confidence level. The red box encloses asexual stages.

The PfeIK1 catalytic domain was amplified from an asexual-stage cDNA library (A. Craig), confirming that it is indeed expressed during asexual stages (data not shown). Further, we raised an anti-peptide antibody, in order to analyse PfeIK1 protein expression; unfortunately, the specific band identified was slightly smaller than expected, which would not have given undue cause for concern. However, critically, this band is unchanged in genotyped *pfeik1*$^{-}$ parasites (4.2.1), which demonstrates that it results from cross-reactivity of the antibody with another protein; PfeIK1 protein expression therefore remains untested. We

have very recently received chicken IgYs directed against PfeIK1-derived peptides from our collaborator Prof. D. Goldring (Univ. of Kwazulu-Natal, South Africa), that will be tested in the near future. RT-PCR and western blot analysis were completed for PfeIK2 and are discussed below (3.4.2.1). We also raised an anti-peptide antibody to PfPK4 that specifically recognizes a band of approximately 80 kDa (Fig. 3-8). Although the full length of PfPK4 is predicted to be a 365 kDa protein, and the kinase domain would also be a relatively large protein of 135 kDa, such that the precise identity of the 80 kDa band is unknown, the size observed here is consistent with previously published data that also report an 80kDa band for PfPK4 (Mohrle et al., 1997). If this band does indeed represent a processed form of PfPK4 then western blot data indicates it is expressed throughout the life cycle but at a higher level in trophozoites and schizonts, than in rings or gametocytes (Fig. 3-8).

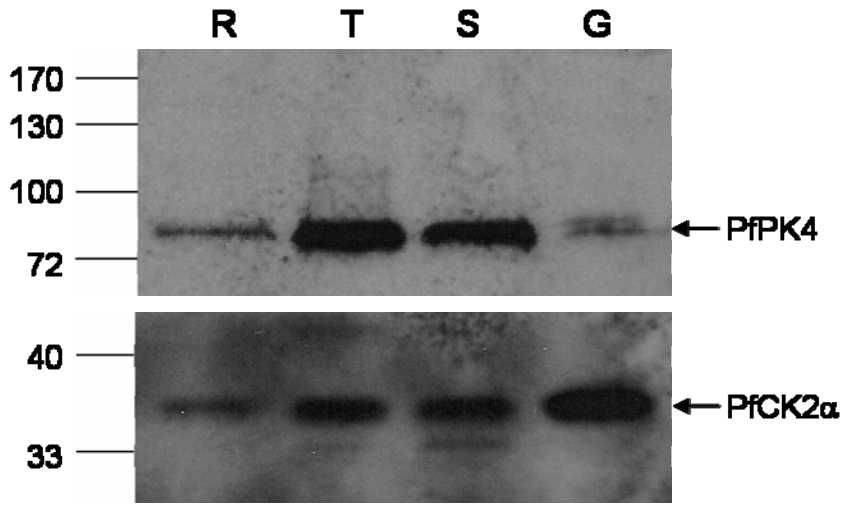

Figure 3-8: Expression of PfPK4.
Western blot analysis of PfPK4 expression in the parasite life cycle. Upper panel, PfPK4; lower panel, PfCK2α as a loading control. R; ring stage, T; trophozoites, S; schizonts, G; gametocyte enriched. Sizes of co-migrating markers are indicated at left.

3.3 Cloning and expression of *P. falciparum* eIF2α

3.3.1 Cloning of PfeIF2α

The PlasmoDB accession number for the *P. falciparum* orthologue of eIF2α is PF07_0117. Oligonucleotide primers were designed to amplify the complete coding sequence by PCR from a cDNA library of the *P. falciparum* clone 3D7, using the Phusion polymerase (Finnzymes). The forward primer (No. 151, Table 6-2, appendix) contained a *Bam*HI restriction site the reverse primer (No.152 Table 6-2, appendix) contained a *Sal*I site. Taq polymerase (Takara) was used to add adenine tails to enable cloning of the 990bp product into the pGEM-T Easy vector (Promega) for amplification and sequencing. The correct sequence was removed by digestion with *Bam*HI/*Sal*I and inserted into the expression vector pGEX-4T3 (Pharmacia) (Fig. 3-9). The pGEX-4T3 vector adds the glutathione-S-transferase (GST) sequence to the N-terminus of PfeIF2α. A mutant of PfeIF2α designed to be refractory to phosphorylation was obtained by site directed mutagenesis (Ser59→Ala) using the overlap extension PCR technique (primers no. 195 and 196) (Ho et al., 1989).

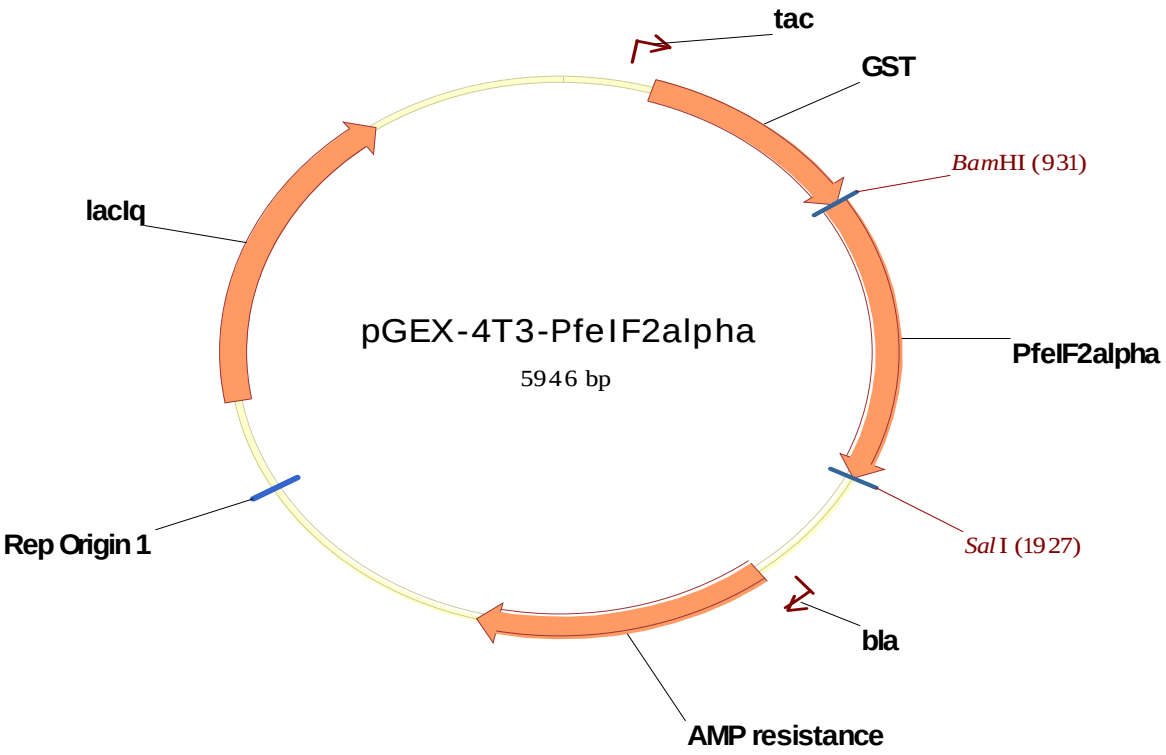

Figure 3-9: Map of the expression vector for PfeIF2α.

3.3.2 Expression of Recombinant PfeIF2α

Different expression conditions were tested in order to optimize the yield of both PfeIF2α wild type and the S59A mutant. *E. coli* BL21codon plus were used; protein expression was induced using 0.1 - 5mM IPTG, at 37°C, or 30°C for 2-4 hours, or 16°C overnight. Samples were taken before induction of protein expression and after induction. Bacteria were harvested after the appropriate time and lysed in lysis buffer 1 (Table 6-7, appendix. Samples were taken of the soluble and insoluble fractions before purification of the soluble fraction on glutathione-agarose beads. Samples were also prepared from the eluted proteins and the beads after elution. Figure 3-10 shows a representative Coomassie-blue stained gel of this series of samples after induction with 0.25mM IPTG, 16°C overnight, which was found to give the best balance of yield of full length protein, whilst minimizing the yield of truncated products, or degradation to GST only. Figure 3-11 shows an anti-GST western blot of the purification stages after induction with 0.5mM IPTG for 2 hours at 30°C; this confirms the expected size of 64 kDa GST-PfeIF2α and illustrates the high proportion of degraded proteins that arose when expression was induced at higher temperatures.

Purification on affinity chromatography columns was also attempted, but batch purification was found to be more reliable and convenient for subsequent experiments.

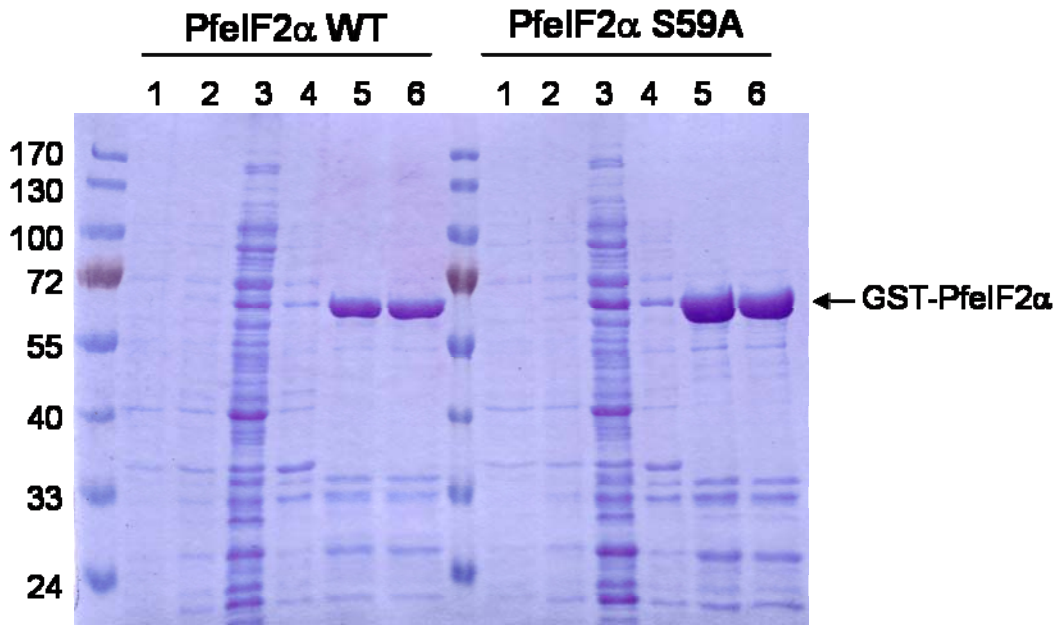

Figure 3-10: Purification of GST-PfeIF2α.
Coomassie blue stained gel showing purification of recombinant GST-PfeIF2α wild type (WT) and Ser→Ala mutant (S59A) in *E. coli*. 1: before induction, 2: after induction (0.25mM IPTG, 16°C over night), 3: soluble fraction, 4: insoluble fraction, 5: eluted proteins, 6: beads, after one elution.

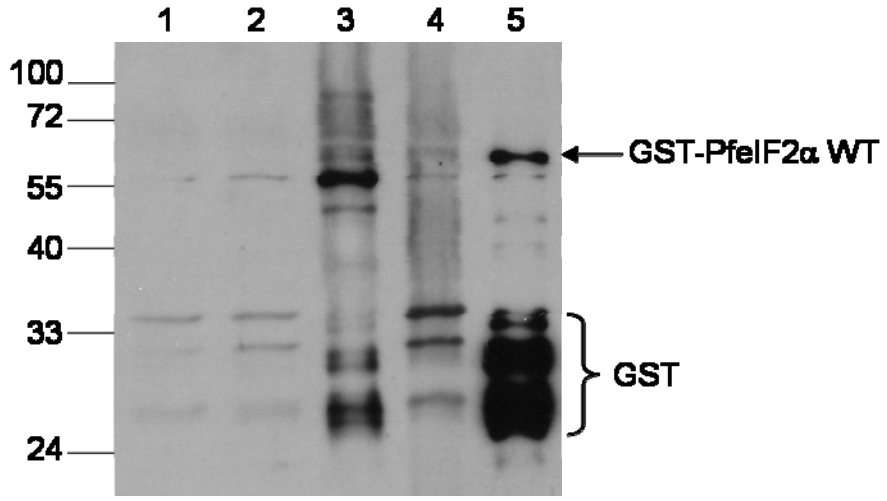

Figure 3-11: Western blot analysis of purification of wild type GST-PfeIF2α.
Samples from successive stages of expression and purification of wild type GST-PfeIF2a were separated by SDS-PAGE, transferred to nitrocellulose and probed with an anti-GST antibody. 1: before induction, 2: after induction (0.5mM IPTG, 2 hours, 30°C), 3: soluble fraction, 4: insoluble fraction, 5: eluate.

3.4 Cloning, expression and characterisation of the *P. falciparum* eIF2α kinases.

3.4.1 PfeIK1

3.4.1.1 Cloning of the PfeIK1 catalytic domain

A 1278bp fragment encoding the catalytic domain of PfeIK1, was amplified from a *P. falciparum* asexual stage cDNA library (A. Craig) using the Phusion polymerase (Finnzymes), (forward including *Bam*HI; no. 146, reverse including *Sal*I; no. 148) followed by Taq for pGEM-T Easy cloning as described for PfeIF2α (3.3.1). A catalytically inactive mutant was obtained by site directed mutagenesis of Lys458→Met using the overlap extension PCR method (nos. 197 & 198, Table 6-2, appendix) (Ho et al., 1989). The correct sequence was removed by digestion with *Bam*HI/*Sal*I and inserted into the expression vector pGEX-4T3, between the same sites. The pGEX-4T3 vector was chosen to express the PfeIK1 catalytic domain with an N-terminal GST tag following the success of this strategy for the expression and characterisation of several other *P. falciparum* kinase domains (for a few examples, see (Dorin et al., 2005, Reininger et al., 2005)(Reininger et al. in prep)(Holland et al. in prep)). Furthermore eIF2α kinases act as dimers (1.8.3.2); expression of the kinase domain of PKR fused to GST, which can form dimers, enabled purification of active kinase, where the kinase domain alone was inactive (Ung et al., 2001).

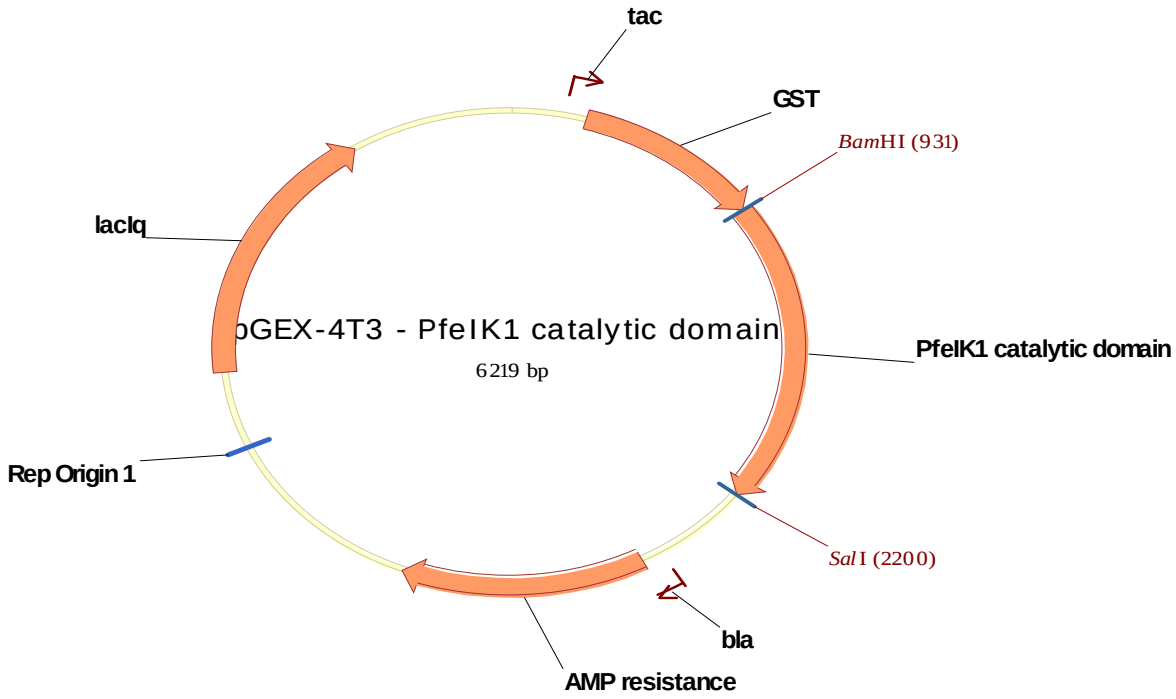

Figure 3-12: Map of the expression vector for GST-PfeIK1.

3.4.1.2 Expression of recombinant PfeIK1

The conditions required for optimal expression of GST-PfeIK1 were investigated; induction was with IPTG at 0.1 - 5.0 mM, or by autoinduction (2.4.6), the temperature was varied from 16°C overnight to 30°C or 37°C for 2-4 hours, and *E. coli* BL21 codon plus cells, or Rosetta2 or RIL cells were tested. Samples were taken at successive stages during induction and purification, as described for PfeIF2α (3.3.2), and analysed by SDS-PAGE followed by Coomassie blue staining or anti-GST western blot (Figs. 3-13 & 3-14). Induction with 0.25mM IPTG at 16°C overnight gave the best yield of active full length GST-PfeIK1 (76 kDa); autoinduction gave less truncated proteins but the full length protein appeared to be inactive in kinase assays (not shown).

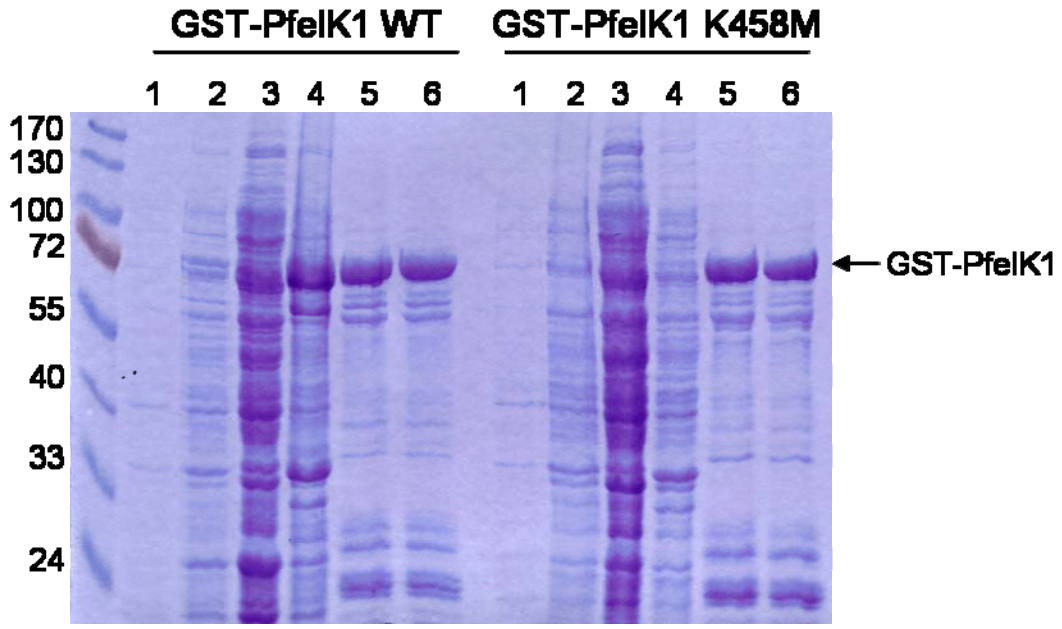

Figure 3-13: Purification of GST-PfeIK1.
Coomassie blue stained gel of purification stages of GST-PfeIK1. 1: before induction, 2: after induction (0.25mM IPTG, 16^{o}C over night), 3: soluble fraction, 4: insoluble fraction, 5: eluate, 6: beads after first elution.

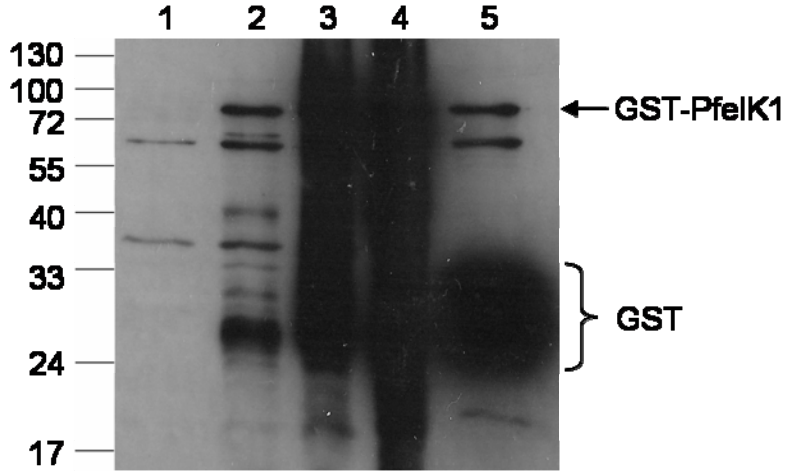

Figure 3-14: Purification of GST-PfeIK1.
Western blot analysis of purification stages of GST-PfeIK1. Samples were collected at successive stages of protein expression which was induced with 0.5mM IPTG, followed by growth at 30^{o}C for 2 hours. Samples were separated by SDS-PAGE, transferred to nitrocellulose and probed with an anti-GST antibody. 1: before induction, 2: after induction, 3: soluble fraction, 4: insoluble fraction, 5: eluted protein. The arrow marks the expected size of full length GST-PfeIK1 at 76 kDa; the bracket marked with GST is likely to contain various truncated proteins including GST.

3.4.1.3 PfeIK1 is an active kinase able to phosphorylate PfeIF2α *in vitro*

In order to test the hypothesis that the *pfeik1* gene encodes a functional kinase I used the GST-PfeIK1 fusion protein in kinase assays. Kinase assays were performed with the non-physiological substrates α- or β-casein, myelin basic protein (MBP) and histone H1, in the presence of wild type GST-PfeIK1, catalytically inactive GST-PfeIK1-K458M, or no kinase (Fig. 3-15). The results demonstrate that PfeIK1 can autophosphorylate; due to the signal at the 76kDa band, which is also clearly observed in Figure 3-16, where the wild type kinase has not been provided with substrate. Autophosphorylation has been shown to be part of the activation mechanism of the eIF2α kinases (reviewed (Mathews, 2007)). Figure 3-15 shows that GST-PfeIK1 can phosphorylate the two non-physiological substrates, α- and β-casein, MBP and histone H1 were not phosphorylated (data not shown). Weaker phosphorylation of β-casein is observed in the catalytically inactive mutant lane; since this activity is also present where there is no recombinant kinase at all, it must derive from a low level of contaminating kinase activity in the substrate itself, providing confidence that the K458M mutant is indeed inactive, and that GST-PfeIK1 is responsible for the kinase activity observed in the wild type lane.

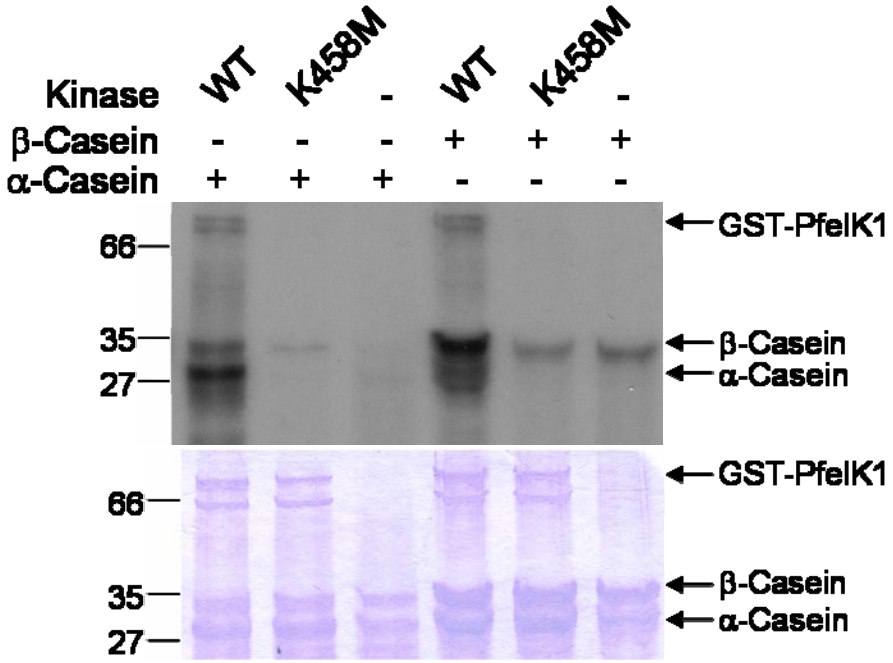

Figure 3-15: PfeIK1 phosphorylates non-physiological substrates.
Kinase assays were carried out using the recombinant catalytic domain of PfeIK1, GST-PfeIK1 using the exogenous substrates α- and β-casein. Assays contained 10μg α-casein (left three lanes), or 10μg β-casein (right three lanes), in the presence of 2μg wild type (WT), 2μg catalytically inactive (K458M), or no kinase (-). Upper panel: autoradiogram, lower panel: Coomassie blue stained gel.

In order to establish whether PfeIK1 is an eIF2α kinase as predicted, I used the recombinant GST-PfeIF2α as a substrate in kinase assays with GST-PfeIK1. Importantly, Figure 3-16 (left lane) shows that GST-PfeIK1 can phosphorylate wild type GST-PfeIF2α. Furthermore, mutation of the predicted target for phosphorylation, Ser59, to alanine, which cannot be phosphorylated, prevents PfeIF2α phosphorylation. This suggests that the mechanism of phosphorylation of eIF2α that, in other systems results in the regulation of translation initiation, may be conserved in *P. falciparum*.

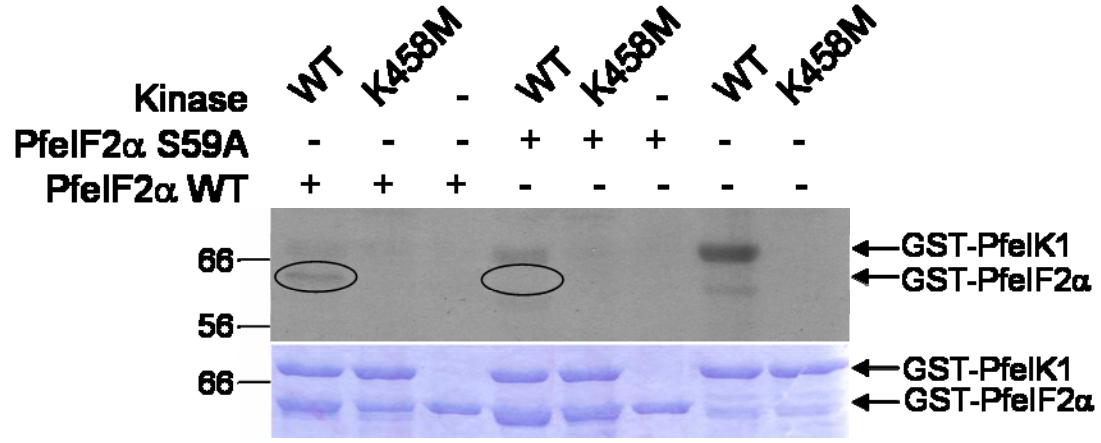

Figure 3-16: GST-PfeIK1 autophosphorylates and phosphorylates wild type PfeIF2α but not the mutant PfeIF2α S59A.
Kinase assays were carried out using 10μg wild type GST-PfeIF2α (left three lanes), 10μg GST-PfeIF2α S59A (centre three lanes), or no substrate (right two lanes), in the presence of 2μg wild type GST-PfeIK1 (WT), 2μg catalytically inactive mutant GST-PfeIK1 (K458M), or no kinase (-). Upper panel: autoradiogram, lower panel: Coomassie blue stained gel.

3.4.2 PfeIK2

3.4.2.1 Verification of *pfeik2* gene structure

The four gene prediction algorithms used by PlasmoDB (Bahl et al., 2003) were not consistent for the exon structure of *pfeik2*. The possible gene structures are shown in Figure 3-17A; RT-PCR was used to investigate which of these is correct. To generate any of these PCR products, it was necessary to use gametocyte cDNA as the template since there was no amplification from asexual material (not shown); this is consistent with the microarray data suggesting PfeIK2 is not expressed during asexual stages. It was possible to amplify the 404 bp fragment corresponding to the 5' end of the single exon prediction (top, Fig. 3-17A), confirming that mRNAs including this region are present. However, neither primer pair selected to amplify across the predicted intron boundaries resulted in any amplification, providing evidence (albeit negative) that the single exon gene structure is correct.

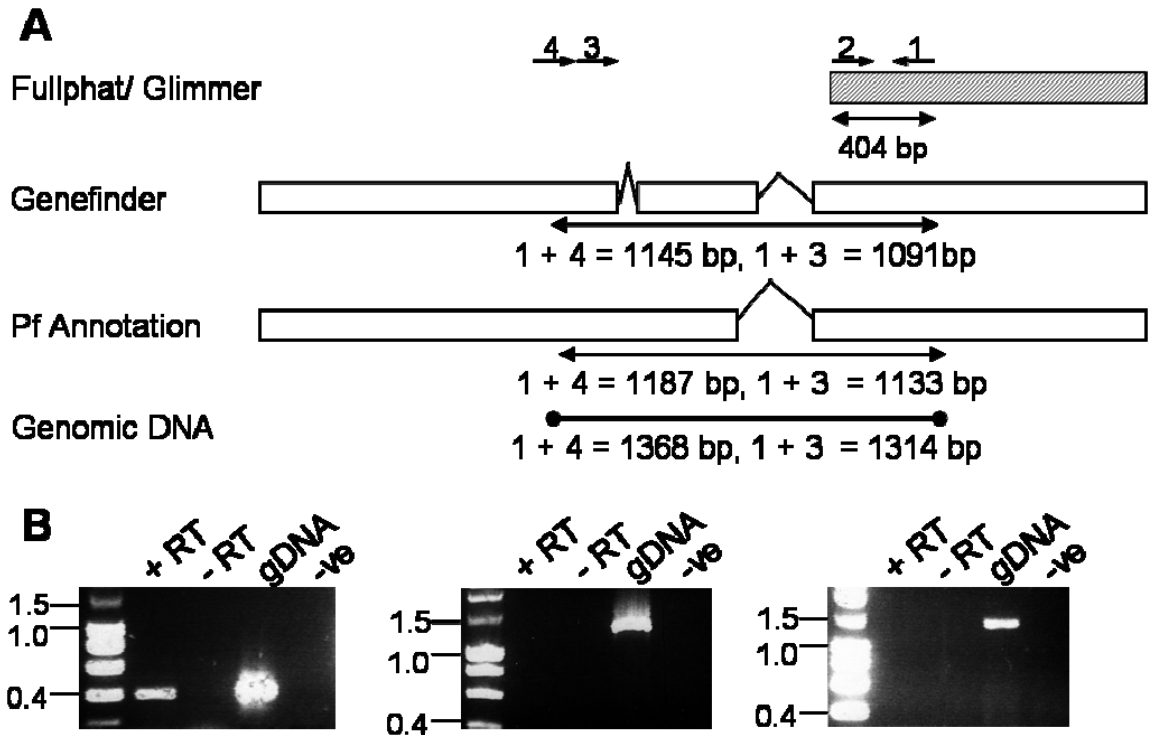

Figure 3-17: Verification of the gene structure of *pfeik2*.
A: Schematic illustrating the three possible gene structures given by the different gene prediction algorithms used by PlasmoDB. Single headed arrows (top) indicate the position of primers used for RT-PCR analysis. Double headed arrows indicate the expected sizes to be amplified by RT-PCR, by each primer combination; the rounded-ended line indicates the expected sizes to be amplified from genomic DNA. B: RT-PCR with different primer pairs; left panel, primers 1+2; centre, 1+3; right, 1+4.

To confirm the RT-PCR results with regard to both the stage of expression, and the length of the open reading frame, a western blot was carried out comparing expression of PfeIK2 in asexual parasites and gametocytes. As shown in Figure3-18, a band of 59 kDa; the expected size of the protein encoded by the single exon gene is recognised exclusively in gametocytes. This supports the RT-PCR data that PfeIK2 is encoded by a single exon, resulting in expression of a 59 kDa protein in gametocytes. The PlasmoDB microarray data (Fig. 3-7) indicates PfeIK2 is also expressed in sporozoites; it would be interesting to extend the analysis presented here to verify this.

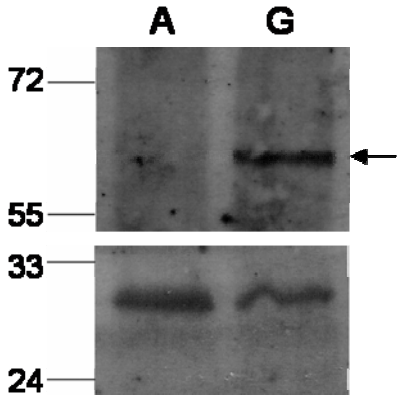

Figure 3-18: Western blot showing the size and stage specific expression of PfeIK2.
Upper panel: Anti-PfeIK2 western blot, the arrow indicates PfeIK2, lower panel; anti-ERD2 loading control. A; mixed asexual parasites, G; gametocyte enriched population.

3.4.2.2 Cloning of the PfeIK2 catalytic domain

Having verified the *pfeik2* gene structure, the 1134 base pair fragment encoding the catalytic domain of PfeIK2 was amplified using the High Fidelity polymerase (Roche) that enables cloning to pGEM-T (Nos. 150 and 185, Table 6-2, appendix). The high AT content of *P. falciparum* genes and the presence of highly repetitive sequence made it difficult to obtain the entire sequence without mutations by PCR; an integral *Bst*BI restriction site was used to piece together correct sequence to produce a construct free from mutations. The correct contiguous sequence was transferred using the *Bam*HI/ *Sal*I restriction sites in the primers, to the expression vector pGEX-4T3 (Fig. 3-19).

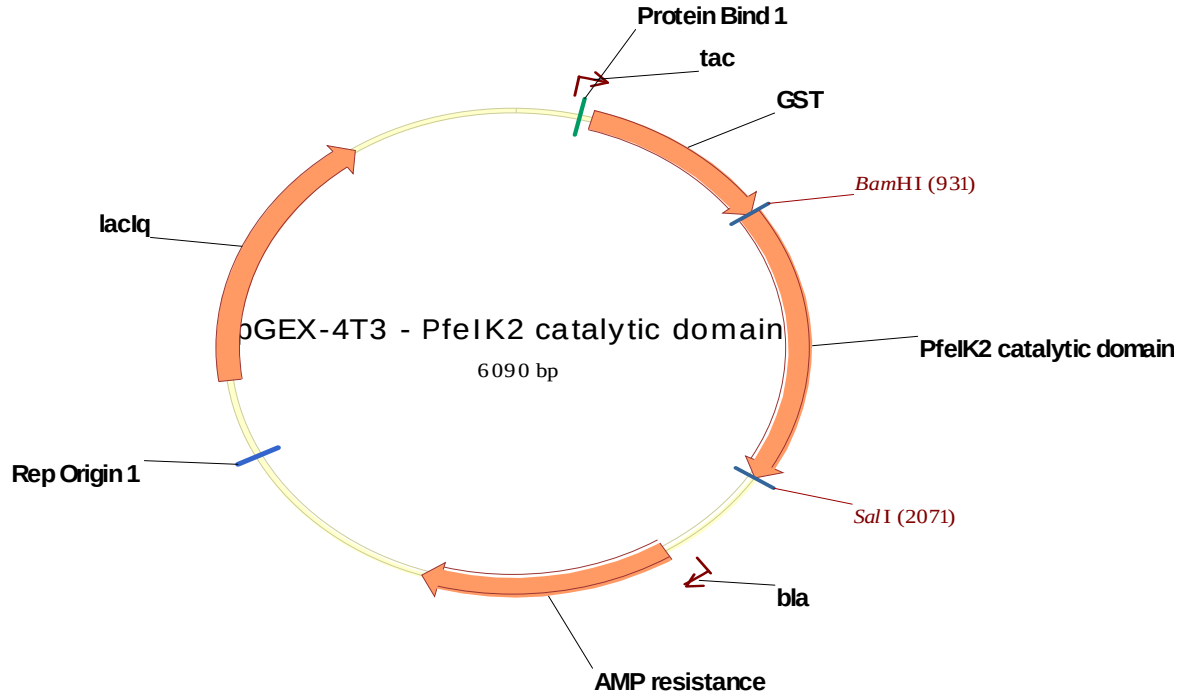

Figure 3-19: Map of the expression vector for GST-PfeIK2.

3.4.2.3 Expression of recombinant PfeIK2

Expression trials for PfeIK2 were carried out using *E. coli* BL21 gold, Rosetta2 and BL21 codonplus, induction of protein expression was by treatment with 0.1mM - 5mM IPTG at 16°C, or 25°C, or autoinduction at 15°C or 20°C for 24 or 48 hours. As indicated in the example of expression and purification in Figure 3-20, induction with 0.25mM IPTG allowed the purification of a low concentration of the expected 73 kDa protein. The anti-GST western blot (Fig. 3-21) confirms that the full length protein was expressed and found in the soluble fraction; this blot suggested that the protein was lost during purification.

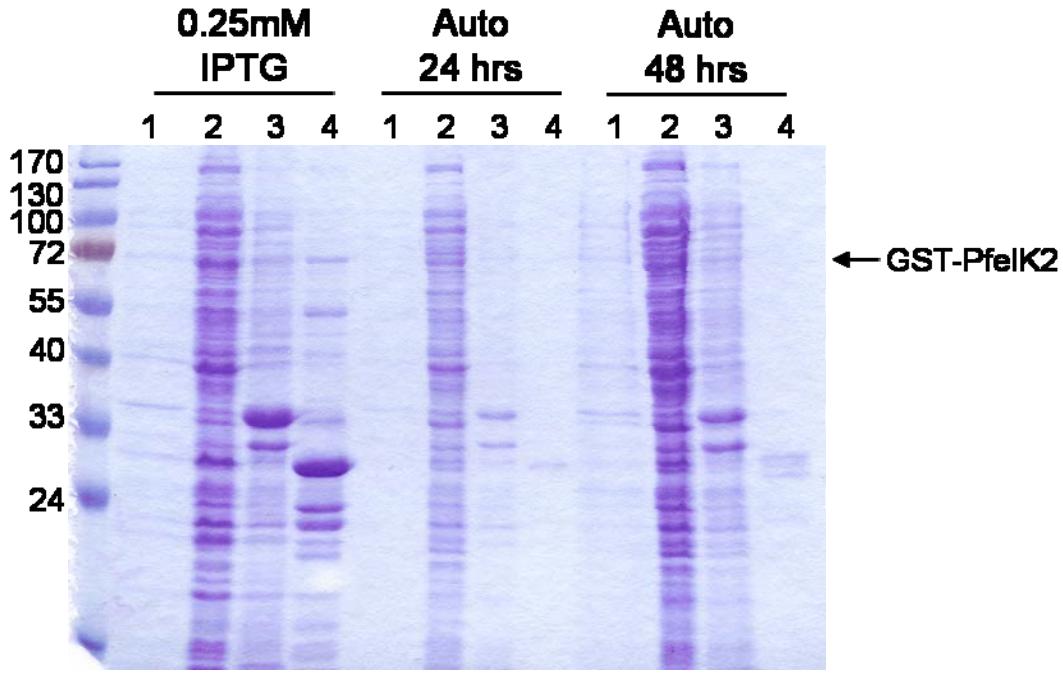

Figure 3-20: Expression of GST-PfeIK2 using *E.coli* BL21c+.
Coomassie blue stained gel of purification of GST-PfeIK2 from three different conditions of expression; left, induced using 0.25mM IPTG; centre, by autoinduction for 24 hours; right, by autoinduction for 48 hours. 1: After induction, 2: soluble fraction, 3: insoluble fraction, 4: beads, without eluting proteins.

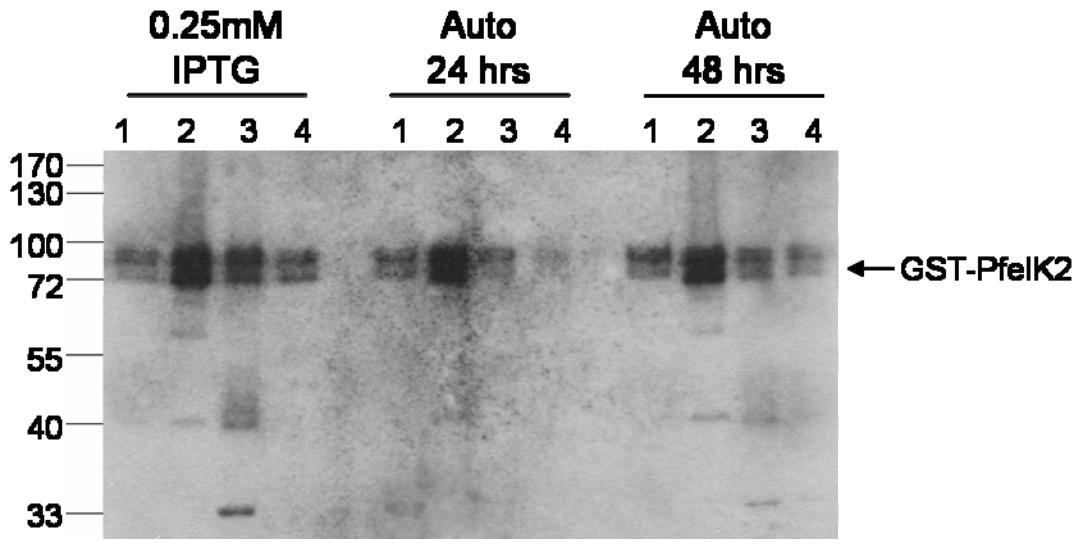

Figure 3-21: Expression of GST-PfeIK2 using *E. coli* BL21 codon plus.
Expression of GST-PfeIK2 was induced under three different conditions; 0.25mM IPTG 15^{o}C overnight or autoinduction at 15^{o}C for 24 or 48 hours. Samples from successive stages of purification were separated by SDS-PAGE, transferred to nitrocellulose and probed with an anti-GST antibody. 1: total extract after induction, 2: soluble fraction, 3: insoluble fraction, 4: beads, without eluting proteins.

3.4.2.4 Initial activity assay of recombinant GST-PfeIK2

Kinase assays can be performed using un-eluted material still bound to the beads; an initial kinase assay was carried out in this way, using those GST-PfeIK2 preparations that contained the 73kDa protein, visible on a Coomassie-blue stained gel. The non-physiological substrates α- and β-casein, myelin basic protein and histone H1 were used, in addition to GST-PfeIF2α and a synthetic peptide comprising the 12 amino acids surrounding PfeIF2αSer59. No activity was detected (data not shown). However, only a small amount of full length recombinant protein was present in any of the preparations used. Before conclusions can be drawn about whether PfeIK2 is indeed a *bona fide* protein kinase, the recombinant protein expression and purification conditions need further optimization. Another approach to address this question would be to immunoprecipitate PfeIK2 from gametocytes, followed by kinase assay. With either approach it remains possible that a lack of detectable activity is not due to the gene product not being a true kinase, but that it requires specific activation stimuli not present under the experimental conditions.

3.4.3 PfPK4

3.4.3.1 Cloning of PfPK4 catalytic domain

According to the PlasmoDB gene prediction, the catalytic domain of PfPK4 is encoded by the 3' 3498 nucleotides of the ORF; this was amplified using primer numbers 161 (forward) and 154 (reverse) (Table 6-2, appendix) and the high fidelity polymerase (Roche), which adds adenine tails allowing for cloning into pGEM-T. The length of the sequence and characteristic high AT content of *P. falciparum* sequences prevented the obtention of a complete mutation-free sequence by PCR. Restriction sites within the catalytic sites were used to piece together mutation free regions to obtain the complete sequence. The *Bam*HI and *Sal*I restriction sites in the primers were used to transfer the complete sequence to the expression vectors pGEX-4T3 and pET-28a (Fig. 3-22). As discussed above, pGEX-4T3 adds the 26 kDa GST sequence to the N-terminus of the protein; the pET-28a vector adds a 6-His tag to the N-terminus.

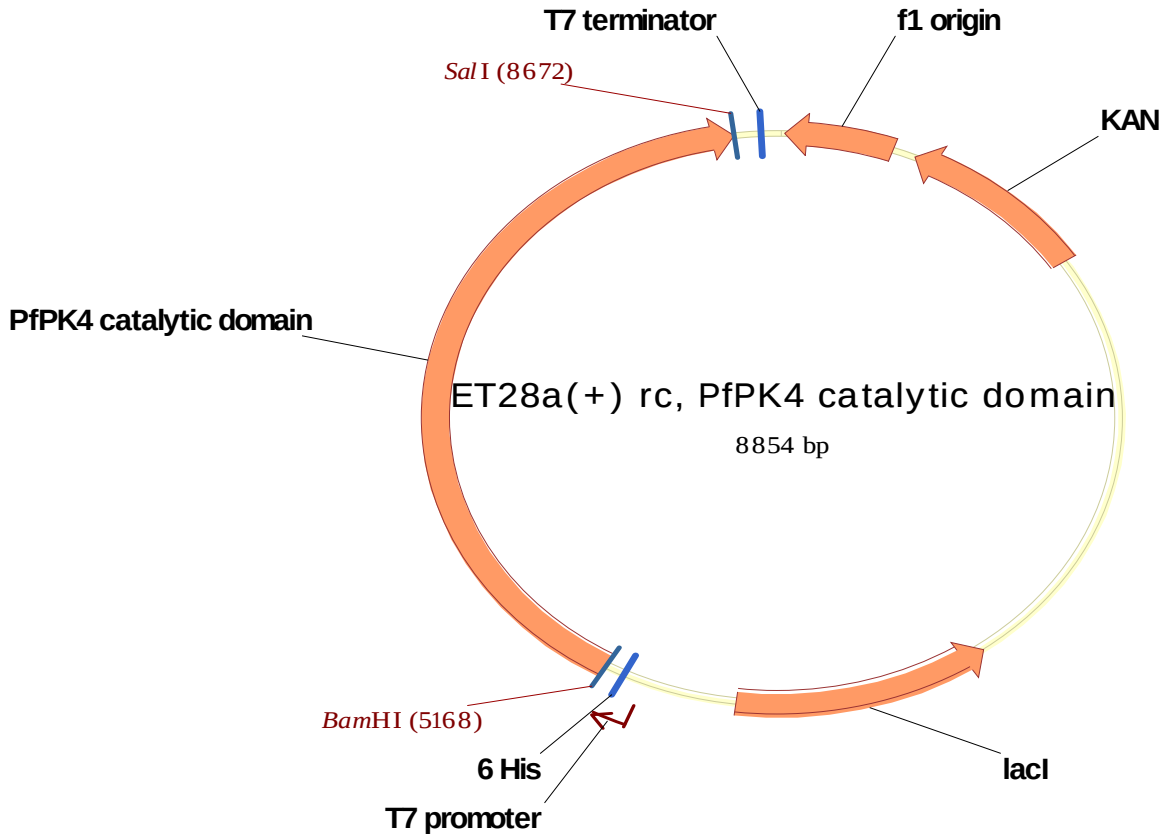

Figure 3-22: Map of the His-PfPK4 expression vector.

3.4.3.2 Expression of recombinant PfPK4

The 3498 nucleotide sequence of the PfPK4 catalytic domain encodes a 136 kDa protein. Initial expression trials were carried out using the pGEX-4T3 construct. However, due to the already large size of the protein I considered that the extra size of the GST tag could exacerbate expression difficulties. Since the catalytic domain of PfPK4 had previously been expressed with a His tag, I switched to using the pET-28a construct, which encodes an N-terminal His tag. As with other recombinant proteins discussed above I used a range of conditions and bacterial strains to attempt to induce expression of His-PfPK4. Examples of the most successful conditions are shown in Figure 1-23, illustrating that the most abundant protein product was approximately 70 kDa. On one occasion an anti-His western blot (not shown) did show a faint band at >100 kDa in the soluble fraction sample, after induction with 5 mM IPTG at 20°C for 1 hour. However, no pure full-length His-PfPK4 was ever obtained.

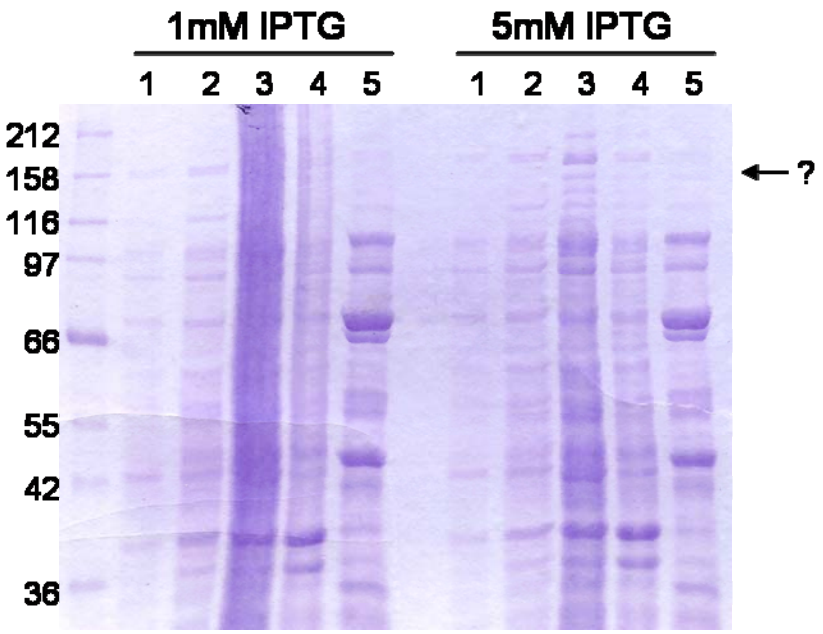

Figure 3-23: Expression of His-PfPK4.
Expression of His-PfPK4 was induced using 1or 5mM IPTG at 15°C overnight. Samples were taken during expression and purification, separated by SDS-PAGE and stained with Coomassie blue. The arrow marks the expected size of His-PfPK4. 1: total extract before induction, 2: after induction, 3: soluble fraction, 4: insoluble fraction, 5: eluate.

3.4.3.3 PfPK4 activity

In spite of poor expression and purification of recombinant PfPK4, kinase assays were nonetheless attempted with some of the recombinant protein preparations to investigate whether any of the truncated proteins had kinase activity, or if any small amount of full length protein had sufficiently high activity to warrant optimization of expression and purification. No kinase activity was observed on a range of non-physiological substrates, recombinant GST-PfeIF2α or the PfeIF2α peptide (not shown). This is in contrast with the activity observed by Mohrle et al, who reported that recombinant PfPK4 was able to phosphorylate an eIF2α-derived peptide (Mohrle et al., 1997). This discrepancy remains unexplained.

Another approach to verify whether PfPK4 in indeed an active protein kinase is to immunoprecipitate the protein from parasite extract and subject this to kinase assays. To improve the chance of specifically immunoprecipitating the kinase, I generated a parasite line expressing a PfPK4 with a double HA epitope at the C-terminus, by allelic replacement (4.1); an anti-HA antibody could then

be used for immunoprecipitation. Results of an initial experiment carried out using these parasites are shown in Figure 3-24. PfPK4 is clearly able to phosphorylate the non-physiological substrates α- and β-casein (lane 1), compared to wild type 3D7 parasites (lane 3). Circumstantial evidence that this activity is indeed derived from PfPK4 and not from some non-specific co-purifying activity is provided by use of the CK2α-HA clone (lane 5); this kinase is significantly more active than PfPK4-HA (only 1/6 of the sample volume used for PfPK4 was loaded). On this occasion PfPK4-HA did not phosphorylate GST-PfeIF2α (data not shown); this may be explained by the presence of the GST tag inhibiting the kinase-substrate interaction, or improper folding of the recombinant substrate. The low level of activity observed in lane 4 where α- and β-casein have been subjected to kinase assay in the absence of additional kinase is often seen when using these substrates (see also Fig. 3-15 and section 3.4.1.3).

The parasites in which wild-type PfPK4 is replace by the HA-tagged enzyme will provide an excellent tool to investigate whether PfPK4 is indeed an eIF2α kinase in *P. falciparum,* and if it can be activated by stress to the parasites. This will be performed, for example, in the amino-acid starvation system used by our collaborator D. Goldberg as described in our joint manuscript (Appendix 6.3).

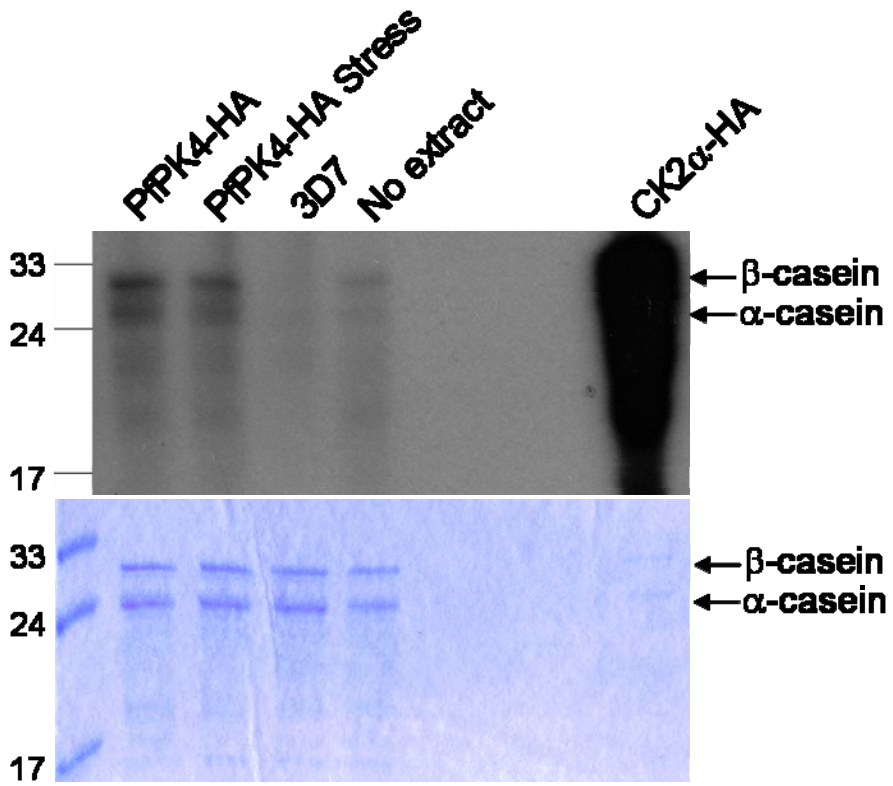

Figure 3-24: PfPK4-HA Kinase assay.
PfPK4-HA was immunoprecipitated from parasite extract and kinase activity assayed using the non-physiological substrates α- and β-casein.

3.5 Perspectives and Discussion

3.5.1 Identification of PfeIF2α and its kinases

Bioinformatic analysis presented here clearly identifies the *P. falciparum* orthologue of eIF2α; conservation of the regulatory Ser and residues involved in formation of the structure that enables interaction with the eIF2α kinases is also observed (3.1). Similarly, *in silico* approaches have identified three kinases of the eIF2α family (3.2). Furthermore, I have shown that GST-PfeIK1 can phosphorylate GST-PfeIF2α at the conserved regulatory Ser (3.4.1.3), validating the bioinformatic observations. Demonstration of the ability of PfeIK1 to phosphorylate PfeIF2α is consistent with (but does not demonstrate) the hypothesis that PfeIK1 may regulate translation through phosphorylation of PfeIF2α *in vivo*.

The amino acid sequence of PfeIK2 suggests it will be an active eIF2α kinase, with the possibility of the non-canonical glycine triad allowing formation of the typical kinase tertiary structure (1.2.2). From the sequence of PfPK4 (1.2.3), and previously published work (Mohrle et al., 1997), PfPK4 is also expected to be an active eIF2α kinase, supported by the preliminary IP data presented here (3.4.3.3). However, to date, I have not been able to confirm that PfeIK2 or PfPK4 can phosphorylate PfeIF2α, largely due to technical problems in recombinant protein production. There are a number of factors to address before further attempts at expression in *E.coli*: i) the location and choice of the tag used for affinity purification; expression of active PfPK4 (see above) was previously reported with a C-terminal His tag (Mohrle et al., 1997) whereas here the tag was at the N-terminus. There are also examples of other kinases in our lab that can be expressed as active enzymes using the His tag, but either cannot be expressed, or are inactive when fused to GST; ii) induction of expression, particularly for PfPK4 where I have evidence for very limited production of the full length protein (3.4.3.2); significantly greater scaling up could be all that is required to obtain useable protein; iii) protein purification; use of the His tag gives greater scope for varying conditions to obtain a more pure product.

Bacterial expression is not the only, and may not be the best route to follow; in addition to further IP experiments (which may also be possible with the anti-PfeIK2 antibody (validated for immunoblotting Fig. 3-18)), another promising strategy for the expression of *P. falciparum* AT rich genes is the wheat germ based cell free system (Sawasaki et al., 2005). The wheat germ system has been used to express a number of previously very challenging *P. falciparum* proteins, in their correctly folded form such that functional analysis was possible (Mudeppa et al., 2007) (Mudeppa et al. Molecular Parasitology Meeting, Woods Hole 2007). Likewise, the protein kinases PfPKA (Sudo et al., 2008) and PfPK2 (Kato et al., 2008) were successfully produced in an active form using this approach. Beyond its demonstrated practicality, one argument presented for use of this system is particularly persuasive for the expression of kinases; since the 'host cells' are propagated in the absence of the plasmodium genes and their products, potential anti-proliferative activity is avoided (Mudeppa et al., 2007).

3.5.2 Characterisation of PfeIF2α and its kinases

Confirmation of kinase activity and ability to phosphorylate PfeIF2α is only the first step in characterizing these proteins; to understand their role in the parasite requires elucidating their expression pattern (spatial and temporal), mechanisms of regulation, and the consequences thereof. Microarray data, RT-PCR and western blotting (3.2.2 & 3.4.2.1), show that the PfeIF2α kinases have distinct temporal expression patterns that suggest they have non-redundant functions. As PfeIK1 is both most similar in overall structure to GCN2 and in the sequence of its catalytic domain (3.2.1.1), we suggest this enzyme is a good candidate for (or may be the orthologue of) GCN2. Furthermore a putative aaRS domain is located in the C-terminal extension of PfeIK1 (3.2.1.1) that may mediate binding to uncharged tRNAs, a function that is performed by the HisRS domain in the C-terminal extension of GCN2 (Wek et al., 1995). One approach to address the function of the putative aaRS domain in PfeIK1 would be to produce the C-terminus as a recombinant protein and analyse its RNA binding properties by northwestern blot, as has been done for GCN2 (Wek et al., 1995).

Sequence analysis of PfeIK2 offers little clue to its regulation. It can be noted that the absence of a transmembrane domain would be consistent with cytoplasmic location. PfPK4 has a putative transmembrane domain at its N-terminus and its catalytic domain is most similar to that of PERK (section 3.2.1.3), suggesting it may play a role in ER stress responses. For both PfeIK2 and PfPK4, localization studies might inform an experimental approach to understanding their regulatory mechanisms, by indicating types of stress to which they might respond (if indeed they are stress responsive). For example, if PfPK4 localises to the ER, then agents which induce ER stress in other eukaryotic cells could be applied, and their effects monitored on kinase activity using the parasite expressing the HA-tagged enzyme, as detailed above (3.4.3.3). For example, tunicamycin is known to cause ER stress (Narasimhan et al., 2008). If it does so in *P. falciparum* as well, and if and PfPK4 plays a PERK-like role, then I would expect to a greater kinase activity to be immunoprecipitated, and see increased phosphorylation of PfeIF2α in parasite extracts, in treated (versus

untreated) parasites. This approach is reliant on hypothesizing appropriate stress stimuli to investigate.

As *P. falciparum* is known to survive in a challenging redox environment (Muller, 2004), oxidative stressors would be interesting to pursue in this respect. In mammalian cells HRI has been shown to be involved in mediating the response to oxidative stress induced by arsenite (Lu et al., 2001). Further, in *T. gondii* arsenite treatment induces TgeIF2α phosphorylation coincident with cyst development (Narasimhan et al., 2008). It remains unknown how this effect is mediated, but it is thought-provoking in that HRI is inhibited by hemin (Fagard and London, 1981), and that recombinant PfPK4 may also be (Mohrle et al., 1997). Hemin has also been observed to inhibit a *P. falciparum in vitro* translation system (Surolia and Padmanaban, 1991). These observations suggest there may be some similarity in the regulatory mechanisms of HRI and PfPK4 (or some unidentified component of the translation machinery), that may extend to activation by oxidative stress.

3.6 Summary

- Bioinformatic analysis reveals *P. falciparum* encodes orthologues of both the translation initiation factor eIF2α, and of three eIF2α kinase related sequences. Furthermore, essential residues appear to be conserved such that the PfeIF2α kinases and PfeIF2α will fold to allow their interaction.

- On the basis of the similarity of the kinase domain sequence, and presence of a putative aaRS domain in its C-terminus, PfeIK1 is proposed as the *P. falciparum* orthologue of GCN2; it may therefore play a role in response to nutrient levels.

- Recombinant GST-PfeIK1 is an active kinase able to phosphorylate recombinant GST-PfeIF2α, confirming our hypothesis that *P. falciparum* has conserved the components of this mechanism for regulation of translation.

- PfeIK2 is encoded by a single exon that is expressed in gametocytes but not in asexual stages; sequence analysis does not provide clues to its regulation.

- The sequence of PfeIK2 contains all residues required for kinase activity but experimental confirmation of this awaits further study.

- PfPK4 protein expression is greatest in trophozoites and schizonts. I was unable to confirm published observations of kinase activity by expression of recombinant protein. However preliminary immunoprecipitation results indicate PfPK4 is indeed a *bona fide* active protein kinase. Sequence analysis suggests PfPK4 may be related to PERK, however other observations suggest it may be regulated in a similar manner to HRI; this also awaits further investigation.

4 Reverse genetics of eIF2α kinases in *P. falciparum*

4.1 Construction of gene disruption and tagging plasmids

To investigate the roles of the eIF2α kinases in *P. falciparum* we first attempted to disrupt the genes, in order to test whether they play an essential role in either asexual multiplication stages, or subsequent stages in mosquito infection. The strategy I used to attempt to disrupt expression of the kinases relied on single cross-over homologous recombination and has been used successfully for other *P. falciparum* protein kinases (Dorin-Semblat et al., 2007, Dorin-Semblat et al., 2008)(Fig. 4-1). A plasmid based on the pCAM-BSD vector (Sidhu et al., 2005) containing an insert comprising the central region of the PfeIK catalytic domain and a cassette conferring resistance to blasticidin was transferred by electroporation into asexual parasites of the 3D7 clone (Figs. 4-2, 4.3 & 4-4). Homologous recombination is predicted to generate a pseudo-diploid locus in which neither of the resulting truncated copies encodes a functional kinase. After recombination the 5' copy is interrupted just prior to the glutamate residue in domain VIII (which provides essential structural stability to the C-terminal lobe), and lacks all downstream coding sequence and the 3'UTR; the 3' copy lacks both the promoter region and the glycine triad in domain I (which is responsible for orientation of the ATP) (Fig. 4-1).

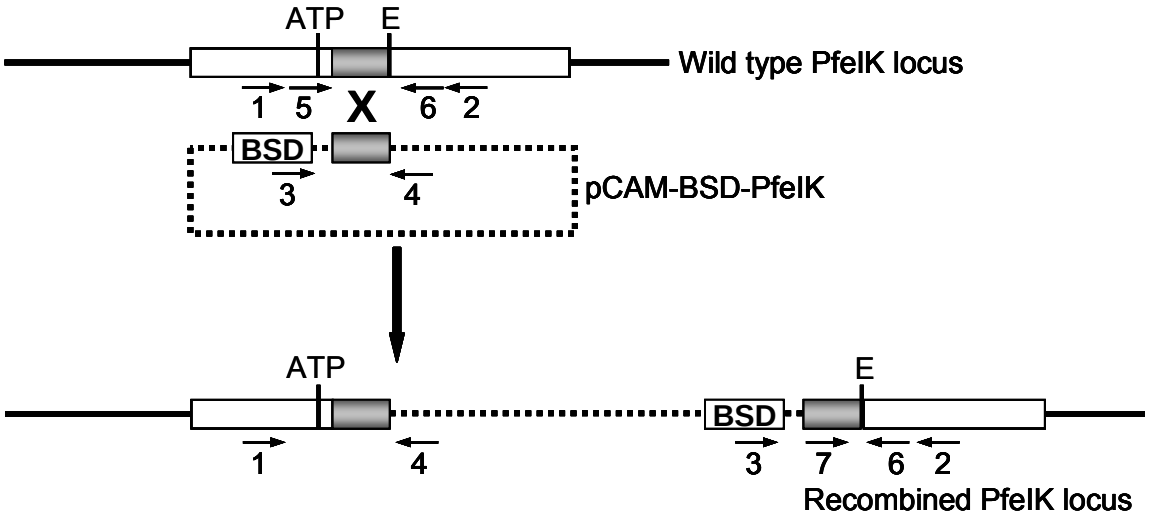

Figure 4-1: Schematic showing the single cross-over homologous recombination strategy used for disruption of the PfeIK genes.
'ATP' represents kinase domain I, a glycine-rich region essential for orientation of ATP by binding the non-transferable phosphates, 'E' is a glutamate residue in domain VIII required for structural stability of the C-terminal lobe of the enzyme; each copy in the resulting psuedo-diploid locus contains only one of these motifs. Numbered arrows indicate the positions of oligonucleotide primers used for PCR analysis of the genotypes of parasite lines. The use of 1 + 2 amplifies the wild-type locus, 3 + 4 the plasmid, 1 + 4 the 5' integration event, 3 + 2 the 3' integration event. Nested PCR was used when analysing the genotypes of infected mosquito midguts; in this case the wild-type locus was amplified by using primers 1 + 2 followed by 5 + 6, and the 3' integration event by using primers 3 + 2 followed by 7 + 6.

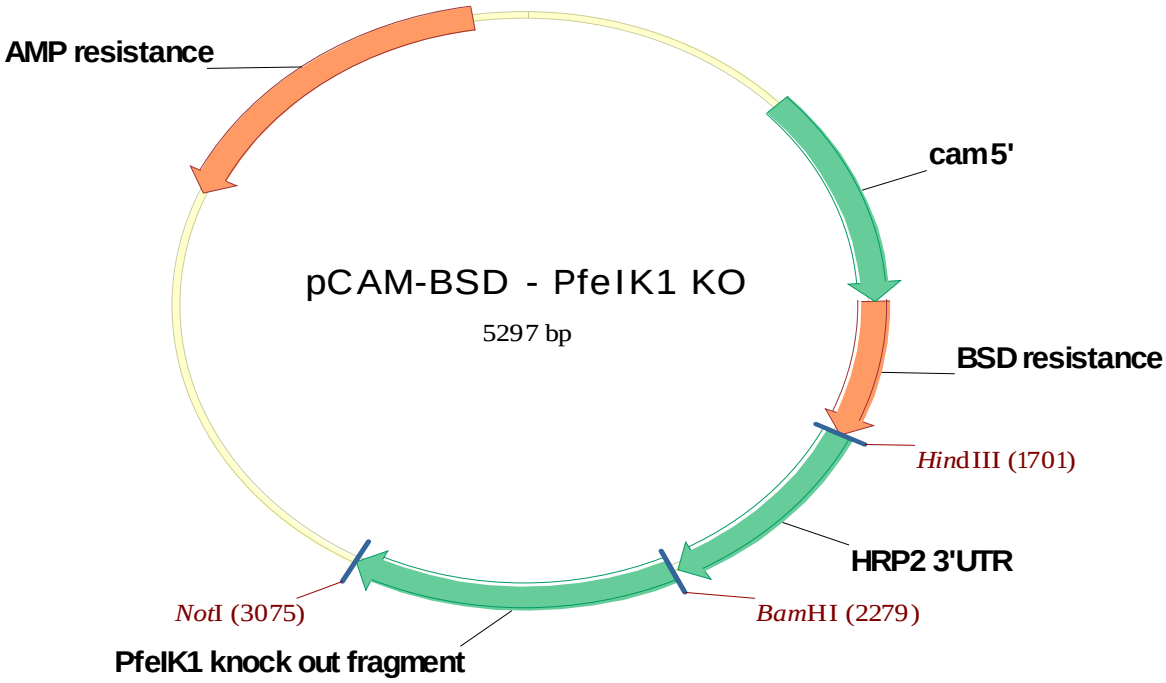

Figure 4-2: Map of the plasmid used for disruption of *pfeik1*.
The transfection plasmid contains a 788bp PCR fragment spanning positions 1467-2255 of the entire 4.8kb *pfeik1* coding sequence (as predicted on PlasmoDB), inserted between *Bam*HI and *Not*I sites(PfeIK1 knock out fragment). The *Hind*III site used in Southern blot analysis is also

shown. cam 5'; *P. falciparum* calmodulin promoter, BSD resistance; gene encoding blasticidin deaminase, HRP2 3' UTR; 3' untranslated region of *P. falciparum* histidine rich protein 2. AMP indicates the ampicillin resistance gene used in preparation of the construct.

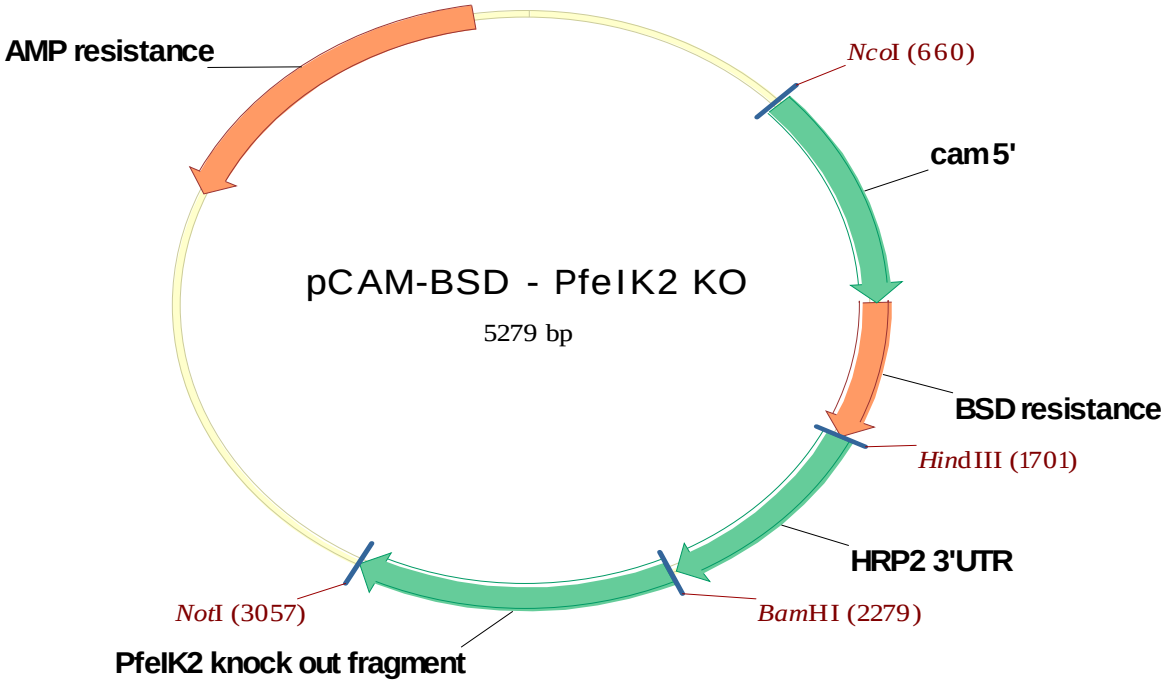

Figure 4-3: Map of the plasmid used for disruption of *pfeik2*.
The transfection plasmid contains a 771bp PCR fragment encompassing positions 430 - 1200 of the verified 1.5kb coding sequence of *pfeik2*, inserted between *Bam*HI and *Not*I sites (PfeIK2 knock out fragment). The *Hind*III and *Nco*I sites used in Southern blot analysis are also shown. cam 5'; *P. falciparum* calmodulin promoter, BSD resistance; gene encoding blasticidin deaminase, HRP2 3' UTR; 3' untranslated region of *P. falciparum* histidine rich protein 2. AMP indicates the ampicillin resistance gene used in preparation of the construct.

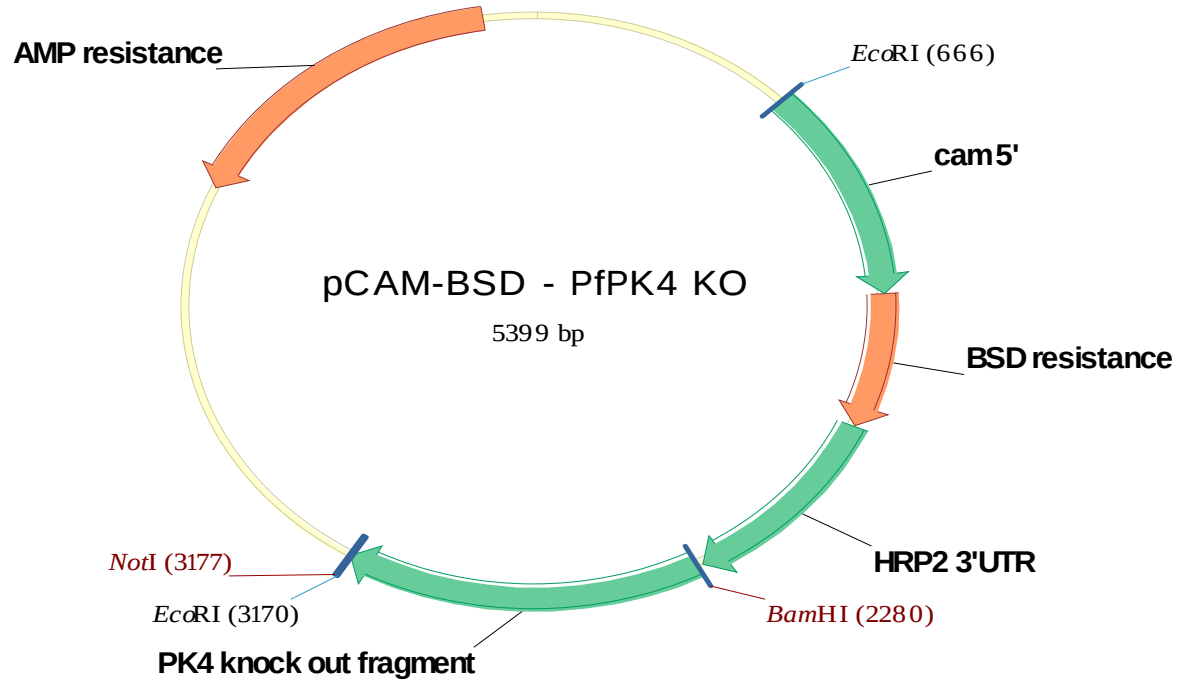

Figure 4-4: Map of the plasmid used to attempt disruption of *pfpk4*.
The transfection plasmid contains an 864bp fragment encompassing positions 7861 - 8724 of the entire coding sequence (as predicted on PlasmoDB), inserted between *Bam*HI and *Not*I sites (PK4 knock out fragment). The *Eco*RI sites used for Southern blot analysis are also shown. cam 5'; *P. falciparum* calmodulin promoter, BSD resistance; gene encoding blasticidin deaminase, HRP2 3' UTR; 3' untranslated region of *P. falciparum* histidine rich protein 2. AMP indicates the ampicillin resistance gene used in preparation of the construct.

If gene knock-out is unsuccessful, it is important to show that the locus is accessible to recombination if the insertion does not cause loss-of-function of the gene product. To do this I used a modification of the single cross-over strategy used for gene disruption (Fig. 4-5). The pCAM-BSD vector was modified to contain a cloning site followed by the 3' untranslated region (UTR) of *P. berghei* DHFR (Jean Halbert, our lab). In addition a tag (either two hemagglutinin [HA] epitopes, or the Green Fluorescent Protein [GFP] (Sylvain Eschenalauer, our lab)) was included, so that if the genes were successfully targeted their tagged products would represent useful tools for molecular analyses. By cloning the 3' end of the gene of interest without its stop codon into this plasmid and transfecting parasites with the resulting construct, single cross over results in reconstitution of a functional gene that encodes a C-terminal double HA, or GFP tag. This strategy was used for PfPK4, since this is the only one of the three PfeIK genes that I was not able to knock-out (4.4.1); vector maps are as shown (Figs. 4-6 & 4-7).

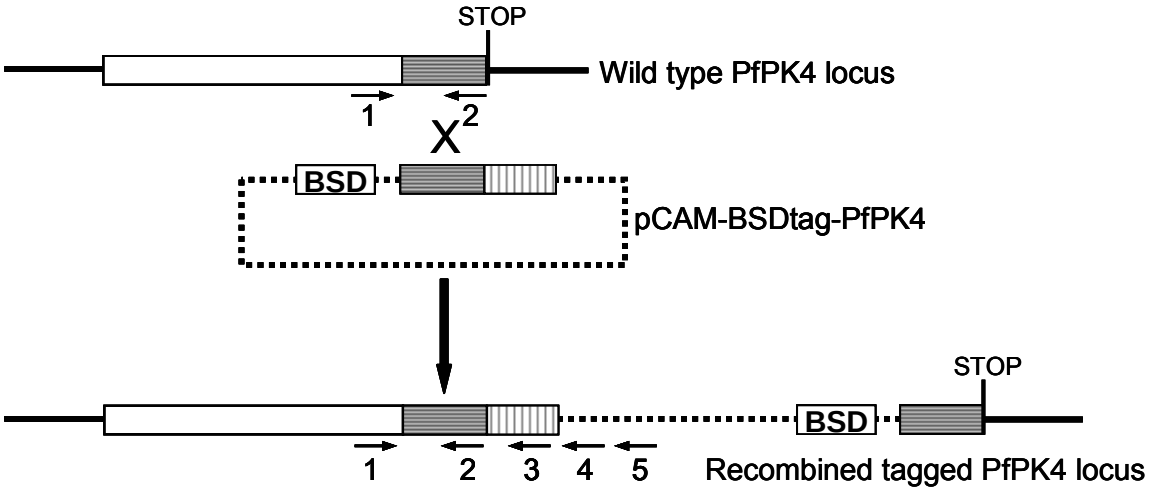

Figure 4-5: Schematic showing the single cross-over recombination strategy used to tag PfPK4.
The horizontally shaded bar represents the 3' 664bp fragment of *pfpk4*, excluding the stop codon (STOP), cloned into the modified pCAM-BSD vector. The vertically hatched bar represents the tag (either double HA or GFP) and the 3'UTR of *P. berghei dhfr*. Numbered arrows indicate the positions of oligonucleotide primers used to analyse the genotypes of parasite lines by PCR.

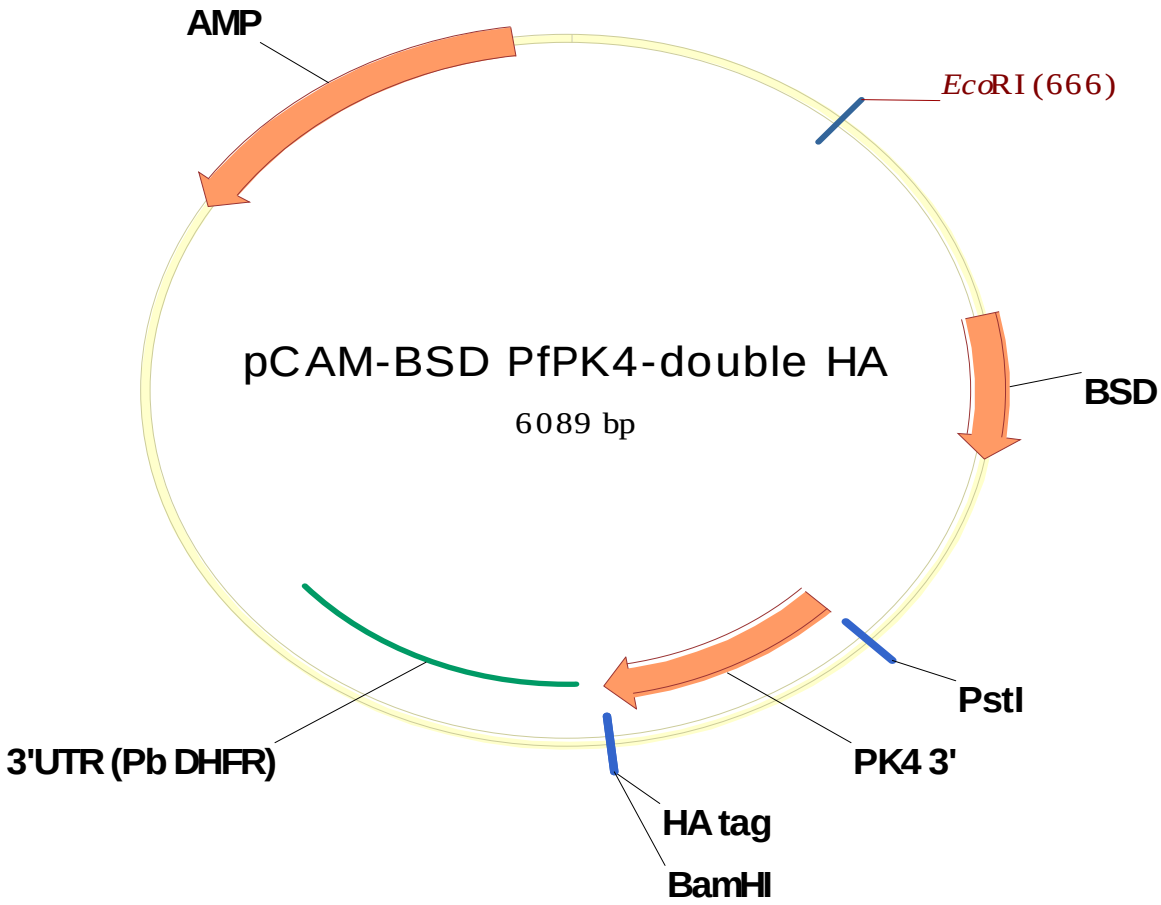

Figure 4-6: Map of the plasmid used to add a C-terminal double HA tag to PfPK4.
A 664bp fragment encompassing positions 8553 - 9216 (PK4 3'), of the *pfpk4* 9219 coding sequence was inserted between *Pst*I and *Bam*HI sites. The *Eco*RI site used subsequently for Southern blot analysis is also shown. BSD indicates the blasticidin deaminse coding sequence, allowing for selection of parasites. 3'UTR (PbDHFR) acts as a 3' UTR for the reconstituted gene to allow expression. AMP indicates the ampicillin resistance gene used in preparation of the construct.

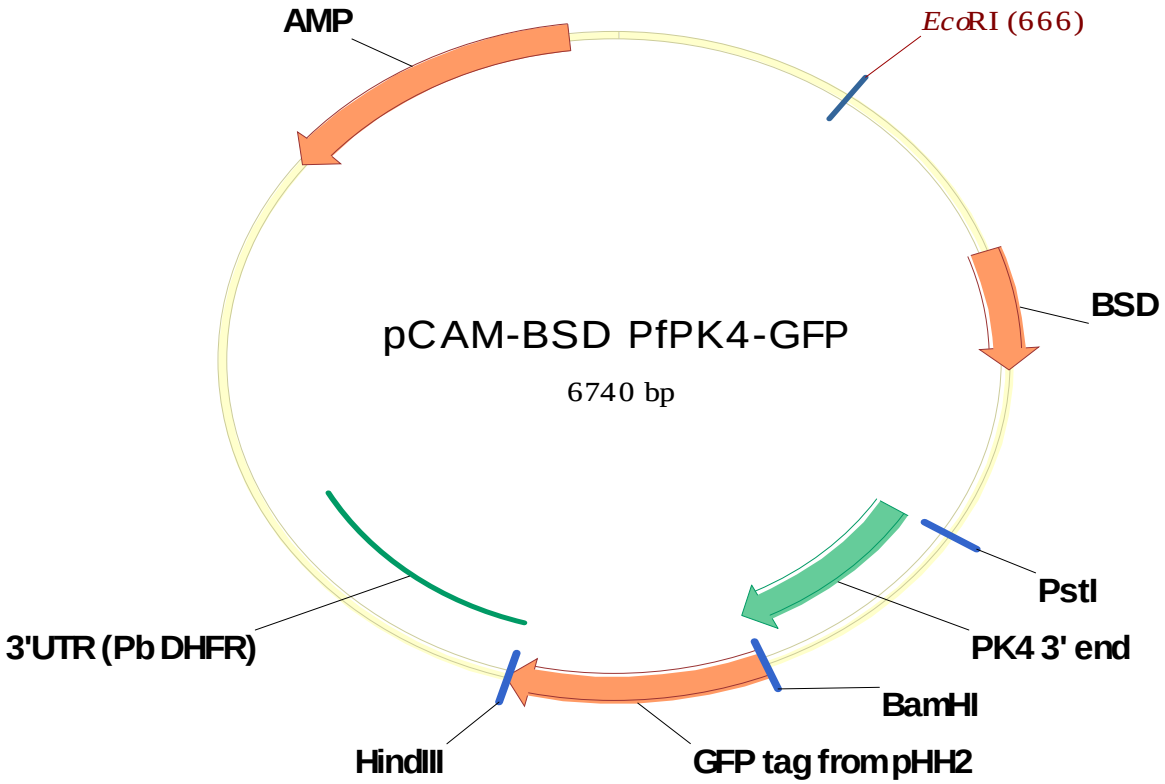

Figure 4-7: Map of the plasmid used to add a C-terminal GFP tag to PfPK4.
A 664bp fragment encompassing positions 8553 - 9216 (PK4 3' end), of the *pfpk4* 9219 coding sequence was inserted between *Pst*I and *Bam*HI sites. The *Eco*RI site used subsequently for Southern blot analysis is also shown.

4.2 PfeIK1

4.2.1 PfeIK1 is not required for asexual growth

PfeIK1 is expressed in asexual parasites (3.2.2 & 3.4.1.1); to investigate whether it plays an essential role in the parasite I attempted to generate *pfeik1*$^{-}$ parasites using the pCAM-BSD-*pfeik1* plasmid shown in Figure 4-2. Blasticidin-resistant parasite populations were obtained from two independent transfection experiments, and PCR analysis indicated that both resistant populations contained parasites whose *pfeik1* locus was disrupted (data not shown). Clonal lines were established by limiting dilution from both independent populations, and the genotypes of one representative clone derived from each transfection experiment (C1 & C8) analysed (Fig. 4-8). The wild-type locus was not detected in clones C1 or C8 (lanes 1& 5), but is observed in the parental wild-type 3D7

parasites. In contrast, fragments diagnostic of plasmid (lanes 2, 6, 10), and both the 5' (lanes 3, 7, 11) and 3' (lanes 4, 8, 12) boundaries of the integrated plasmid are amplified from C1 and C8, but not wild-type 3D7 parasites.

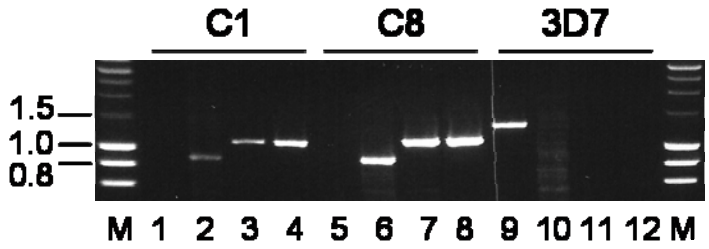

Figure 4-8: PCR analysis of two *pfeik1*⁻ clones.
Lanes 1, 5, 9 are diagnostic of the wild-type locus: primers 1 + 2 (1278bp), lanes 2, 6, 10 are diagnostic of the episome: primers 3 + 4 (847bp), lanes 3, 7, 11 are diagnostic of the 5' boundary of the integrated plasmid: primers 1 + 4 (1050bp), lanes 4, 8, 12 are diagnostic of the 3' boundary of the integrated plasmid: primers 2 + 3 (1075bp). Primers are as follows: 1= 146, 2= 148, 3= 169, 4= 170, see Table 6-2, appendix for details. See Figure 4-1 for primer positions.

Integration of the gene disruption construct was verified by Southern blot analysis; using *Hind*III digestion a 12 kb band containing the wild-type locus is replaced in the mutant clones by the expected two bands resulting from integration; the 10.4 kb fragment contains the 5' boundary of the integrated plasmid and the 6.8 kb band contains the 3' boundary of the integrated plasmid. The 5.3kb band is derived from linearised plasmid or from digestion of concatemers of plasmid (which may or may not be integrated into the chromosome) (Figs. 4-9 & 4-10).

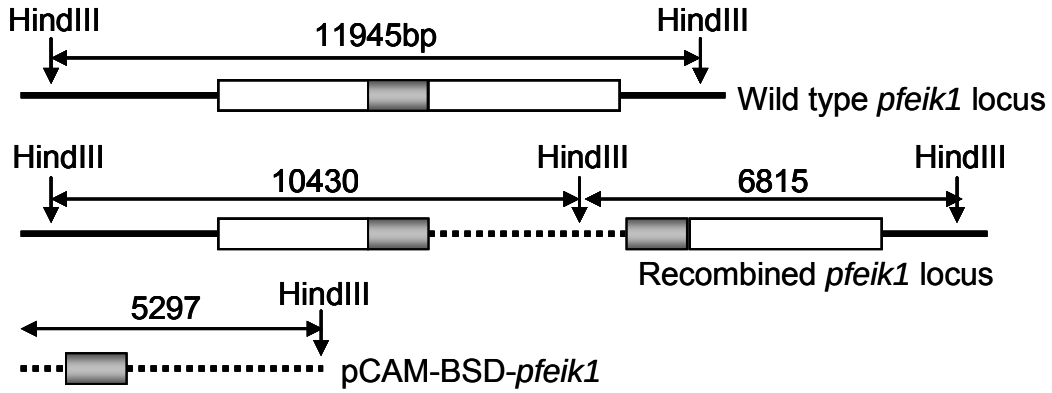

Figure 4-9: Schematic for *pfeik1*⁻ Southern blot.
The fragments expected after *Hind*III digestion of the wild-type locus (top), disrupted *peik1* locus (middle) and disruption plasmid (bottom), are shown.

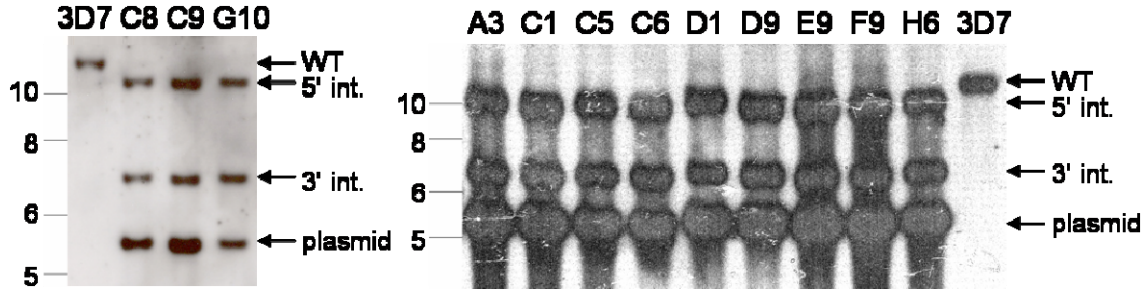

Figure 4-10: Southern blot analysis of *pfeik1*⁻ clones.
Several clones derived from two independent populations (left and right) were analysed. The expected sizes illustrated in Figure 4-9 are shown on the right of each gel: WT: 11945bp, 5' integration: 10430bp, 3' integration: 6815bp, and the pfeik1 disruption plasmid: 5297bp. Sizes of co-migrating markers are indicated on the left.

The results shown in Figures 4-8 and 4-10 confirm that the *pfeik1* locus was indeed disrupted in clones C1 and C8, and demonstrate that PfeIK1 is not required for completion of the asexual cycle of *P. falciparum* under *in vitro* culture conditions. Furthermore, the Goldberg lab has produced growth curves to compare cell cycle progression in *pfeik1*⁻ and 3D7 parasites (Fig. 4-11). Cultured asexual parasites were synchronized and carefully monitored through several life cycles. There was no significant difference in cell cycle progression of parental and knockout clones; cycle times of 49.0 hr +/- 0.5 and 49.2 hr +/- 0.7, respectively, were measured (see also our joint manuscript, appendix 6.3).

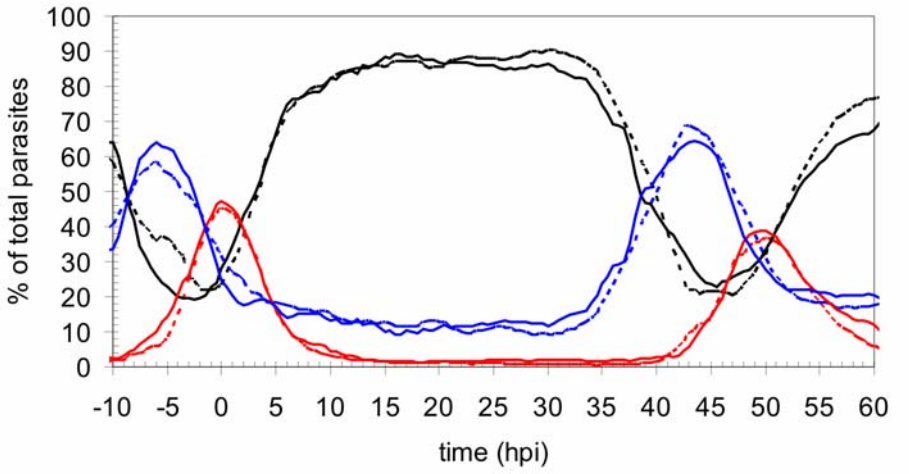

Figure 4-11: Growth of *pfeik1*⁻ parasites.

Representative cycles of *pfeik1*$^{-}$, clone E6 (solid line) and wild-type 3D7 (dashed line); samples were taken every 30 minutes, fixed and DNA content analysed by flow cytometry. Red; mature schizonts, blue; S-phase, black; G phase (G1), hpi; hours post invasion.

4.2.2 PfeIK1 is not required for gametocytogenesis

It was hypothesised that PfeIK1 plays a role in the parasite's stress response, and may therefore be involved in the regulation of gametocytogenesis. To test this hypothesis, I used published methods (Carter et al., 1993) to determine whether the *pfeik1*$^{-}$ parasites could produce male gametocytes. As shown in Figure 4-12, morphologically normal gametocytes at all stages of maturation were produced, suggesting that there is no defect in the ability of *pfeik1*$^{-}$ parasites to differentiate from asexual stages to sexual forms. That both male and female gametocytes were produced by the *pfeik1*$^{-}$ clones was ascertained by their ability to productively infect mosquitoes (see next section).

Although gametocytogenesis appeared to be qualitatively unimpaired, it is also possible that if PfeIK1 plays a role in regulation of differentiation, it could be involved at the stage of detecting the stimuli that result in the life cycle stage switch. Since it remains unknown what these stimuli are in a natural infection of the human host, or indeed if there are one or many, gametocytogenesis could be quantitatively changed in *pfeik1*$^{-}$ parasites, or qualitatively changed but under different conditions than were tested here. We can nevertheless conclude from our experiments that PfeIK1 is not required for gametocytogenesis *in vitro*.

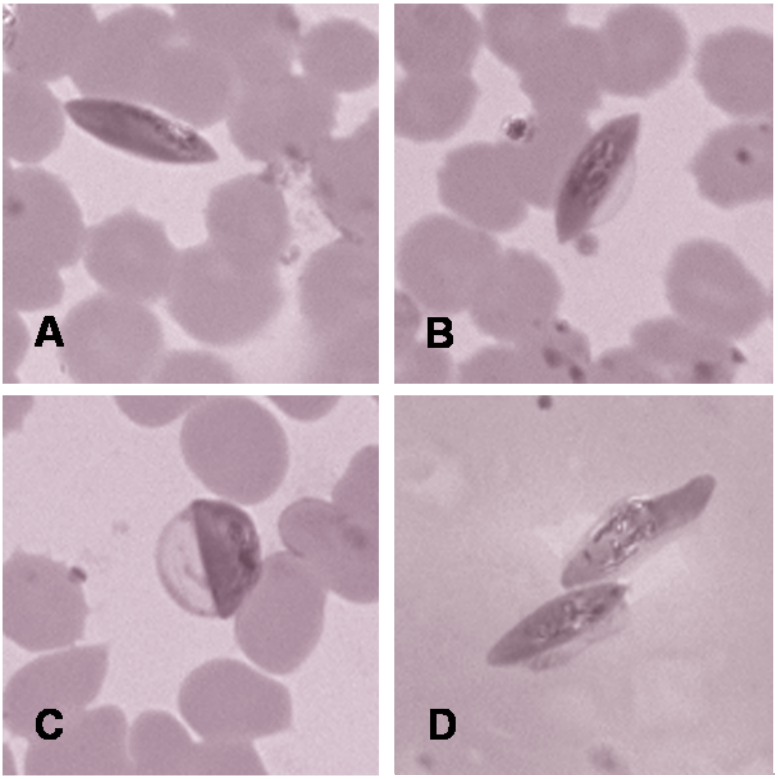

Figure 4-12: Giemsa stained *pfeik1*⁻ gametocytes.
A range of gametocyte developmental stages are shown; A: stage IV, B: stage III, C: stage: II, D: stage V or mature gametocytes.

4.2.3 PfeIK1 is not required for infection of mosquitoes or progression to sporozoites

Since I had not detected a critical role of PfeIK1 in asexual stages or gametocytogenesis, I continued by investigating the viability of *pfeik1*⁻ parasites in mosquito infection experiments. First, I obtained qualitative evidence that male *pfeik1*⁻ gametocytes were competent to continue development to produce gametes (*in vitro* exflagellation, data not shown). Subsequently, *pfeik1*⁻ gametocytes were fed to *Anopheles gambiae*, and their infectivity examined by dissecting the parasite fed mosquitoes for oocysts and sporozoites, after the appropriate development periods (10 and 16 days post feeding, respectively) had elapsed. As shown in Table 4-1 both the *pfeik1*⁻ clones tested were able to infect mosquitoes, and in the one instance I was able to investigate, the infection resulted in development of sporozoites that reached the salivary

glands. The proportion of sporozoite-positive mosquitoes was not significantly different from the proportion of infected mosquitoes (p= 0.74).

Clone	Exp. No.	Infection prevalence	Median oocyst no. per infected mosquito (range)	Sporozoite presence
C1	1	15% (2/14)	1.5 (0-2)	ND
C8	1	44% (7/16)	10 (0-34)	37% (7/19)
C1	2	not fed, insufficient gametocytes	ND	ND
C8	2	20% (5/25)	2 (0-5)	ND

Table 4-1: Mosquito infection with *pfeik1*$^{-}$ parasites.
The two independent clonal lines C1 and C8 were stimulated to produce gametocytes on two separate occasions (Experiments 1 & 2). Experience has shown that a gametocytaemia lower than ~0.4% is extremely unlikely to be infectious, such that clone C1, experiment 2 was not continued. When a feed took place, the mosquitoes were dissected 10 days later when midguts were examined and oocysts counted. The infection prevalence is given, followed by the number of mosquitoes this observation derives from. The median number of oocysts per infected mosquito is shown, followed by the range in number of oocysts found on individual midguts. If examination of midguts established that the parasites were infectious, and sufficient mosquitoes had fed to be able to continue the experiment for a further 6 days, the remaining mosquitoes were then dissected and examined for presence of sporozoites in the salivary glands. Mosquitoes were scored as positive or negative for sporozoites. ND= not done.

It is clear this experiment has limitations: the first is the lack of wild-type 3D7 control. Long term *in vitro* culture of *P. falciparum* tends to result in the loss of the parasites' ability to produce gametocytes at all, or loss of their infectious capacity. In this instance I maintained sham-transfected 3D7 in culture along side the *pfeik1*$^{-}$ parasites throughout the transfection and cloning process; consequently all these parasites had been in culture for ~7 months before mosquito experiments could commence. It was therefore not unduly surprising to find that sham-transfected parasites were unable to produce gametocytes.

Without a wild-type control I cannot investigate whether the prevalence or intensity of infection is changed by *pfeik1* disruption, however experience suggests that both levels observed here are within the expected range for such 'old' parasites. It is possible that the fact that the *pfeik1*$^{-}$ could still produce gametocytes is specifically mediated by the knock out, however I suspect it is most likely a chance event.

It was important to verify that the parasites had had not reverted to a wild-type *pfeik1* locus, which remains a possibility when using the single cross-over strategy. To this end I collected midguts from infected mosquitoes 10 days post feeding, extracted genomic DNA and carried out nested PCR (one round of PCR is not sufficient when starting from the small amount of DNA present in these samples). The wild-type locus could be amplified as expected from mosquitoes infected with wild-type 3D7 parasites, but not from those infected with *pfeIK1*$^{-}$ C8 parasites (Fig. 4-13 lower panel, lanes 1, 3, 5). Conversely, the amplicon diagnostic of the 3' integration event could only be amplified from midguts of *pfeIK1*$^{-}$ C8-infected mosquitoes, but not from mosquitoes infected with wild-type parasites (Fig. 4-13 lanes 2, 4, 8). The wild-type infected mosquitoes used here came from a separate experiment and were used only to control for PCR amplification of the wild-type amplicon from infected midguts (and did not serve as controls for infection prevalence; see above).

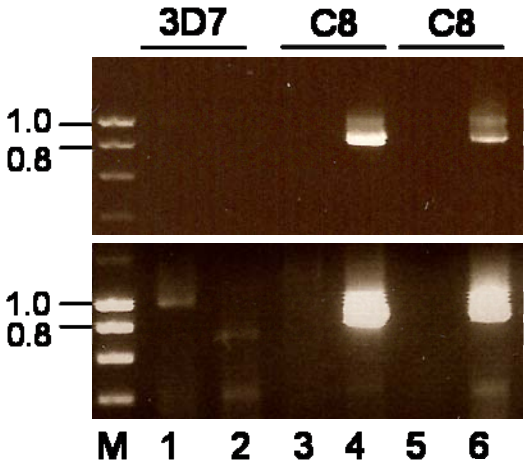

Figure 4-13: PCR analysis of *pfeik1*$^{-}$ infected mosquito midguts.
Nested PCR was used to analyse presence of the wild-type locus; lanes 1, 3, 5 using primers 1 + 2, followed by 5 + 6; expected size =1012bp, and the 3' integration event; lanes 2, 4, 6 using primers 3 + 2, followed by 7 + 6, expected size = 889bp. The upper panel shows the 3' integration amplicons (lanes 4 & 6); the lower panel is a longer exposure to reveal the wild-type amplicon (lane

1). Primers used are as follows: 1= 146, 2= 148, 3= 169, 4= 170, 5= 979, 6= 980, 7= 179, see Table 6-2, appendix, for details. Primer positions are shown in Figure 4-2.

4.2.4 Expression levels of remaining PfeIF2α kinases in pfeik1⁻ *parasites.*

It is conceivable that the parasite can sustain disruption of one gene by modulating the expression of another gene that performs a related function. To address this I aimed to examine protein levels of the remaining eIF2α kinases, after the *pfeik1* gene had been disrupted. At the time of writing these experiments were not completed. However, Figure 4-14 suggests that expression of PfPK4 may be increased in asexual *pfeik1*⁻ clones is in comparison to wild-type parasites, which will be an important consideration for further analysis of the *pfeik1*⁻ parasites. I am cautious in interpreting this result since I have shown that PfPK4 levels are higher in trophozoites and schizonts (3.2.2), so that the difference observed between wild type and *pfeik1*⁻ parasites in Figure 4-14 could be due to a different mix of life cycle stages at the time of parasite harvest; this must now be confirmed with synchronized parasites.

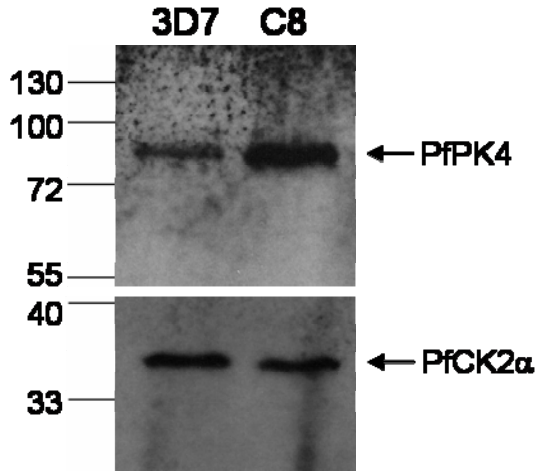

Figure 4-14: Western blot showing expression of PfPK4 in *pfeik1*⁻ parasites.
Parasite pellets of wild-type parasites (3D7) and *pfeik1*⁻ clone C8 were resuspended in parasite solubilising buffer before addition of reducing Laemlli buffer. Equal amounts of protein were separated by SDS-PAGE and transferred to nitrocellulose. The membrane was cut to probe the upper part with anti-PfPK4, while the lower part provided a loading control with anti PfCK2α.

Further experiments to complete this analysis would be to examine expression of PfeIK2 and PfPK4 in *pfeik1*$^{-}$ gametocytes, which could be purified from asexual stages using a Percoll gradient. Furthermore, it is also possible that in the absence of PfeIK1, expression of PfeIK2 could be induced in asexual stages.

4.3 PfeIK2

4.3.1 PfeIK2 is not required for asexual growth

As PfeIK2 is not expressed in asexual stages (3.4.2.1) we predicted that it would be possible to generate PfeIK2 knock-out parasites. I proceeded to two independent transfection experiments using the pCAM-BSD-*pfeik2* plasmid (Fig. 1-3), from which two independent series of clones were obtained by limiting dilution. PCR analysis of five clones (Fig. 4-15) shows that PfeIK2 is indeed dispensable for asexual growth; C3 and F12 are independent from F4 and H1 and D7. In each case the wild type amplicon is only amplified from the wild-type 3D7 parasites, but not from any of the *peik2*$^{-}$ clones. Similarly, the amplicons diagnostic of the gene disruption plasmid, and the 5' and 3' boundaries of the integrated plasmid can only be amplified from *peik2*$^{-}$ clones, and not from wild-type parasites. The *peik2* locus has not been disrupted in clone D7 hence amplicons for the wild-type and the gene disruption plasmid are seen in lanes 21 and 22 respectively, but not for the integrated plasmid in lanes 23 or 24.

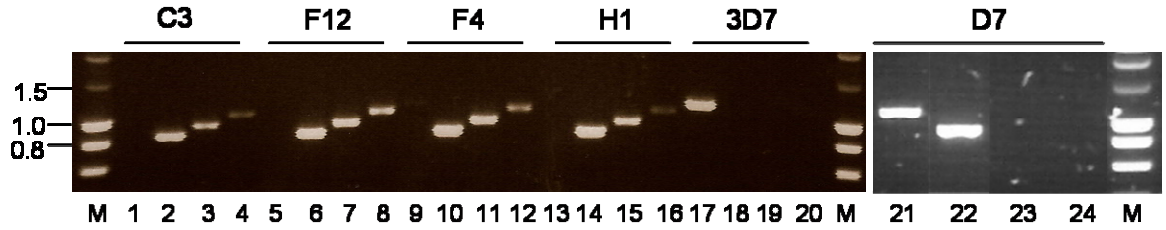

Figure 4-15: PCR analysis of *pfeik2*$^{-}$ clones.
Lanes 1, 5, 9, 13, 17 & 21 are diagnostic of the wild-type locus: primers 1 + 2 = 1134bp, lanes 2, 6, 10, 14, 18 & 22 are diagnostic of the transfection plasmid: primers 3 + 4 = 829bp, lanes 3, 7, 11, 15, 19 & 23 are diagnostic of 5' integration: 1 + 4 = 923bp, lanes 4, 8, 12, 16, 20 & 24 are diagnostic of 3' integration: 3 + 2 = 1066bp. Primers are as follows: 1= 185, 2= 150, 3= 169, and for primer 4, two adjacent sequences were used; either 170 for amplification of the episome, or 168 for amplification of the 5' integration amplicon, see Table 6-2, appendix for details. Primer positions are indicated in Figure 4-1.

The genotype of *peik2*$^-$ clones was verified by Southern blot; digestion with *Hind*III and *Nco*I yields a 6635bp fragment containing the wild-type locus, a 5650bp fragment that contains the 5' boundary of the integrated plasmid, and a 5225bp fragment containing the 3' boundary. The 4239bp band derives from linearised plasmid or from digestion of concatemers of plasmid (which may or may not be integrated into the chromosome) (Figs. 4-16 & 4-17). One of the clones shown here (D7) contains the gene disruption plasmid, but has not integrated it into the genomic locus so shows only the wild-type and plasmid bands.

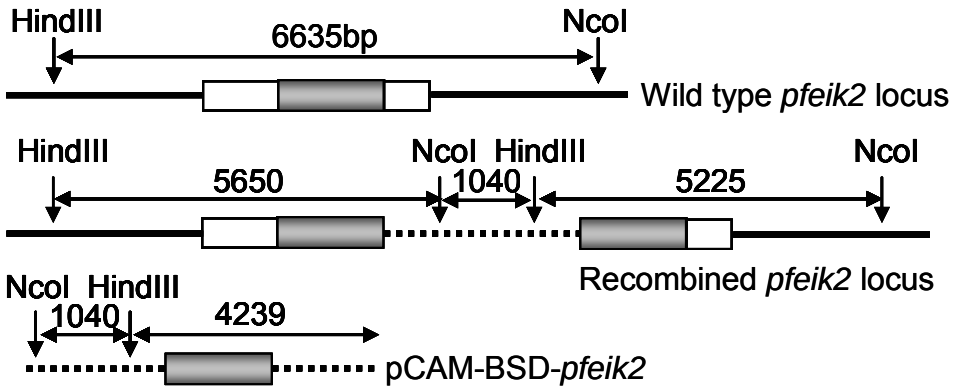

Figure 4-16: Schematic for *pfeik2*$^-$ Southern blot.
The fragments expected following *Hind*III/*Nco*I digestion of the wild-type *pfeik2*$^-$ locus (top), disrupted *pfeik2* locus (middle) and *pfeik2* gene disruption plasmid (bottom), are shown.

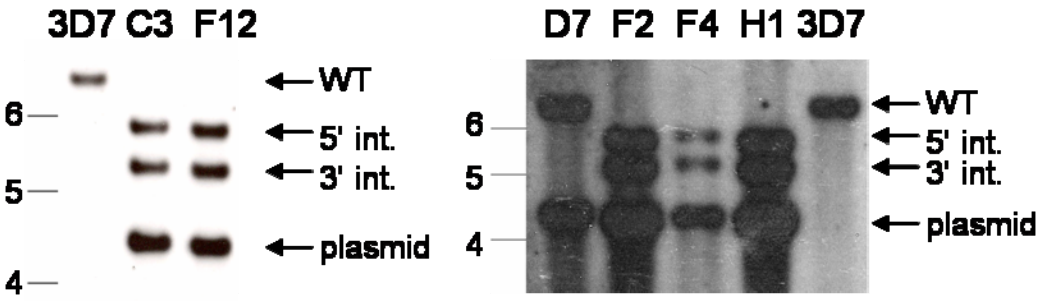

Figure 4-17: Southern blot analysis of *pfeik2*$^-$ clones.
Several clones from two independent populations were analysed. Fragments illustrated in Figure 4-16 are marked here: WT: 6635bp, 5' integration: 5650bp, 3' integration 5225 bp and the transfection plasmid 4239bp. Positions of co-migrating markers are indicated on the left of each gel.

4.3.2 PfeIK2 is not required for gametocytogenesis

Since PfeIK2 is expressed in gametocytes but not asexual stages, I was more interested to investigate whether gene disruption had any effect on the parasites during sexual development. I used standard methods to produce *pfeik2*$^{-}$ gametocytes (Carter et al., 1993), which as shown in Figure 4-18 are morphologically normal and span all developmental stages. Further, that both male and female gametocytes were produced by the *pfeik2*$^{-}$ clones was ascertained by their ability to productively infect mosquitoes (4.3.3). PfeIK2 therefore has no apparent essential role in gametocytogenesis.

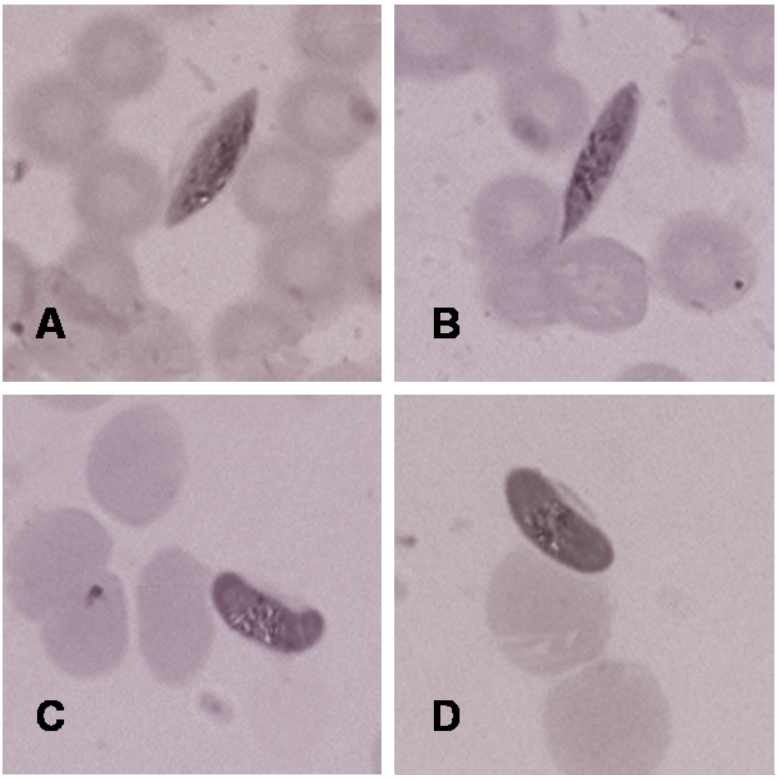

Figure 4-18: Giemsa stained *pfeik2*$^{-}$ gametocytes.
A range of developmental stages is shown; A: stage III, B: stage IV, C: stage V, D: mature gametocyte.

4.3.3 PfeIK2 is not required for infection of mosquitoes or progression to sporozoites

As with PfeIK1, I wanted to investigate whether disruption of PfeIK2 impaired the ability of the parasite to infect mosquitoes. *pfeik2*$^-$ gametocytes were fed to *Anopheles gambiae* that were dissected in order to count oocysts on midguts 10 days post feeding, or 16 days post feeding for sporozoites in the salivary glands. As shown in Table 4-2 *pfeik2*$^-$ parasites are able to infect mosquitoes and parasite development can proceed, resulting in sporozoites invading the salivary glands. In experiment 1 we compared the prevalence of infection between *pfeik2*$^-$ H1 and wild-type; in this instance there was no reduction in the ability of *pfeik2*$^-$ parasites to infect mosquitoes compared to wild-type parasites ($p=0.05$). Indeed, infection with wild-type parasites yielded fewer oocysts/sporozoites than infection with *pfeik2*$^-$ parasites. It seems unlikely that the loss of PfeIK2 has rendered the parasites more infectious; this experiment would need to be repeated several times to be able to demonstrate such an effect. In the one experiment carried through to sporozoite stage, a significantly smaller proportion of mosquitoes contained sporozoites, than oocyts ($p=0.003$), suggesting sporozoite development might be impaired. Clearly this is a single small scale experiment and would require verification. However, it is conceivable that there could be an important role for PfeIK2 in the development of sporozoites inside oocysts, or in their ability to reach the salivary glands.

It took only ~3 months from the transfection procedure to generate one set of *pfeik2*$^-$ 'clones' ready for mosquito infection; the results shown here are for 2 'clones' (F4 & H1) derived from this population and compared with sham-transfected 3D7 parasites maintained in culture over the same period. I recognize that F4 and H1 may not be truly independent, since they derive from the same transfection experiment; however, use of two parasite lines provided some control for experimental variation, and for the possibility that one line could have lost the ability to produce gametocytes (or subsequent functions) after dilution cloning. It required ~ 7months of culture to generate the second, independent set of *pfeik2*$^-$ lines, along side *pfeik1*$^-$ parasites and the sham-transfected 3D7 parasites that had lost the ability to produce gametocytes

(discussed in 4.2.3); these *pfeik2*$^-$ parasites were also unable to produce gametocytes.

Clone	Exp. No.	Infection prevalence	Median oocyst no. per infected mosquito (range)	Sporozoite presence
F4	1	Insufficient gametocytes to feed	ND	ND
H1	1	84% (21/25)	3 (1-30)	42% (10/24)
3D7	1	57% (13/23)	2 (2-41)	ND
F4	2	22% (6/27)	2 (1-7)	ND
H1	2	0% (0/21)	0 (0)	ND
3D7	2	0% (0/24)	0 (0)	ND

Table 4-2: Mosquito infection with *pfeik2*$^-$ parasites.
Two *pfeik2*$^-$ clonal lines, F4 and H1 were stimulated to produce gametocytes on two separate occasions (experiments 1 & 2). Experience has shown that a gametocytaemia lower than ~0.4% is extremely unlikely to be infectious, such that clone F4, experiment 1 was not continued. When a feed took place the mosquitoes were dissected 10 days later, midguts were examined and oocysts counted. The infection prevalence is given, followed by the number of mosquitoes this observation derives from. The median number of oocysts per infected mosquito is shown, followed by the range in number of oocysts found on individual midguts. If examination of midguts established that the parasites were infectious, and sufficient mosquitoes had fed to be able to continue the experiment for a further 6 days, the remaining mosquitoes were dissected and examined for presence of sporozoites in the salivary glands. Mosquitoes were scored as positive or negative for sporozoites. Note that parasite lines F4 and H1 are not truly independent clones as they derive from the same population.

Genomic DNA was extracted and nested PCR was performed to verify that *pfeik2*$^-$ infected mosquitoes had retained their disrupted genotype. Using a set of well characterized sensitive primers designed to amplify the *pfmdr* gene (Duraisingh et al., 2000) I was able to confirm that parasite DNA was present in both the wild-type and *pfeik2*$^-$ infected midguts (data not shown). Furthermore, in support of the maintainance of the disrupted locus, a single round of PCR was sufficient to amplify the wild-type locus from wild-type infected mosquitoes,

while no amplicon was detected in *pfeik2*$^{-}$ infected mosquitoes (data not shown). Although I was unable to amplify the fragments containing either the 5' or 3' boundaries of the integrated plasmid by nested PCR (data not shown), I suspect this is due to differences in the sensitivity of the primers used to amplify the different loci.

We consider that the probability of reversion to the wild-type locus occurring during development in the mosquito is sufficiently small to result in no more than one or two oocysts per midgut. Therefore, since I observed greater numbers of oocysts than this in several midguts and as the wild-type locus was readily amplified from wild-type, but not from *pfeik2*$^{-}$ infected mosquitoes this suggests that the parasites had indeed retained the *pfeik2*$^{-}$ genotype.

Taken together, these results strongly suggest that PfeIK2 does not play an essential role in the developmental stages required to establish mosquito infection, but raises the interesting possibility that it may perform a key function during oocyst maturation or subsequent sporozoite migration.

4.4 PfPK4

4.4.1 PfPK4 is essential for asexual growth

PfPK4 is expressed in asexual stages (3.2.2); to address whether it performs an essential function in the life cycle I used the plasmid shown in Figure 4-4 to attempt to disrupt the gene by single cross-over. Three separate transfections were performed on different occasions; in each case a blasticidin-resistant population was obtained. However after at least six months in culture I never saw evidence of integration of the construct into the *pfpk4* locus, (Figs. 4-19 & 4-21). PCR analysis of one representative population is shown in Figure 4-19; an amplicon diagnostic of the wild-type locus was amplified from both the transfected population and wild-type parasites (lanes 1& 5, Fig. 4-19), demonstrating that wild-type parasites were still present in both populations.

The amplicon diagnostic of the gene disruption plasmid was amplified, as expected from the transfected parasites, but not from wild-type parasites (lanes 2 & 6, Fig. 4-19). If integration occurred it would have been detected as a 3kb band in lane 3, and a 1.5kb band in lane 4; this was never seen, suggesting an essential role for PfPK4 in the asexual life cycle.

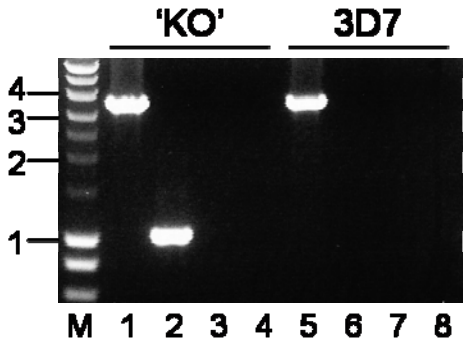

Figure 4-19: PCR analysis of attempted disruption of *pfpk4*.
Lanes 1 & 5, WT primers 1+ 2, expected size = 3508bp, lanes 2 & 6 episome: = 1054bp, lanes 3 & 7 5' integration = 3069bp, lanes 4 & 8 3' integration = 1474bp. Primers used were as follows: 1= 161, 2= 154, 3= 167, 4= 168, see Table 6-2, appendix for details. Primer positions are indicated in Figure 1-1.

To verify the PCR data I also analysed the blasticidin-resistant populations transfected with the *pfpk4* gene disruption plasmid by Southern blot. *Eco*RI digestion yields the fragments illustrated in Figure 4-20; the wild type locus at 3347bp is detected in both transfected ('KO') and wild-type (3D7) parasites, confirming that wild type parasites are still present in the transfected population. The gene disruption plasmid gives rise to the expected 2480 bp fragment in the transfected parasite sample. If integration had occurred two intermediate sized fragments would be present, at 2832 bp for the 5' truncated copy, and 3015 bp for the 3' truncated copy; these bands were never observed, confirming the PCR data. Together these data suggest that PfPK4 performs an essential function in the asexual replication cycle.

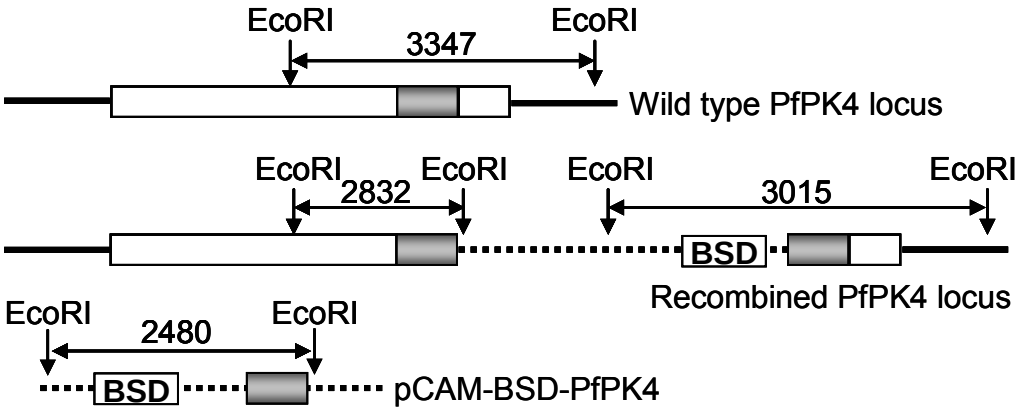

Figure 4-20: Schematic of expected fragments on Southern blot analysis of *pfpk4*.
*Eco*RI digestion results in a 3347bp fragment from the wild-type locus (top), a 2832bp fragment if 5' integration occurs and a 3015bp fragment if 3' integration occurs, and the locus is disrupted (middle), the 2480bp fragment derives from the digested gene disruption plasmid.

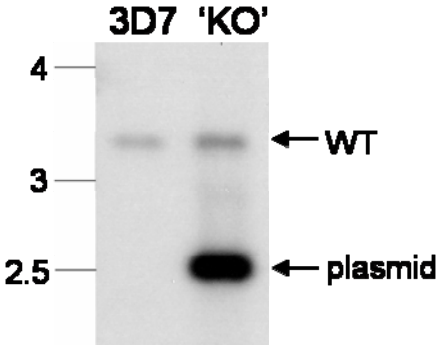

Figure 4-21: Southern blot analysis of attempted *pfpk4* disruption.
The left hand lane contains wild-type parasites (3D7); the right hand lane contains parasites transfected with the *pfpk4* disruption construct ('KO'), sizes of co-migrating markers are shown on the left. Fragments corresponding to the wild-type locus (WT) and gene disruption plasmid (as shown in Figure 4-20) are indicated.

As discussed in section 4.1, it is important to verify that inability to disrupt the function of a gene is not due to an inability to target the locus. I elected to use the circumstantial evidence provided by the 3' tagging strategy (due to the 9.2kb size of the coding region of *pfpk4*, it would have been very difficult to implement a complementation strategy as described for other, smaller protein kinases such as Pfmap-2 and PfPK7 (Dorin-Semblat et al., 2007, Dorin et al., 2005)).

Wild-type parasites were transfected with a plasmid containing the 3' end of *pfpk4* without the stop codon, and either a double HA epitope, or a GFP coding sequence (Figs. 4-6 & 4-7). In contrast to the lack of integration of the gene

disruption plasmid, blasticidin-resistant populations were obtained that rapidly showed integration of the gene modification plasmids (Fig. 4-22). Analysis of both HA and GFP-transfected populations by PCR (Fig. 4-5, for schematic) reveals presence of all the expected amplicons for integration (Fig. 4-22, lanes 6-8 and 10-12). This provides evidence that *pfpk4* can be targeted for recombination if the locus modification does not cause loss-of-function, and therefore supports the conclusion that the *pfpk4* gene cannot be disrupted due to an essential function in asexual replication.

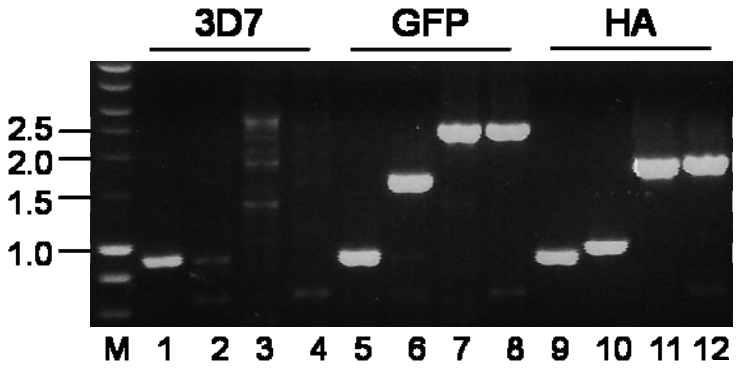

Figure 4-22: PCR analysis of integration of *pfpk4* 3' tags.
Lanes 1, 5, 9: 3' fragment of wild type gene used in plasmid, such that amplicons in lanes 5 and 9 may derive from wild type, integrated, or free plasmid (1+ 2 = 898bp), lanes 2, 6, 10: 3' integration (1+ 3, GFP = 1652bp, HA = 1000bp), lanes 3, 7, 11: 3' integration (1 + 4, GFP = 2504, HA = 1853), lanes 4, 8, 12: 3' integration (1+ 5, GFP = 2530, HA = 1879bp). Primers used to analyse integration of the 3' tags are as follows: 1= 177, 2= 154, 3=275, 4=170, 5= 168; see Table 6-2, appendix for details. Primer positions are illustrated in Figure 4-5.

Southern blot analysis was used to confirm the genotypes of the *pfpk4* HA and GFP-transfected parasites. As expected, the fragments obtained by *Eco*RI digestion of the integrated locus (Fig. 4-23) are seen in both HA and GFP transfected parasites, but not wild-type (Fig. 4-24). The analysis was performed on uncloned populations, such that the wild-type locus is still present in the transfected populations (Fig. 4-24). Provided the tags do not impair the function of PfPK4 it is expected that the integrated parasites will overgrow parasites that carry the drug resistance cassette on the episome, since unlike the genomic copy, this will not segregate equally to all daughter merozoites. Figure 4-24 shows that in the HA transfected parasites the wild-type band is dramatically reduced in intensity compared to the two bands diagnostic for integration in this

lane, or the wild-type band in the other two samples, suggesting that integrated parasites are indeed able to overgrow the wild-type parasites.

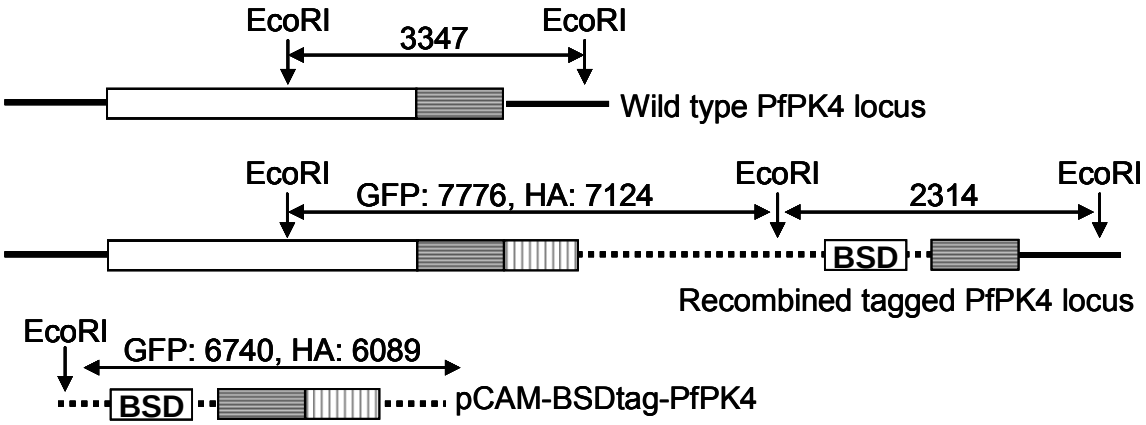

Figure 4-23: Schematic of expected sizes for Southern blot analysis of *pfpk4* 3' tags.
*Eco*RI digestion will yield the following fragments: wild-type: 3347bp; 5' integration: 7776bp for GFP transfected parasites, 7124bp for HA transfected parasites; 3' integration: 2314bp for both HA and GFP transfectants; transfection plasmid: 6740bp for GFP and 6089bp for the HA construct.

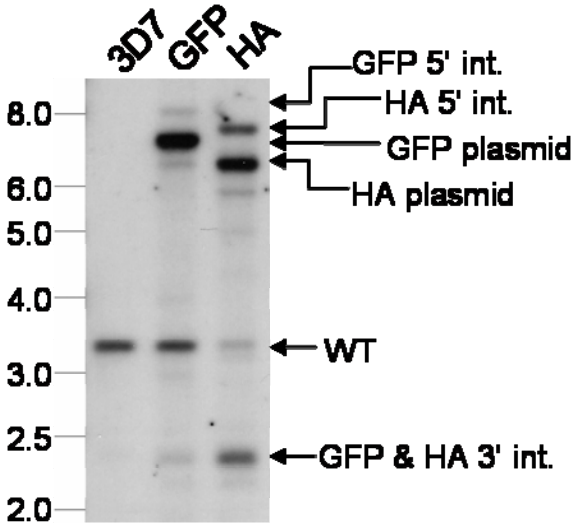

Figure 4-24: Southern blot analysis of *pfpk4* 3' tag populations.
Left lane: wild-type 3D7 parasites, centre: pCAM-BSD-*pfpk4*GFP transfected parasites, right: pCAM-BSD-*pfpk4*HA transfected parasites. The expected fragments diagnostic of the parasite genotypes illustrated in Figure 4-23 are indicated on the right. Sizes of co-migrating markers are shown on the left.

In addition to analysis of the locus by PCR and Southern blot, I was also interested to know whether functional PfPK4 is expressed with the double HA tag. To date I have not been able to show this by western blot. However as discussed in section 3.4.3.3, preliminary IP results suggest that the tagged protein is expressed and active.

4.5 Discussion and Perspectives

4.5.1 PfeIK1

It would be informative to compare the prevalence and intensity of *pfeik1*$^-$ mosquito infections with those of wild-type parasites, as it remains possible that their infectious capacity is reduced; this would require new transfections in the hope of integration occurring more rapidly in order to limit the effects of prolonged *in vitro* parasite culture on the experiment.

As discussed in section 3.2.1, PfeIK1 is a putative GCN2 orthologue and may therefore play a role in the parasites' response to nutrient deprivation. This is particularly interesting in the context of a recent report that amino acid starvation of *P. falciparum* does result in increased phosphorylation of PfeIF2α (Dan Goldberg, Molecular Approaches to Malaria, Lorne 2008; see our joint manuscript in Appendix 6.3). We are collaborating with the Goldberg lab to investigate this in *pfeik1*$^-$ clones. Whether or not increased phosphorylation of PfeIF2α is observed in *pfeik1*$^-$ parasites (in which, as discussed in section 4.2.4, increased expression of PfPK4 could compensate for loss of PfeIK1) it would be ideal to be able to immunoprecipitate PfeIK1 from starved parasites for *in vitro* kinase assay in order to assess whether it is activated by starvation. Chicken anti-PfeIK1 IgYs have recently been produced by our collaborator Dean Goldring (Pietermaritzbutg), which if specific will provide a useful tool; otherwise the C-terminal tagging strategy deployed for PfPK4 should be used.

4.5.2 PfeIK2

As for PfeIK1, the mosquito infection experiments should be repeated before it can be concluded that PfeIK2 does not play an essential role during sexual development; in particular, PCR analysis of the disrupted *pfeik2* locus from the minute amounts of DNA present in infected midguts must be optimized to enable comprehensive analysis of the genotypes of the oocysts. Furthermore, since evidence suggests PfeIK2 is highly expressed in sporozoites (3.2.2) it would be

fascinating to see if *pfeik2*$^-$ sporozoites are competent to invade and proliferate in hepatocytes; this clearly poses considerable technical challenges, but we are setting up collaborations to try to address this question.

4.5.3 PfPK4

I have presented evidence that PfPK4 is essential for asexual multiplication of *P. falciparum*. However, since I have been unable to generate *pfpk4*$^-$ parasites, I do not have a tool to investigate whether PfPK4 plays a specific role in gametocytogenesis, which we hypothesized as a possible role for the PfeIF2α kinases (1.3.1). It would be interesting to investigate whether the essential functions of PfPK4 occur at particular life cycle stages; several possible strategies could be used to address this. The first is to generate a 'chemical genetics' mutant (Bishop et al., 2001). Briefly, mutation of a large-side chain residue known as the gate-keeper residue (Met2776 in PfPK4) to an amino acid with a small side chain such as glycine sensitizes the enzyme to a specific inhibitor that is too bulky to inhibit wild-type kinases. The Met$\rightarrow$Gly mutant enzyme is predicted to retain activity in the absence of compound. It would be theoretically possible to produce such mutants using the single cross-over strategy employed for gene disruption and tagging; parasite populations could then be synchronized and the inhibitor added at different stages of the life cycle and effects on parasite survival observed. Secondly, a tetracycline inducible system has also been described for *P. falciparum* that could be deployed to express proteins with dominant negative function, or to generate conditional knockouts as has been shown in *T. gondii* (Meissner et al., 2005) (Meissner et al., 2002). Thirdly, use of FKBP destabilization domain-fusion proteins has been described in *P. falciparum* (Armstrong and Goldberg, 2007). Briefly, the FKBP domain promotes degradation of the protein to which it is fused, unless the ligand of the destabilization domain, Shld1, is present. It is therefore possible that the FKBP domain could be integrated at the 3' end of the gene of interest (as described here for HA or GFP, section 4.1) to produce a C-terminal fusion, transgenic parasites would have to be established in the presence of the Shld1, but its removal would activate the destabilisation domain thus creating a conditional knock out.

4.5.4 Expression levels of remaining PfeIF2α kinases, following disruption of one of the three genes.

Section 1.2.4 described initial western blot experiments to investigate the expression of PfPK4 in *pfeik1*$^{-}$ parasites, PfeIK2 could also be investigated in this way. It would also be possible to analyse asexual *pfeik2*$^{-}$ parasites for a change in PfPK4 or PfeIK1 expression. However, since PfeIK2 is not expressed in asexual stages I consider it unlikely that there would be any change in expression of the other eIF2α kinases in these parasites during the asexual cycle. As PfeIK2 is expressed in gametocytes it would be more important to investigate expression of PfPK4 in *pfeik2*$^{-}$ gametocytes. Clearly the same principles apply to the investigation of PfeIK1 expression levels in the absence of PfeIK2; this may now be possible with the very recently acquired chicken IgYs.

Alternative strategies exist to address the possible compensation of knock-out of one kinase by the function of another; one would be to tag the remaining kinase(s) in a knock-out clone, and use the tags to monitor protein expression by western blot as described, and their activity by immunoprecipitation followed by kinase assay. Another, would be to look at localisation of the remaining kinase(s), either with the antibodies to the native proteins, or to tags. Thirdly, attempts to generate double knock-outs of *pfeik1* and *pfeik2* would in principle answer the question of whether one compensates for another, although this would clearly be complicated in mosquito stage experiments due to the problem of lengthy *in vitro* culture that would be required.

4.6 Summary

- Using the single cross over strategy I have shown PfeIK1 and PfeIK2 are dispensable for asexual replication.

- Further, disruption of neither PfeIK1 nor PfeIK2 affects the ability of the parasite to infect mosquitoes and produce sporozoites.

- I provide evidence that PfPK4 is essential for asexual replication.

- Without *pfpk4*$^{-}$ parasites I was unable to determine if PfPK4 plays a specific role in gametocytogenesis.

5 Discussion and conclusions

5.1 Identification of PfeIF2α and its kinases

As discussed above (3.5.1), I have identified the *P. falciparum* orthologue of eIF2α and a phylogenetic cluster of PfeIF2α kinases. Furthermore I have confirmed that PfeIK1 is able to phosphorylate PfeIF2α on Ser 59, providing support for the hypothesis that regulation of translation initiation may occur in *P. falciparum* by this mechanism. However, crucially, I have not verified whether the other two putative PfeIF2α kinases, PfeIK2 and PfPK4, are able to phosphorylate PfeIF2α, because I was unable to produce these two enzymes in the form of active recombinant enzymes. With regard to PfPK4, this is at odds with Mohrle et al. who published activity of PfPK4-His on an eIF2α-derived peptide (Mohrle et al., 1997); the most obvious way to reconcile our different findings is the location of the tag used in recombinant protein production (see below, 5.2.1 for further comment). I have described factors which should be considered prior to any further attempts to express these two proteins in *E. coli* (3.5.1). In addition, as the mammalian and yeast eIF2α kinases dimerize for activity through their accessory domains (reviewed (Mathews, 2007)), it is possible that production of recombinant proteins incorporating more than the kinase domain alone may allow expression of active enzymes. I also described the possibility of using the wheat germ cell free system to produce recombinant PfeIF2α kinases (Sawasaki et al., 2005, Mudeppa et al., 2007). Although the wheat germ system appears attractive, it may also not be practical; if (as seems likely), the wheat eIF2α sequence is as well conserved as rice (Fig. 3-1), it is probable that if the proposed PfeIF2α kinases are indeed active, they will phosphorylate the eIF2α in the cell free system and thus inhibit translation, and therefore their own synthesis.

An alternative approach to identifying the kinase that is responsible for phosphorylation of a given residue has been described by Maly et al. (Maly et al., 2004). In this approach, the residue that is the target for phosphorylation is mutated to cysteine (i.e. Ser59→Cys in PfeIF2α), and a kinase reaction allowed

to proceed containing the Ser-Cys mutant substrate, potential upstream kinases (e.g. a whole cell extract) and a specific crosslinking compound. The crosslinker utilizes on one hand the reactive cysteine that has been introduced into the substrate, and on the other hand a conserved lysine in the catalytic cleft of the kinase, which results in a covalent bond between the substrate and the kinase. The complex can then be purified via a tag in the substrate, and the trapped kinase identified by immunoblotting where there are known candidates, or mass spectrometry if there are not.

5.2 Investigation of the role of PfeIF2α kinases

5.2.1 Activation stimuli

I have presented preliminary data showing that PfPK4-HA can be immunoprecipitated from parasite extracts and used in *in vitro* kinase assays (3.4.3.3), an approach that has been successfully used to show activity of two divergent eIF2α kinases in *T. gondii* (Narasimhan et al., 2008). This approach may be effective to verify whether PfPK4-HA can phosphorylate PfeIF2α by using GST-PfeIF2α as the substrate in *in vitro* kinase assays, including the Ser59→Ala mutant as a control to confirm the target of phosphorylation. These experiments are required to confirm and extend previously published results; Mohrle et al. (1997) described activity of PfPK4-His against an eleven-residue peptide representing the human eIF2α sequence containing the target serine (Ser51 in human) (Mohrle et al., 1997). The data they presented suggests that the recombinant protein was quite active, since other eIF2α kinases have been found to have 1000-fold less activity on a short peptide, than on the whole eIF2α molecule (Mellor and Proud, 1991) (subsequently explained by the crystal structure of PKR and eIF2α, which shows the large surface area involved in the kinase-substrate interaction (3.1) (Dar et al., 2005)). However, the Mohrle et al. study did not include a kinase-dead mutant, and was carried out by scintillation counting, as against SDS-PAGE followed by autoradiography, so that the identity of the phosphorylated substrate remains uncertain.

Similarly, immunoprecipitation from gametocyte extracts can be tried with our anti-PfeIK2 antibody, but the possibility remains that the kinases may be maintained in an inhibited condition, so that no activity would be detected.

5.2.1.1 Starvation

I suggest that such immunoprecipitation experiments should be carried out in conjunction with investigation of activation stimuli. It is possible to detect phosphorylation of PfeIF2α by immunoblotting after amino acid deprivation of the parasites (Babbitt & Goldberg, MAM 2008; our joint manuscript, Appendix 6.3). We hypothesize that since PfeIK1 appears to be the orthologue of GCN2, then it will be the kinase responsible for mediating this starvation response. The *pfeik1*$^{-}$ parasites are one useful tool with which to investigate this (in progress). It would clearly be advantageous to be able imunoprecipitate PfeIK1 from starved parasites for *in vitro* kinase assay; either a very recently available anti-sera will facilitate this, or PfeIK1-HA parasites should be generated. Both PfeIK2 and PfPK4 could be investigated in this way.

5.2.1.2 Oxidative stress

Consideration of other candidate stress stimuli should take into account the conditions in which the parasite must survive. For example, as discussed previously (3.5.2), *P. falciparum* is vulnerable to oxidative stress, and has limited capacity to neutralize damaging oxidative agents (Muller, 2004); it would not be surprising therefore, to find additional mechanisms that function to protect the parasite in the event of redox mechanisms being overwhelmed. It has been shown in other eukaryotic systems that arsenite mediates oxidative stress (Patel et al., 2002, Novoa et al., 2003), and that HRI is activated under these conditions as part of the cellular stress response (Lu et al., 2001). In view of speculated HRI-like activity in *P. falciparum* (3.5.2), (and unknown mechanism of HRI activation by arsenite (Lu et al., 2001)), but also the interesting finding that arsenite induces differentiation from tachyzoites to bradyzoites in conjunction with eIF2α phosphorylation in *T. gondii* (Narasimhan et al., 2008), this is certainly a candidate stressor to investigate.

5.2.1.3 Heat shock

I am intrigued by the possibility that *P. falciparum* must regulate its functions in response to the greater than 10°C difference between its mosquito vector and human host, in addition to the repeated exposure to heat shock on account of the febrile episodes that are part of malaria pathology. In view of this substantial exposure to heat shock, inherent in the parasite life cycle it is not surprising that the major classes of heat shock proteins are well represented in *P. falciparum* (reviewed (Acharya et al., 2007)). In addition to the characterized activation stimuli of eIF2α kinases (1.8.3.2), other stress stimuli including heat shock are also known to induce phosphorylation of eIF2α (Brostrom and Brostrom, 1998). It has been demonstrated that in erythroid cells HRI is the principle eIF2α kinase activated by heat shock. Furthermore, evidence suggests that hsp90 and hsc70 are required for this effect (Uma et al., 1997, Uma et al., 1999, Lu et al., 2001). Heat shock is therefore also a candidate activator for the PfeIF2α kinases.

5.2.2 Complementation of yeast mutants

I have provided evidence that components of the mechanism for phosphorylation of eIF2α are conserved in *P. falciparum*, and that therefore translation may be regulated in response to stress; this remains to be shown experimentally. Since *S. cerevisiae* has only a single eIF2α kinase (GCN2) that is not essential for growth under normal conditions, mutant strains have been established that enable analysis of other eIF2α kinases (Vattem et al., 2001), including the divergent eIF2α kinases of *T. gondii* (Sullivan et al., 2004) and *T. brucei* (Moraes et al., 2007). There are two key isogenic strains in which GCN2 has been deleted, one expresses wild type eIF2α (such as strain H1894), the other expresses the Ser51→Ala mutant of eIF2α that cannot be phosphorylated (strain J82, SUI2-S51A); a galactose-inducible promoter is used to express a GST fusion of the heterologous eIF2α kinase. If the exogenous kinase is active, the resulting hyperphosphorylation of eIF2α results in a significant reduction in translation initiation and reduced growth. The Ser51→Ala strain is used to

confirm that any growth defect observed in the GCN2Δ strain is mediated by phosphorylation at this position; growth of the Ser51→Ala strain is expected to be unaffected by the heterologous kinase. We initiated a collaboration to carry out these experiments with the PfeIF2α kinases; initial trials were unsuccessful (R. Wek lab), likely due to poor expression of the *P. falciparum* proteins in yeast. Just as it may be necessary to improve prokaryotic expression of AT-rich plasmodium genes, by use of cells with additional tRNA genes, so codon optimisation could be required for expression of the same genes in yeast. PfeIK1 and PfeIK2 have more modest sized catalytic domains (than PfPK4); gene synthesis could be a practical approach. If expression in yeast is achieved then the Ser51→Ala strain can also provide a useful means of producing GST-tagged proteins for *in vitro* kinase assay.

5.2.3 Effect of phosphorylation of PfeIF2α on translation?

Three strategies are under consideration to address whether certain stress conditions influence translation rates in *P. falciparum*, and whether this is via phosphorylation of PfeIF2α.

The first strategy is to use published methods to set up an *in vitro* translation system using *P. falciparum* components (Surolia and Padmanaban, 1991) (Ferreras et al., 2000). Theoretically, the system described by Ferreras et al. 2000 could be generated from parasites cultured under normal or stress conditions, or from wild type or *pfeik*$^{-}$ parasites. Use of an *in vitro* system has the advantage of being more readily manipulated, for example by supplementing with a recombinant PfeIK, or potential inhibitor (Ferreras et al., 2002). In the second strategy, protein production can be examined by replacing the methionine and cysteine in the culture medium with [^{35}S]Met/Cys and monitoring [^{35}S] incorporation; it is expected that if a stress stimulus leads to phosphorylation of eIF2α and translation arrest, then in the same amount of total protein the stressed sample will only have incorporated a fraction of the [^{35}S], compared to an unstressed sample (Narasimhan et al., 2008). Finally, a third strategy might be to directly address whether phosphorylation of PfeIF2α

is accompanied by a reduction in translation initiation by examining polyribosome profiles. It is expected that in stressed parasites if the eIF2α mechanism is operative a reduction in polysomes will be seen, and free ribosomes and monosomes correspondingly increased (Han et al., 2001, Narasimhan et al., 2008). If this can be shown to be the case, then purifying the polysomes that are maintained in these conditions might allow the identification of the mRNAs that are translated under stress, which would yield interesting information with respect to the mediation of the stress response.

5.3 Perspectives

5.3.1 Phosphoregulation is a two way process.

Phosphorylation is such a widely used post translational signaling mechanism largely because it can be readily reversed by the action of protein phosphatases, resulting in systems that can be tightly regulated. In general, organisms have fewer Ser/Thr phosphatases than their corresponding complement of Ser/Thr kinases (Gallego and Virshup, 2005), and *P. falciparum* is no exception to this (Wilkes, 2008). It is increasingly clear that phosphatases operate as hetero-oligomeric complexes, where the diverse regulatory subunits with which a catalytic subunit associates, provide specificity of action by targeting specific substrates (Barford et al., 1998, Bollen, 2001). Regulation of translation by the dephosphorylation of eIF2α is less well understood than the action of the eIF2α kinases, however it is clear that since the downstream consequences of eIF2α phosphorylation include changes in gene expression, translation must be allowed to continue, if a new complement of proteins is to be produced (Novoa et al., 2003). Interestingly, many viruses can block the activity of PKR and hence phosphorylation of eIF2α, (Mohr, 2007), others prevent translational arrest by modulating dephosphorylation of eIF2α (Mulvey et al., 2003); this contributed to the identification of protein phosphatase 1 (PP1) as the catalytic subunit responsible for eIF2α-P dephosphorylation (He et al., 1997, He et al., 1998). In mammalian cells, growth arrest and DNA damage gene (GADD)34 has been identified as a regulatory subunit of a holophosphatase complex that includes

PP1 and specifically promotes the dephosphorylation of eIF2α *in vitro* (Novoa et al., 2001). Furthermore GADD34 expression is induced by stress downstream of eIF2α kinase activity (the precise mechanism is not know, but it does depend on phosphorylation of eIF2α), thereby orchestrating a programmed shift from translational repression to stress-induced gene expression (Novoa et al., 2003).

P. falciparum has been shown to encode a functional PP1 enzyme (Bhattacharyya et al., 2002), and one interaction and regulatory effect has been identified (Daher et al., 2006). It is expected from the mechanisms of regulation of other eukaryotic phosphatases, and particularly in view of the small size of the *P. falciparum* Ser/Thr phosphatome (Wilkes, 2008), that many more regulatory interactions (that may include a GADD34-like protein) will be found. Recently, the ubiquitously expressed adaptor protein Nck that is composed of Src homology domains, has been shown to reduce eIF2α phosphorylation in mammalian cells, in a stress specific manner (Cardin et al., 2007). Queries of PlasmoDB for Src-homology domains, does not return any matches (Interpro IDs: Src homology-3 domain; IPR001452, SH2 motif; IPR000980, SH3, type-5 bacterial; IPR013667, SH3, type 3; IPR013247, Variant SH3; IPR011511 and Bacterial SH3-like region; IPR003646). As *P. falciparum* does not encode classical tyrosine kinases (Ward et al., 2004) it is not surprising that there are no apparent Src homology domains making it unlikely that this mechanism operates in *P. falciparum*.

5.3.2 Gametocytogenesis; a stress induced response?

As discussed in section 1.3.1, commitment to gametocytogenesis remains an enigmatic process; in particular, although environmental conditions modulate its induction, no single molecule or signalling pathway has been shown to act as an inducing factor (reviewed (Alano, 2007)). *T. gondii* differentiates from rapidly dividing tachyzoites to quiescent bradyzoites on exposure to a number of cellular stresses that also induce phosphorylation of TgeIF2α (Sullivan et al., 2004, Narasimhan et al., 2008). These observations led us to hypothesise that the withdrawal from proliferation and switch to differentiation into gametocytes could represent an analogous series of events in *P. falciparum*, rendering

phosphorylation of PfeIF2α a candidate mediator of this process. Although I have shown that neither PfeIK1or PfeIK2are required for production of gametocytes or subsequent completion of the sexual cycle, our reverse genetics data do not allow us to formally exclude that one of the eIF2α kinases is indeed a mediator of the switch to sexual development. First, the PfPK4 gene cannot be inactivated; it is conceivable that superimposed to its essential function in asexual growth (which we demonstrated), PfPK4 also plays a role in gametocytogenesis (which we cannot demonstrate due to the lack of a *pfpk4*$^{-}$ clone). Second, our preliminary data suggest that *pfeik1*$^{=}$ parasites appear to overexpress PfPK4. This may complement for a function of the former gene in asexual growth or in sexual development.

It remains an open question as to how the observed inducers of gametocytogenesis function. Conditions shown to increase gametocytogenesis, such as sub-lethal concentrations of chloroquine (Buckling et al., 1997) are therefore candidates for inclusion in experiments seeking to identify conditions inducing PfeIF2α phosphorylation and activation of PfeIF2α kinases.

5.3.3 Relative importance of translation control in P. falciparum

When I began this project, the prevailing view was that translation might play a highly significant role in the regulation of *P. falciparum* gene expression (discussed in section 1.7). This was largely based on the small number of identified transcription-associated proteins, and dearth of well conserved promoter elements (reviewed (Coleman and Duraisingh, 2008)). However, these observations did not detract from the unusual, and clearly tightly regulated cascade of gene expression observed through the *P. falciparum* life cycle (Le Roch et al., 2003), or the interesting finding that distinct transcriptional states were observed in clinical isolates that did not correlate with anything previously observed *in vitro* (Daily et al., 2007). Recent discoveries of *cis*-regulatory elements and the ApiAP2 plant-like transcription factors (Balaji et al., 2005) (Young et al., 2008) are calling into question the view that transcriptional control in *P. falciparum* is relatively uncomplicated (reviewed (Coleman and Duraisingh, 2008)). While the evidence that post-transcriptional regulation plays

a key role in *P. falciparum* gene expression still stands, it is unlikely to be as significant as was previously thought.

5.3.4 Search for new therapeutic targets

As outlined in section 1.5.1, regulation of reversible phosphorylation, specifically by targeting kinases is a promising therapeutic approach; the eIF2α are no exception. It has been proposed that inhibition of PERK may synergise with other cancer therapies (Blais and Bell, 2006), however a cautionary note was added recently in view of the heterogeneous nature of tumour cells. PERK activity can promote cell survival, which provides the basis of rationale for its inhibition, however it may also be responsible for maintaining the slow dividing or dormant state of some regions of primary tumours or disseminated cells, such that inhibition would have a harmful effect (Ranganathan et al., 2008). In addition, proof of concept for selectively targeting dephosphorylation has been provided with the identification of salubrinal, a compound that inhibits dephosphorylation of eIF2α; this approach may be beneficial in diseases involving ER stress or viral infection (Boyce et al., 2005).

The underlying aim of our laboratory is to identify new therapeutic targets for the treatment of malaria, via the absorbing route of seeking to decipher events that control proliferation and differentiation in *P. falciparum*; kinases are strong candidates. In the context of this overall aim, I can conclude that PfeIK1 and PfeIK2 are not therapeutic targets, as I have shown they are not required for asexual multiplication, and notwithstanding as yet unidentified essential roles in sporozoites stages, do not have potential as transmission blocking targets either. A possible essential role in exo-erythrocytic (liver) stages would provide rationale for prophylaxis. We are currently establishing a collaboration with a laboratory that has access to infection of hepatocytes with *P. falciparum* sporozoites, in order to assess the ability of the *pfeik1*$^{-}$ or *pfeik2*$^{-}$ sporozoites to establish a productive infection of hepatocytes. On the contrary, due to its apparent essential role in the asexual cycle, PfPK4 is promising, but cannot be pursued until active recombinant protein, the basis of a high throughput screen, can be produced.

6 Appendix

6.1 Biological and chemical reagents

General chemicals were purchased from Sigma.

Biogenes	Custom antibody production
Biorad	Bradford reagent, 30% Acrylamide/Bis mix
Blood transfusion service	Human full blood
Calbiochem	Gentamycin, Blasticidin S hydrochloride
Eurogentec	Smartladder, DNA ladder
Fermentas	PageRuler™ prestained protein ladder
Finnzymes	Phusion DNA polymerase
GE Healthcare	γ-^{32}[P]ATP, Gene Images AlkPhos Direct Labelling and Detection system, Gene-Images CDP-Star detection kit, Amersham Hyperfilm, Hybond-N^{+}
Genscript	PfeIF2α S59 peptide (ILMSELSKRRFR)
GIBCO	RPMI 1640
Invitrogen	DNase I, SuperScript II, T4 DNA ligase
Kodak	Medical X-Ray film
Qiagen	DNA miniprep kit, maxiprep kit, gel extraction kit
New England Biolabs	Restriction enzymes, BSA, Broad Range protein marker

Novagen	pET-28a
Perkin-Elmer	Western Lightning Chemiluminescence reagent Plus
Pharmacia	pGEX-4T3
Promega	pGEM-T easy
Roche	High fidelity polymerase, complete protease inhibitor tablets +/- EDTA
Takara	Ex Taq DNA polymerase

Table 6-1: Supppliers of biological and chemical reagents.

6.1.1 Oligonucleotide primers

Oligonucleotide primers were designed to amplify genes for recombinant protein expression, gene disruption, 3' tagging and sequencing. Where PCR products were to be subcloned into appropriate destination plasmids, the oligonucleotide primers included a 5' extension containing the relevant restriction site.

081	pGEX, GST forward	GGG CTG GCA AGC CAG GTT TGG TGG
082	pGEX, GST reverse	GGG GGA GCT GCA TGT GTC AGC GC
95	SP6	ATT TAG GTG ACA CTA TAG
123	T7	TAA TAC GAC TCA CTA TAG GG
145	PfeIK1 (PF14_0423) full length, forward (*Bam*HI)	G**GG ATC C**AT GAC AAG TGA GGA CAA GAC AGC
146	PfeIK1 (PF14_0423) catalytic domain, forward (*Bam*HI)	GGG G**GG ATC C**AT GGG GAA AAA AAA ACA TGG

147	PfeIK1 (PF14_0423) full length, reverse (*Sal*I)	GGG G**GT CGA C**TT AAA AAT ATT TAA TTA GGT AG
148	PfeIK1 (PF14_0423) catalytic domain, reverse (*Sal*I)	GGG G**GT CGA C**CG TAA AAA GTA CAC TTT CGT G
149	PfeIK2 (PFA0380w) 5' end of longest predictions (*Bam*HI)	GGG G**GG ATC C**AT GCT AAT AAA TAA AAG AAA AAG
150	PfeIK2 (PFA0380w) catalytic domain, reverse (*Sal*I)	GGG G**GT CGA C**TC AAT ATA TAT ATA TAT TTT TTT TTT TC
151	PfeIF2α (PF11_0117) forward (*Bam*HI)	GGG G**GG ATC C**AT GAC TGA AAT GCG AGT AAA AGC
152	PfeIF2α (PF11_0117) reverse (*Sal*I)	GGG G**GT CGA C**TT AAT CTT CCT CCT CCT CGT C
153	PfPK4 entire gene, forward (*Bam*HI)	GGG GG**G GAT CC**A TGT GTA ATT TTA TAA AAA AAG GT
154	PfPK4 catalytic domain, reverse (*Sal*I)	GGG G**GT CGA C**CT ATT TGT CTG CAC CAT TAT TCT C
161	PfPK4 catalytic domain forward (*Bam*HI)	GGG G**GG ATC C**AT GAA AAA ACG GAT ACG TAG TAG T
167	pCAM-BSD forward	TAT TCC TAA TCA TGT AAA TCT TAA A
168	pCAM-BSD reverse	CAA TTA ACC CTC ACT AAA G
169	pCAM-BSD forward, 2	ATT TAT TAA ACT GCA GCC C
170	pCAM-BSD reverse, 2	AAG CTG GAG CTC CAC CGC
171	PfeIF2α S59C, forward	GTC CGA ACT ATG CAA AAG AAG

172	PfeIF2α S59C, reverse	CTT CTT TTG CAT AGT TCG GAC
173	PfPK4 F3, sequencing	GTT CGA GTG CTA GGA ATT TGT C
174	PfPK4 F4, sequencing	GTA GTT GTT ATA GTG CTA GTA G
175	PfPK4 F5, sequencing	GTT TTC GCC GAT AAT GAA GAA TC
176	PfPK4 F6, sequencing	CCA AAT TCT CGA ACC GAA ACG
177	PfPK4 F7, sequencing	GCA GAT GGA ATT GTG TAA AGG
178	PfPK4 F8, sequencing	GGA CAA ATT ATA GGA ACC CCT GG
179	PfeIK1 gene disruption F (*Bam*HI)	GGG G**GG ATC C**GT AAT GAA AGT AAA AAA TAA G
180	PfeIK1 gene disruption R (*Not*I)	GGG G**CG CCG GCG** AGG TGA AAT ATA ATG AAT TGT TCC
183	PfeIK2 gene disruption, forward (*Bam*HI)	GGG G**GG ATC C**AT GAA TAT AAC AAC CAC TTA TTT A
184	PfeIK2 gene disruption, reverse (*Not*I)	GGG G**CG CCG GCG** TGG AGC TGC ATA TAT TTT TGT TCC
185	PfeIK2 catalytic domain, forward (*Bam*HI)	GGG G**GG ATC C**AT GTT CAT AAA ATC ATG TAA TGA TAA AAG C
186	PfPK4 gene disruption reverse (*Bam*HI)	GGG G**GG ATC C**CC AAA TTC TCG AAC CGA AAC G
187	PfPK4 gene disruption reverse	GGG G**CG CCG GCG** TGG TGC TGT ATA ACC AGG GG
195	PfeIF2α S59A forward	GTC CGA ACT AGC CAA AAG AAG

196	PfeIF2α S59A reverse	GTC CGA ACT AGC CAA AAG AAG
197	PfeIK1 K458M forward	CTT ATG CAT TAA TGA TTA TAA G
198	PfeIK1 K458M reverse	CTT ATA ATC ATT AAT GCA TAA G
199	PfeIK2 K157M forward	ATG AAA ATA AGG ATG ATA TTA AAT
200	PfeIK2 K157M reverse	ATT TAA TAT CAT CCT TAT TTT CAT
201	PfPK4 K2177M forward	CCA ACA TAT GCT GTG ATG TTT ATT
202	PfPK4 K2177M reverse	CCA ACA TAT GCT GTG ATG TTT ATT
224	PfeIK2 gene structure long forward (*Bam*HI)	GGG G**GG ATC C**CC AAC AAA TAT ATT ATC ACC ACA AG
225	PfeIK2 gene structure short, forward (*Bam*HI)	GGG G**GG ATC C**AT GTA TTA TTT CAC AAA AGT TGT ATC C
226	PfeIK2 gene structure reverse (*Sal*I)	GGG G**GT CGA C**CG CAA GCA TTT GGT AGG GAA TGC
275	pHGB reverse	CGA ACA TTA AGC TGC CAT ATC C
470	PfPK4 reverse, integral *Bst*API	GGA TTT CTT TTG **GCA TCA GAT GC**A TAG G
486	PfeIK1 Kdead D660N reverse	GAT ATT TGA AGG TTT AAT ATT TCT ATG C
487	PfeIK1 K dead D660N forward	GCA TAG AAA TAT TAA ACC TTC AAA TAT C
589	PfeIK2 intron forward	CTC GAA CCA TCC TAA ATA GCA GAG GAC

635	GFP reverse	CAG GTA GTT TTC CAG TAG TGC
616	PfPK4 3' end forward (*Pst*I)	GGG G**CT GCA G**GA TTG GAG ATT TAG GAT TAG TAC G
617	PfPK4 3' end reverse (*Bam*HI)	GGG G**GG ATC C**TT TGT CTG CAC CAT TAT TCT C
979	PfeIK1 nested forward	CCT TTA ACT GTT CAG TTA GC
980	PfeIK1 nested, reverse	CCA TAG AAG TCG AAA ATG GTT C

Table 6-2: Oligonucleotide primers.
Sequences are given 5' to 3', restriction sites are in bold.

6.1.2 Bacterial strains

XL10-gold	Tet^r Δ(mcrA)183 Δ(mcrCB-hsdSMR-mrr)173 endA1 supE44 thi-1 recA1 gyrA96 relA1 lac Hte [F′ proAB lacI $^qZ\Delta M15$ Tn10 (Tet^r) Amy Cam^r]
BL21-codon plus	
Rosetta 2 (DE3)pLysS (Novagen)	F^- *ompT hsd*S_B(r_B^- m_B^-) *gal dcm* (DE3) pLysSRARE2 (Cam^R)
BL21-CodonPlus-RIL (Stratagene)	E. coli B F– ompT hsdS(rB– mB–) dcm+ Tetr gal endA Hte [argU ileY leuW Camr]

6.1.3 P. falciparum *strain*

3D7

6.1.4 Mosquitoes

Anopheles gambiae

6.1.5 Antibodies

Target	Animal	Dilution	Source
PfeIK2	Rabbit	Serum, 1/1500	Biogenes
PfPK4	Rabbit	Immunopurified, 1/600	Biogenes
ERD2	Rat	Serum, 1/500	Gift from Dr Helen Taylor
GST	Rabbit	Immunopurified 1/5000	Sigma
His	Rabbit	Immunopurified 1/1000	Santa Cruz
HA (either HRP coupled, or not)	Mouse monoclonal	1/1000	Roche

Table 6-3: Primary antibodies.

Target	Dilution	Source
Rabbit IgG	1/10,000	Sigma
Rat IgG	1/15,000	Gift from Dr Helen Taylor
Mouse IgG	1/10,000	Sigma

Table 6-4: Secondary antibodies.

6.2 Buffers, solutions and media

6.2.1 General Buffers

1X PBS	137mM NaCl, 2,7mM KCl, 10mM Na_2HPO_4, 2mM KH_2PO_4

Table 6-5: General buffer composition.

6.2.2 DNA analysis

1X TAE	40mM Tris-Acetate, 1mM EDTA
6X DNA loading dye	0.25% (w/v) bromophenol blue, 0.25% (w/v) xylene cyanol FF, 30% (w/v) glycerol
10X Ex Taq buffer	Contains 20mM $Mg2^+$
20X SSC	0.3M Na_3Citrate, 3M NaCl
Denaturation solution	1.5M NaCl, 0.5MNaOH
Depurination solution	0.25mM HCl
Southern hybridization buffer	Gene Images Alk Phos Hybridization buffer, containing 0.5M NaCl and 4% (w/v) blocking reagent (from kit).
Southern primary wash	1M Urea, 0.1% (w/v) SDS, 50mM Na phosphate (pH 7.0), 150mM NaCl, 1mM $MgCl_2$, 0.2% (w/v) blocking reagent.
Southern secondary wash	50mM Tris base, 100mM NaCl, 2mM $MgCl_2$.

Table 6-6: Composition of buffers used for DNA analysis.

6.2.3 Protein analysis

Coomassie Stain	0.25g Coomassie brilliant blue/ 100ml destain solution
Destain solution	5% acetic acid, 22% methanol
Kinase buffer	20mM Tris-HCl, pH 7.5, 20mM $MgCl_2$, 2mM $MnCl_2$, phosphatase inhibitors (10mM NaF, 10mM β glycerophosphate), 10μM ATP and 0.1MBq [γ-^{32}P] ATP
4X Laemmli loading buffer	40% Glycerol, 20% β-mercaptoethanol (14M stock), 2% SDS, 0.25M Tris, pH 6.9, plus bromophenol blue to a dense colour.
Lysis Buffer 1, for GST-fusion protein preparation	2mM EDTA, 1mM DTT, 1mM BHH, 0.5% (w/v) Triton X100, 1X complete protease inhibitor (Roche), 1mM PMSF
Lysis buffer 2, for His-fusion protein preparation	100mM Tris-HCl pH 7.5, 300mM NaCl, 1X EDTA-free protease inhibitor (Roche), 1mM PMSF.
Parasite solubilisation buffer	0.1% SDS, 0.05% Sodium deoxycholate, complete protease inhibitor (1tablet per 10ml), in PBS
RIPA buffer	150mM NaCl, 20mM $MgCl_2$, 1% NP-40, 0.5% Triton, 30mM Tris (pH 8.0), 10mM NaF, 1mM PMSF, 1X complete protease inhibitor cocktail (Roche).
1X TGS, running buffer	25mM Tris, 192mM glycine, 0.1% (w/v) SDS, pH 8.3

Towbin buffer - standard	25mM Tris pH 8.3, 192mM glycine, 20% methanol,
Towbin buffer - high molecular weight	50mM Tris pH 8.3, 384mM glycine, 20% methanol, 0.1% SDS,

Table 6-7: Composition of buffers used for protein analyses, including recombinant protein preparation.

6.2.4 Bacterial culture

Ampicillin	1000X stock: 50mg/ml in dH_2O
Autoinduction medium	400ml LB, 8 ml 50X 'M' (see below), 8 ml 50X 5052, 0.8 ml 1M MgSO4
Chloramphenicol	1000X stock, 34mg/ml in ethanol
Kanamycin	1000X stock: 10mg/ml in dH_2O
Luria-Bertani medium	10g/L tryptone, 5g/L yeast extract, 10g/L NaCl, pH 7.5
Luria-Bertani agar	Luria-Bertani medium plus 15g/L Tayo Agar
50X 'M'	1.25 M Na_2HPO_4, 1.25 M KH_2PO_4, 2.5 M NH_4Cl, 0.25 M Na_2SO_4
Tetracycline	100X stock: 5mg/ml in ethanol
TFB1	30mM potassium acetate, 10mM $CaCl_2$, 50mM $MnCl_2$, 100mM RbCl, 15% glycerol. pH 5.8 (using 1M acetic acid), filter sterilized
TFB2	100mM MOPS (pH6.5), 75mM $CaCl_2$, 10mM RbCl, 15% glycerol. pH 6.5 (using 1M KOH), filter sterilized

2YT	16g/L tryptone, 10g/L NaCl, 10g/L yeast extract, pH 7.6
50X 5052	25 % glycerol, 2.5 % glucose, 10 % lactose

Table 6-8: Buffers, medium and antibiotics used for bacterial preparation and culture.

6.2.5 P. falciparum *culture*

Blasticidin	2.5μg/ml in complete RPMI
Complete RPMI 1640 medium	For 5L: 79.45g RPMI 1640 powder (GIBCO), 0.25g hypoxanthine (Sigma), 10g $NaHCO_3$, 0.25mg gentamycine sulphate (VWR International), 0.5% w/v of Albumax II-lipid rich bovine serum albumin (Invitrogen), pH 7.2. Note: for gametocyte cultures for mosquito infection Albumax was replaced with heat inactivated (1 hour, 56°C) human AB serum, 10% v/v.
Cytomix	120 mM KCl, 0.15 mM $CaCl_2$, 2mM EGTA, 5 mM $MgCl_2$, 10 mM K_2HPO_4/KH_2PO_4, 25 mM HEPES
Deep freeze solution	4.2 % (w/v) sorbitol, 0.9 % (w/v) NaCl, 28% (v/v) glycerol
Giemsa buffer	21.1mM Na_2HPO_4, 4.4mM KH_2PO_4, pH 7.4
Incomplete medium	For 5L: 79.45g RPMI 1640 powder (GIBCO), 0.25g hypoxanthine (Sigma), pH 7.2.
Malstat reagent	13mg/ml Tris/HCl pH 9.0, 20mg/ml Lithium-L-lactate, 0.66mg/ml APAD, 0.2% Triton X100.

Solution A	12% (w/v) NaCl
Solution B	1.6% (w/v) NaCl
Solution C	0.9% (w/v) NaCl, 0.2% dextrose
Sorbitol	50g/L

Table 6-9: Composition of solutions used for *P. falciparum* culture.

6.2.6 Mosquito breeding

Glucose solution for adult mosquitoes	5.0% (w/v) D-glucose, 0.05% (w/v) PABA

Table 6-10: Solution for mosquitoes.

6.3 Submitted manuscript

PfeIK1, a eukaryotic initiation factor 2α kinase of the human malaria parasite *Plasmodium falciparum*.

Prepared for submission to Malaria Journal, December 2008 (see over).

References

The Protein Kinase Resource.

ABRAHAMSEN, M. S., TEMPLETON, T. J., ENOMOTO, S., ABRAHANTE, J. E., ZHU, G., LANCTO, C. A., DENG, M., LIU, C., WIDMER, G., TZIPORI, S., BUCK, G. A., XU, P., BANKIER, A. T., DEAR, P. H., KONFORTOV, B. A., SPRIGGS, H. F., IYER, L., ANANTHARAMAN, V., ARAVIND, L. & KAPUR, V. (2004) Complete genome sequence of the apicomplexan, Cryptosporidium parvum. *Science,* 304**,** 441-5.

ACHARYA, P., KUMAR, R. & TATU, U. (2007) Chaperoning a cellular upheaval in malaria: heat shock proteins in Plasmodium falciparum. *Mol Biochem Parasitol,* 153**,** 85-94.

ALANO, P. (2007) Plasmodium falciparum gametocytes: still many secrets of a hidden life. *Mol Microbiol,* 66**,** 291-302.

ANAMIKA, SRINIVASAN, N. & KRUPA, A. (2005) A genomic perspective of protein kinases in Plasmodium falciparum. *Proteins,* 58**,** 180-9.

ARAVIND, L., IYER, L. M., WELLEMS, T. E. & MILLER, L. H. (2003) Plasmodium biology: genomic gleanings. *Cell,* 115**,** 771-85.

ARMSTRONG, C. M. & GOLDBERG, D. E. (2007) An FKBP destabilization domain modulates protein levels in Plasmodium falciparum. *Nat Methods,* 4**,** 1007-9.

BAHL, A., BRUNK, B., CRABTREE, J., FRAUNHOLZ, M. J., GAJRIA, B., GRANT, G. R., GINSBURG, H., GUPTA, D., KISSINGER, J. C., LABO, P., LI, L., MAILMAN, M. D., MILGRAM, A. J., PEARSON, D. S., ROOS, D. S., SCHUG, J., STOECKERT, C. J., JR. & WHETZEL, P. (2003) PlasmoDB: the Plasmodium genome resource. A database integrating experimental and computational data. *Nucleic Acids Res,* 31**,** 212-5.

BAIRD, J. K. (2007) Neglect of Plasmodium vivax malaria. *Trends Parasitol,* 23**,** 533-9.

BALAJI, S., BABU, M. M., IYER, L. M. & ARAVIND, L. (2005) Discovery of the principal specific transcription factors of Apicomplexa and their implication for the evolution of the AP2-integrase DNA binding domains. *Nucleic Acids Res,* 33**,** 3994-4006.

BALDAUF, S. L. (2003) The deep roots of eukaryotes. *Science,* 300**,** 1703-6.

BANNISTER, L. H., HOPKINS, J. M., FOWLER, R. E., KRISHNA, S. & MITCHELL, G. H. (2000) A brief illustrated guide to the ultrastructure of Plasmodium falciparum asexual blood stages. *Parasitol Today,* 16**,** 427-33.

BARFORD, D., DAS, A. K. & EGLOFF, M. P. (1998) The structure and mechanism of protein phosphatases: insights into catalysis and regulation. *Annu Rev Biophys Biomol Struct,* 27**,** 133-64.

BARKAN, D., GINSBURG, H. & GOLENSER, J. (2000) Optimisation of flow cytometric measurement of parasitaemia in plasmodium-infected mice. *Int J Parasitol,* 30**,** 649-53.

BARR, M. M., TU, H., VAN AELST, L. & WIGLER, M. (1996) Identification of Ste4 as a potential regulator of Byr2 in the sexual response pathway of Schizosaccharomyces pombe. *Mol Cell Biol,* 16**,** 5597-603.

BAUER, B. N., RAFIE-KOLPIN, M., LU, L., HAN, A. & CHEN, J. J. (2001) Multiple autophosphorylation is essential for the formation of the active and stable homodimer of heme-regulated eIF2alpha kinase. *Biochemistry,* 40**,** 11543-51.

BERTOLOTTI, A., ZHANG, Y., HENDERSHOT, L. M., HARDING, H. P. & RON, D. (2000) Dynamic interaction of BiP and ER stress transducers in the unfolded-protein response. *Nat Cell Biol,* 2**,** 326-32.

BHATTACHARYYA, M. K., HONG, Z., KONGKASURIYACHAI, D. & KUMAR, N. (2002) Plasmodium falciparum protein phosphatase type 1 functionally complements a glc7 mutant in Saccharomyces cerevisiae. *Int J Parasitol,* 32**,** 739-47.

BISHOP, A. C., BUZKO, O. & SHOKAT, K. M. (2001) Magic bullets for protein kinases. *Trends Cell Biol,* 11**,** 167-72.

BLAIS, J. & BELL, J. C. (2006) Novel therapeutic target: the PERKs of inhibiting the integrated stress response. *Cell Cycle,* 5**,** 2874-7.

BOGOYEVITCH, M. A. & FAIRLIE, D. P. (2007) A new paradigm for protein kinase inhibition: blocking phosphorylation without directly targeting ATP binding. *Drug Discov Today,* 12**,** 622-33.

BOLLEN, M. (2001) Combinatorial control of protein phosphatase-1. *Trends Biochem Sci,* 26**,** 426-31.

BOUDEAU, J., MIRANDA-SAAVEDRA, D., BARTON, G. J. & ALESSI, D. R. (2006) Emerging roles of pseudokinases. *Trends Cell Biol,* 16**,** 443-52.

BOYCE, M., BRYANT, K. F., JOUSSE, C., LONG, K., HARDING, H. P., SCHEUNER, D., KAUFMAN, R. J., MA, D., COEN, D. M., RON, D. & YUAN, J. (2005) A selective inhibitor of eIF2alpha dephosphorylation protects cells from ER stress. *Science,* 307**,** 935-9.

BOZDECH, Z., LLINAS, M., PULLIAM, B. L., WONG, E. D., ZHU, J. & DERISI, J. L. (2003) The transcriptome of the intraerythrocytic developmental cycle of Plasmodium falciparum. *PLoS Biol,* 1**,** E5.

BROSTROM, C. O. & BROSTROM, M. A. (1998) Regulation of translational initiation during cellular responses to stress. *Prog Nucleic Acid Res Mol Biol,* 58**,** 79-125.

BROSTROM, M. A., LIN, X. J., CADE, C., GMITTER, D. & BROSTROM, C. O. (1989) Loss of a calcium requirement for protein synthesis in pituitary cells following thermal or chemical stress. *J Biol Chem,* 264**,** 1638-43.

BRUCE, M. C., ALANO, P., DUTHIE, S. & CARTER, R. (1990) Commitment of the malaria parasite Plasmodium falciparum to sexual and asexual development. *Parasitology,* 100 Pt 2**,** 191-200.

BUCKLING, A. G., TAYLOR, L. H., CARLTON, J. M. & READ, A. F. (1997) Adaptive changes in Plasmodium transmission strategies following chloroquine chemotherapy. *Proc Biol Sci,* 264**,** 553-9.

CARDIN, E., LATREILLE, M., KHOURY, C., GREENWOOD, M. T. & LAROSE, L. (2007) Nck-1 selectively modulates eIF2alphaSer51 phosphorylation by a subset of eIF2alpha-kinases. *Febs J,* 274**,** 5865-75.

CARLTON, J. M., ANGIUOLI, S. V., SUH, B. B., KOOIJ, T. W., PERTEA, M., SILVA, J. C., ERMOLAEVA, M. D., ALLEN, J. E., SELENGUT, J. D., KOO, H. L., PETERSON, J. D., POP, M., KOSACK, D. S., SHUMWAY, M. F., BIDWELL, S. L., SHALLOM, S. J., VAN AKEN, S. E., RIEDMULLER, S. B., FELDBLYUM, T. V., CHO, J. K., QUACKENBUSH, J., SEDEGAH, M., SHOAIBI, A., CUMMINGS, L. M., FLORENS, L., YATES, J. R., RAINE, J. D., SINDEN, R. E., HARRIS, M. A., CUNNINGHAM, D. A., PREISER, P. R., BERGMAN, L. W., VAIDYA, A. B., VAN LIN, L. H., JANSE, C. J., WATERS, A. P., SMITH, H. O., WHITE, O. R., SALZBERG, S. L., VENTER, J. C., FRASER, C. M., HOFFMAN, S. L., GARDNER, M. J. & CARUCCI, D. J. (2002) Genome sequence and comparative analysis of the model rodent malaria parasite Plasmodium yoelii yoelii. *Nature,* 419**,** 512-9.

CARTER, R. & MILLER, L. H. (1979) Evidence for environmental modulation of gametocytogenesis in Plasmodium falciparum in continuous culture. *Bull World Health Organ,* 57 Suppl 1**,** 37-52.

CARTER, R., RANFORD-CARTWRIGHT, L. & ALANO, P. (1993) The culture and preparation of gametocytes of Plasmodium falciparum for immunochemical, molecular, and mosquito infectivity studies. *Methods Mol Biol,* 21**,** 67-88.

CHEFALO, P. J., OH, J., RAFIE-KOLPIN, M., KAN, B. & CHEN, J. J. (1998) Heme-regulated eIF-2alpha kinase purifies as a hemoprotein. *Eur J Biochem,* 258**,** 820-30.

CHEN, J. J. & LONDON, I. M. (1995) Regulation of protein synthesis by heme-regulated eIF-2 alpha kinase. *Trends Biochem Sci,* 20**,** 105-8.

CHOI, S. Y., SCHERER, B. J., SCHNIER, J., DAVIES, M. V., KAUFMAN, R. J. & HERSHEY, J. W. (1992) Stimulation of protein synthesis in COS cells transfected with variants of the alpha-subunit of initiation factor eIF-2. *J Biol Chem,* 267**,** 286-93.

COHEN, P. (2002) Protein kinases--the major drug targets of the twenty-first century? *Nat Rev Drug Discov,* 1**,** 309-15.

COLEMAN, B. I. & DURAISINGH, M. T. (2008) Transcriptional control and gene silencing in Plasmodium falciparum. *Cell Microbiol*.

COLTHURST, D. R., CAMPBELL, D. G. & PROUD, C. G. (1987) Structure and regulation of eukaryotic initiation factor eIF-2. Sequence of the site in the alpha subunit phosphorylated by the haem-controlled repressor and by the double-stranded RNA-activated inhibitor. *Eur J Biochem,* 166**,** 357-63.

COULSON, R. M., HALL, N. & OUZOUNIS, C. A. (2004) Comparative genomics of transcriptional control in the human malaria parasite Plasmodium falciparum. *Genome Res,* 14**,** 1548-54.

COX-SINGH, J., DAVIS, T. M., LEE, K. S., SHAMSUL, S. S., MATUSOP, A., RATNAM, S., RAHMAN, H. A., CONWAY, D. J. & SINGH, B. (2008) Plasmodium knowlesi malaria in humans is widely distributed and potentially life threatening. *Clin Infect Dis,* 46**,** 165-71.

CRABB, B. S. & COWMAN, A. F. (1996) Characterization of promoters and stable transfection by homologous and nonhomologous recombination in Plasmodium falciparum. *Proc Natl Acad Sci U S A,* 93**,** 7289-94.

DAHER, W., BROWAEYS, E., PIERROT, C., JOUIN, H., DIVE, D., MEURICE, E., DISSOUS, C., CAPRON, M., TOMAVO, S., DOERIG, C., CAILLIAU, K. & KHALIFE, J. (2006) Regulation of protein phosphatase type 1 and cell cycle progression by PfLRR1, a novel leucine-rich repeat protein of the human malaria parasite Plasmodium falciparum. *Mol Microbiol,* 60**,** 578-90.

DAILY, J. P., SCANFELD, D., POCHET, N., LE ROCH, K., PLOUFFE, D., KAMAL, M., SARR, O., MBOUP, S., NDIR, O., WYPIJ, D., LEVASSEUR, K., THOMAS, E., TAMAYO, P., DONG, C., ZHOU, Y., LANDER, E. S., NDIAYE, D., WIRTH, D., WINZELER, E. A., MESIROV, J. P. & REGEV, A. (2007) Distinct physiological states of Plasmodium falciparum in malaria-infected patients. *Nature,* 450**,** 1091-5.

DAR, A. C., DEVER, T. E. & SICHERI, F. (2005) Higher-order substrate recognition of eIF2alpha by the RNA-dependent protein kinase PKR. *Cell,* 122**,** 887-900.

DAR, A. C. & SICHERI, F. (2002) X-ray crystal structure and functional analysis of vaccinia virus K3L reveals molecular determinants for PKR subversion and substrate recognition. *Mol Cell,* 10**,** 295-305.

DAVIS, R. J. (2000) Signal transduction by the JNK group of MAP kinases. *Cell,* 103**,** 239-52.

DE SILVA, E. K., GEHRKE, A. R., OLSZEWSKI, K., LEON, I., CHAHAL, J. S., BULYK, M. L. & LLINAS, M. (2008) Specific DNA-binding by apicomplexan AP2 transcription factors. *Proc Natl Acad Sci U S A,* 105**,** 8393-8.

DENG, W., PARBHU-PATEL, A., MEYER, D. J. & BAKER, D. A. (2003) The role of two novel regulatory sites in the activation of the cGMP-dependent protein kinase from Plasmodium falciparum. *Biochem J,* 374**,** 559-65.

DEVER, T. E. (2002) Gene-specific regulation by general translation factors. *Cell,* 108**,** 545-56.

DEY, M., CAO, C., DAR, A. C., TAMURA, T., OZATO, K., SICHERI, F. & DEVER, T. E. (2005) Mechanistic link between PKR dimerization, autophosphorylation, and eIF2alpha substrate recognition. *Cell,* 122**,** 901-13.

DOERIG, C. (2004a) Protein kinases as targets for anti-parasitic chemotherapy. *Biochim Biophys Acta,* 1697**,** 155-68.

DOERIG, C., BILLKER, O., PRATT, D. & ENDICOTT, J. (2005) Protein kinases as targets for antimalarial intervention: Kinomics, structure-based design, transmission-blockade, and targeting host cell enzymes. *Biochim Biophys Acta,* 1754**,** 132-50.

DOERIG, C. & MEIJER, L. (2007) Antimalarial drug discovery: targeting protein kinases. *Expert Opin Ther Targets,* 11**,** 279-90.

DOERIG, C. C., D (2004b) *Cell Cycle control in Plasmodium falciparum: a genomics perspective*.

DONG, J., QIU, H., GARCIA-BARRIO, M., ANDERSON, J. & HINNEBUSCH, A. G. (2000) Uncharged tRNA activates GCN2 by displacing the protein kinase moiety from a bipartite tRNA-binding domain. *Mol Cell,* 6**,** 269-79.

DORIN-SEMBLAT, D., QUASHIE, N., HALBERT, J., SICARD, A., DOERIG, C., PEAT, E., RANFORD-CARTWRIGHT, L. & DOERIG, C. (2007) Functional characterization of both MAP kinases of the human malaria parasite Plasmodium falciparum by reverse genetics. *Mol Microbiol,* 65**,** 1170-80.

DORIN-SEMBLAT, D., SICARD, A., DOERIG, C., RANFORD-CARTWRIGHT, L. & DOERIG, C. (2008) Disruption of the PfPK7 gene impairs schizogony and sporogony in the human malaria parasite Plasmodium falciparum. *Eukaryot Cell,* 7**,** 279-85.

DORIN, D., ALANO, P., BOCCACCIO, I., CICERON, L., DOERIG, C., SULPICE, R. & PARZY, D. (1999) An atypical mitogen-activated protein kinase (MAPK) homologue expressed in gametocytes of the human malaria parasite Plasmodium falciparum. Identification of a MAPK signature. *J Biol Chem,* 274**,** 29912-20.

DORIN, D., SEMBLAT, J. P., POULLET, P., ALANO, P., GOLDRING, J. P., WHITTLE, C., PATTERSON, S., CHAKRABARTI, D. & DOERIG, C. (2005) PfPK7, an atypical MEK-related protein kinase, reflects the absence of classical three-component MAPK pathways in the human malaria parasite Plasmodium falciparum. *Mol Microbiol,* 55**,** 184-96.

DURAISINGH, M. T., VON SEIDLEIN, L. V., JEPSON, A., JONES, P., SAMBOU, I., PINDER, M. & WARHURST, D. C. (2000) Linkage disequilibrium between two chromosomally distinct loci associated with increased resistance to chloroquine in Plasmodium falciparum. *Parasitology,* 121 (Pt 1)**,** 1-7.

DYER, M. & DAY, K. (2000) Expression of Plasmodium falciparum trimeric G proteins and their involvement in switching to sexual development. *Mol Biochem Parasitol,* 110**,** 437-48.

ENGELBERG, D. (2004) Stress-activated protein kinases-tumor suppressors or tumor initiators? *Semin Cancer Biol,* 14**,** 271-82.

FAGARD, R. & LONDON, I. M. (1981) Relationship between phosphorylation and activity of heme-regulated eukaryotic initiation factor 2 alpha kinase. *Proc Natl Acad Sci U S A,* 78**,** 866-70.

FERNANDEZ, J., YAMAN, I., SARNOW, P., SNIDER, M. D. & HATZOGLOU, M. (2002) Regulation of internal ribosomal entry site-mediated translation by phosphorylation of the translation initiation factor eIF2alpha. *J Biol Chem,* 277**,** 19198-205.

FERRERAS, A., TRIANA, L., CORREIA, H., SANCHEZ, E. & HERRERA, F. (2000) An in vitro system from Plasmodium falciparum active in endogenous mRNA translation. *Mem Inst Oswaldo Cruz,* 95**,** 231-5.

FERRERAS, A., TRIANA, L., SANCHEZ, E. & HERRERA, F. (2002) Effect of antimalarial drugs on plasmodia cell-free protein synthesis. *Mem Inst Oswaldo Cruz,* 97**,** 377-80.

FINN, R. D., MISTRY, J., SCHUSTER-BOCKLER, B., GRIFFITHS-JONES, S., HOLLICH, V., LASSMANN, T., MOXON, S., MARSHALL, M., KHANNA, A., DURBIN, R., EDDY, S. R., SONNHAMMER, E. L. & BATEMAN, A. (2006) Pfam: clans, web tools and services. *Nucleic Acids Res,* 34**,** D247-51.

FISCHER, P. M. (2004) The design of drug candidate molecules as selective inhibitors of therapeutically relevant protein kinases. *Curr Med Chem,* 11**,** 1563-83.

GAJRIA, B., BAHL, A., BRESTELLI, J., DOMMER, J., FISCHER, S., GAO, X., HEIGES, M., IODICE, J., KISSINGER, J. C., MACKEY, A. J., PINNEY, D. F., ROOS, D. S., STOECKERT, C. J., JR., WANG, H. & BRUNK, B. P. (2008) ToxoDB: an integrated Toxoplasma gondii database resource. *Nucleic Acids Res,* 36**,** D553-6.

GALLEGO, M. & VIRSHUP, D. M. (2005) Protein serine/threonine phosphatases: life, death, and sleeping. *Curr Opin Cell Biol,* 17**,** 197-202.

GARDNER, M. J., HALL, N., FUNG, E., WHITE, O., BERRIMAN, M., HYMAN, R. W., CARLTON, J. M., PAIN, A., NELSON, K. E., BOWMAN, S., PAULSEN, I. T., JAMES, K., EISEN, J. A., RUTHERFORD, K., SALZBERG, S. L., CRAIG, A., KYES, S., CHAN, M. S., NENE, V., SHALLOM, S. J., SUH, B., PETERSON, J., ANGIUOLI, S., PERTEA, M., ALLEN, J., SELENGUT, J., HAFT, D., MATHER, M. W., VAIDYA, A. B., MARTIN, D. M., FAIRLAMB, A. H., FRAUNHOLZ, M. J., ROOS, D. S., RALPH, S. A., MCFADDEN, G. I., CUMMINGS, L. M., SUBRAMANIAN, G. M., MUNGALL, C., VENTER, J. C., CARUCCI, D. J., HOFFMAN, S. L., NEWBOLD, C., DAVIS, R. W., FRASER, C. M. & BARRELL, B. (2002) Genome sequence of the human malaria parasite Plasmodium falciparum. *Nature,* 419**,** 498-511.

GELB, M. H. (2007) Drug discovery for malaria: a very challenging and timely endeavor. *Curr Opin Chem Biol,* 11**,** 440-5.

GIAMAS, G., STEBBING, J., VORGIAS, C. E. & KNIPPSCHILD, U. (2007) Protein kinases as targets for cancer treatment. *Pharmacogenomics,* 8**,** 1005-16.

GRAVES, P. M., CARTER, R. & MCNEILL, K. M. (1984) Gametocyte production in cloned lines of Plasmodium falciparum. *Am J Trop Med Hyg,* 33**,** 1045-50.

GREENWOOD, B. & MUTABINGWA, T. (2002) Malaria in 2002. *Nature,* 415**,** 670-2.

GUERRA, C. A., SNOW, R. W. & HAY, S. I. (2006) Mapping the global extent of malaria in 2005. *Trends Parasitol,* 22**,** 353-8.

HALL, N., KARRAS, M., RAINE, J. D., CARLTON, J. M., KOOIJ, T. W., BERRIMAN, M., FLORENS, L., JANSSEN, C. S., PAIN, A., CHRISTOPHIDES, G. K., JAMES, K., RUTHERFORD, K., HARRIS, B., HARRIS, D., CHURCHER, C., QUAIL, M. A., ORMOND, D., DOGGETT, J., TRUEMAN, H. E., MENDOZA, J., BIDWELL, S. L., RAJANDREAM, M. A., CARUCCI, D. J., YATES, J. R., 3RD, KAFATOS, F. C., JANSE, C. J., BARRELL, B., TURNER, C. M., WATERS, A. P. &

SINDEN, R. E. (2005) A comprehensive survey of the Plasmodium life cycle by genomic, transcriptomic, and proteomic analyses. *Science,* 307**,** 82-6.

HAN, A. P., YU, C., LU, L., FUJIWARA, Y., BROWNE, C., CHIN, G., FLEMING, M., LEBOULCH, P., ORKIN, S. H. & CHEN, J. J. (2001) Heme-regulated eIF2alpha kinase (HRI) is required for translational regulation and survival of erythroid precursors in iron deficiency. *Embo J,* 20**,** 6909-18.

HANKS, S. K. (2003) Genomic analysis of the eukaryotic protein kinase superfamily: a perspective. *Genome Biol,* 4**,** 111.

HANKS, S. K. & HUNTER, T. (1995) Protein kinases 6. The eukaryotic protein kinase superfamily: kinase (catalytic) domain structure and classification. *Faseb J,* 9**,** 576-96.

HARDING, H. P., CALFON, M., URANO, F., NOVOA, I. & RON, D. (2002) Transcriptional and translational control in the Mammalian unfolded protein response. *Annu Rev Cell Dev Biol,* 18**,** 575-99.

HARDING, H. P., ZHANG, Y. & RON, D. (1999) Protein translation and folding are coupled by an endoplasmic-reticulum-resident kinase. *Nature,* 397**,** 271-4.

HE, B., GROSS, M. & ROIZMAN, B. (1997) The gamma(1)34.5 protein of herpes simplex virus 1 complexes with protein phosphatase 1alpha to dephosphorylate the alpha subunit of the eukaryotic translation initiation factor 2 and preclude the shutoff of protein synthesis by double-stranded RNA-activated protein kinase. *Proc Natl Acad Sci U S A,* 94**,** 843-8.

HE, B., GROSS, M. & ROIZMAN, B. (1998) The gamma134.5 protein of herpes simplex virus 1 has the structural and functional attributes of a protein phosphatase 1 regulatory subunit and is present in a high molecular weight complex with the enzyme in infected cells. *J Biol Chem,* 273**,** 20737-43.

HO, S. N., HUNT, H. D., HORTON, R. M., PULLEN, J. K. & PEASE, L. R. (1989) Site-directed mutagenesis by overlap extension using the polymerase chain reaction. *Gene,* 77**,** 51-9.

HOLCIK, M. & SONENBERG, N. (2005) Translational control in stress and apoptosis. *Nat Rev Mol Cell Biol,* 6**,** 318-27.

HTTP://WWW.ROLLBACKMALARIA.ORG/ Roll Back Malaria Factsheet 10: Economic costs of Malaria.

HUSON, D. H. & BRYANT, D. (2006) Application of phylogenetic networks in evolutionary studies. *Mol Biol Evol,* 23**,** 254-67.

JOHNSON, L. N., LOWE, E. D., NOBLE, M. E. & OWEN, D. J. (1998) The Eleventh Datta Lecture. The structural basis for substrate recognition and control by protein kinases. *FEBS Lett,* 430**,** 1-11.

JOSHI, H., PRAJAPATI, S. K., VERMA, A., KANG'A, S. & CARLTON, J. M. (2008) Plasmodium vivax in India. *Trends Parasitol,* 24**,** 228-35.

KATO, K., SUDO, A., KOBAYASHI, K., TOHYA, Y. & AKASHI, H. (2008) Characterization of Plasmodium falciparum protein kinase 2. *Mol Biochem Parasitol,* 162**,** 87-95.

KAWAGISHI-KOBAYASHI, M., SILVERMAN, J. B., UNG, T. L. & DEVER, T. E. (1997) Regulation of the protein kinase PKR by the vaccinia virus pseudosubstrate inhibitor K3L is dependent on residues conserved between the K3L protein and the PKR substrate eIF2alpha. *Mol Cell Biol,* 17**,** 4146-58.

KIM, K. & WEISS, L. M. (2004) Toxoplasma gondii: the model apicomplexan. *Int J Parasitol,* 34**,** 423-32.

KIM, Y. A., CHA, J. E., AHN, S. Y., RYU, S. H., YEOM, J. S., LEE, H. I., KIM, C. G., SEOH, J. Y. & PARK, J. W. (2007) Plasmodium falciparum cultivation using the Petri Dish: revisiting the effect of the 'age' of erythrocytes and the interval of medium change. *J Korean Med Sci,* 22**,** 1022-5.

KIRKMAN, L. A., SU, X. Z. & WELLEMS, T. E. (1996) Plasmodium falciparum: isolation of large numbers of parasite clones from infected blood samples. *Exp Parasitol,* 83**,** 147-9.

KUMAR, S., TAMURA, K. & NEI, M. (2004) MEGA3: Integrated software for Molecular Evolutionary Genetics Analysis and sequence alignment. *Brief Bioinform,* 5**,** 150-63.

LAMBROS, C. & VANDERBERG, J. P. (1979) Synchronization of Plasmodium falciparum erythrocytic stages in culture. *J Parasitol,* 65**,** 418-20.

LE ROCH, K. G., ZHOU, Y., BLAIR, P. L., GRAINGER, M., MOCH, J. K., HAYNES, J. D., DE LA VEGA, P., HOLDER, A. A., BATALOV, S., CARUCCI, D. J. & WINZELER, E. A. (2003) Discovery of gene function by expression profiling of the malaria parasite life cycle. *Science,* 301**,** 1503-8.

LEROY, D. & DOERIG, C. (2008) Drugging the Plasmodium kinome: the benefits of academia-industry synergy. *Trends Pharmacol Sci,* 29**,** 241-9.

LIN, D. T., GOLDMAN, N. D. & SYIN, C. (1996) Stage-specific expression of a Plasmodium falciparum protein related to the eukaryotic mitogen-activated protein kinases. *Mol Biochem Parasitol,* 78**,** 67-77.

LIU, C. Y., SCHRODER, M. & KAUFMAN, R. J. (2000) Ligand-independent dimerization activates the stress response kinases IRE1 and PERK in the lumen of the endoplasmic reticulum. *J Biol Chem,* 275**,** 24881-5.

LIU, J., GLUZMAN, I. Y., DREW, M. E. & GOLDBERG, D. E. (2005) The role of Plasmodium falciparum food vacuole plasmepsins. *J Biol Chem,* 280**,** 1432-7.

LU, L., HAN, A. P. & CHEN, J. J. (2001) Translation initiation control by heme-regulated eukaryotic initiation factor 2alpha kinase in erythroid cells under cytoplasmic stresses. *Mol Cell Biol,* 21**,** 7971-80.

LUCHAVEZ, J., ESPINO, F., CURAMENG, P., ESPINA, R., BELL, D., CHIODINI, P., NOLDER, D., SUTHERLAND, C., LEE, K. S. & SINGH, B. (2008) Human Infections with Plasmodium knowlesi, the Philippines. *Emerg Infect Dis,* 14**,** 811-3.

MACKINNON, M. J. & READ, A. F. (2004) Virulence in malaria: an evolutionary viewpoint. *Philos Trans R Soc Lond B Biol Sci,* 359**,** 965-86.

MAIR, G. R., BRAKS, J. A., GARVER, L. S., WIEGANT, J. C., HALL, N., DIRKS, R. W., KHAN, S. M., DIMOPOULOS, G., JANSE, C. J. & WATERS, A. P. (2006) Regulation of sexual development of Plasmodium by translational repression. *Science,* 313**,** 667-9.

MAKLER, M. T. & HINRICHS, D. J. (1993) Measurement of the lactate dehydrogenase activity of Plasmodium falciparum as an assessment of parasitemia. *Am J Trop Med Hyg,* 48**,** 205-10.

MAKLER, M. T., RIES, J. M., WILLIAMS, J. A., BANCROFT, J. E., PIPER, R. C., GIBBINS, B. L. & HINRICHS, D. J. (1993) Parasite lactate dehydrogenase as an assay for Plasmodium falciparum drug sensitivity. *Am J Trop Med Hyg,* 48**,** 739-41.

MALY, D. J., ALLEN, J. A. & SHOKAT, K. M. (2004) A mechanism-based cross-linker for the identification of kinase-substrate pairs. *J Am Chem Soc,* 126**,** 9160-1.

MANNING, G., WHYTE, D. B., MARTINEZ, R., HUNTER, T. & SUDARSANAM, S. (2002) The protein kinase complement of the human genome. *Science,* 298**,** 1912-34.

MATHEWS, M. B., SONENBERG N. & HERSHEY, J.W.B. (2007) *Translational Control in Biology and Medicine,* Cold Spring Harbor Laboratory Press.

MATUSCHEWSKI, K. & MUELLER, A. K. (2007) Vaccines against malaria - an update. *Febs J,* 274**,** 4680-7.

MEISSNER, M., KREJANY, E., GILSON, P. R., DE KONING-WARD, T. F., SOLDATI, D. & CRABB, B. S. (2005) Tetracycline analogue-regulated transgene expression in Plasmodium falciparum blood stages using Toxoplasma gondii transactivators. *Proc Natl Acad Sci U S A,* 102**,** 2980-5.

MEISSNER, M., SCHLUTER, D. & SOLDATI, D. (2002) Role of Toxoplasma gondii myosin A in powering parasite gliding and host cell invasion. *Science,* 298**,** 837-40.

MELLOR, H. & PROUD, C. G. (1991) A synthetic peptide substrate for initiation factor-2 kinases. *Biochem Biophys Res Commun,* 178**,** 430-7.

MERCKX, A., ECHALIER, A., LANGFORD, K., SICARD, A., LANGSLEY, G., JOORE, J., DOERIG, C., NOBLE, M. & ENDICOTT, J. (2008) Structures of P. falciparum protein kinase 7 identify an activation motif and leads for inhibitor design. *Structure,* 16**,** 228-38.

MEURS, E., CHONG, K., GALABRU, J., THOMAS, N. S., KERR, I. M., WILLIAMS, B. R. & HOVANESSIAN, A. G. (1990) Molecular cloning and characterization of the human double-stranded RNA-activated protein kinase induced by interferon. *Cell,* 62**,** 379-90.

MIRANDA-SAAVEDRA, D., STARK, M. J., PACKER, J. C., VIVARES, C. P., DOERIG, C. & BARTON, G. J. (2007) The complement of protein kinases of the microsporidium Encephalitozoon cuniculi in relation to those of Saccharomyces cerevisiae and Schizosaccharomyces pombe. *BMC Genomics,* 8**,** 309.

MOHR, I. J., PE'ERY, T., MATHEWS,M.B. (2007) *Protein Synthesis and Translational control during Viral Infection (in Translational Control in Biology and Medicine),* Cold Spring Harbor Laboratory Press.

MOHRLE, J. J., ZHAO, Y., WERNLI, B., FRANKLIN, R. M. & KAPPES, B. (1997) Molecular cloning, characterization and localization of PfPK4, an eIF-2alpha kinase-related enzyme from the malarial parasite Plasmodium falciparum. *Biochem J,* 328 (Pt 2)**,** 677-87.

MORAES, M. C., JESUS, T. C., HASHIMOTO, N. N., DEY, M., SCHWARTZ, K. J., ALVES, V. S., AVILA, C. C., BANGS, J. D., DEVER, T. E., SCHENKMAN, S. & CASTILHO, B. A. (2007) Novel membrane-bound eIF2alpha kinase in the flagellar pocket of Trypanosoma brucei. *Eukaryot Cell,* 6**,** 1979-91.

MUDEPPA, D. G., PANG, C. K., TSUBOI, T., ENDO, Y., BUCKNER, F. S., VARANI, G. & RATHOD, P. K. (2007) Cell-free production of functional Plasmodium falciparum dihydrofolate reductase-thymidylate synthase. *Mol Biochem Parasitol,* 151**,** 216-9.

MULLER, S. (2004) Redox and antioxidant systems of the malaria parasite Plasmodium falciparum. *Mol Microbiol,* 53**,** 1291-305.

MULVEY, M., POPPERS, J., STERNBERG, D. & MOHR, I. (2003) Regulation of eIF2alpha phosphorylation by different functions that act during discrete phases in the herpes simplex virus type 1 life cycle. *J Virol,* 77**,** 10917-28.

MURTHA-RIEL, P., DAVIES, M. V., SCHERER, B. J., CHOI, S. Y., HERSHEY, J. W. & KAUFMAN, R. J. (1993) Expression of a phosphorylation-resistant eukaryotic initiation factor 2 alpha-subunit mitigates heat shock inhibition of protein synthesis. *J Biol Chem,* 268**,** 12946-51.

NANDURI, S., RAHMAN, F., WILLIAMS, B. R. & QIN, J. (2000) A dynamically tuned double-stranded RNA binding mechanism for the activation of antiviral kinase PKR. *Embo J,* 19**,** 5567-74.

NARASIMHAN, J., JOYCE, B. R., NAGULESWARAN, A., SMITH, A. T., LIVINGSTON, M. R., DIXON, S. E., COPPENS, I., WEK, R. C. & SULLIVAN, W. J., JR. (2008) Translation regulation by eukaryotic initiation factor-2 kinases in the development of latent cysts in Toxoplasma gondii. *J Biol Chem,* 283**,** 16591-601.

NEBREDA, A. R. & PORRAS, A. (2000) p38 MAP kinases: beyond the stress response. *Trends Biochem Sci,* 25**,** 257-60.

NIEDNER, R. H., BUZKO, O. V., HASTE, N. M., TAYLOR, A., GRIBSKOV, M. & TAYLOR, S. S. (2006) Protein kinase resource: an integrated environment for phosphorylation research. *Proteins,* 63**,** 78-86.

NOVOA, I., ZENG, H., HARDING, H. P. & RON, D. (2001) Feedback inhibition of the unfolded protein response by GADD34-mediated dephosphorylation of eIF2alpha. *J Cell Biol,* 153**,** 1011-22.

NOVOA, I., ZHANG, Y., ZENG, H., JUNGREIS, R., HARDING, H. P. & RON, D. (2003) Stress-induced gene expression requires programmed recovery from translational repression. *Embo J,* 22**,** 1180-7.

O'LOGHLEN, A., PEREZ-MORGADO, M. I., SALINAS, M. & MARTIN, M. E. (2003) Reversible inhibition of the protein phosphatase 1 by hydrogen peroxide. Potential regulation of eIF2 alpha phosphorylation in differentiated PC12 cells. *Arch Biochem Biophys,* 417**,** 194-202.

PADYANA, A. K., QIU, H., ROLL-MECAK, A., HINNEBUSCH, A. G. & BURLEY, S. K. (2005) Structural basis for autoinhibition and mutational activation of eukaryotic initiation factor 2alpha protein kinase GCN2. *J Biol Chem,* 280**,** 29289-99.

PATEL, J., MCLEOD, L. E., VRIES, R. G., FLYNN, A., WANG, X. & PROUD, C. G. (2002) Cellular stresses profoundly inhibit protein synthesis and modulate the states of phosphorylation of multiple translation factors. *Eur J Biochem,* 269**,** 3076-85.

PATON, M. G., BARKER, G. C., MATSUOKA, H., RAMESAR, J., JANSE, C. J., WATERS, A. P. & SINDEN, R. E. (1993) Structure and expression of a post-transcriptionally regulated malaria gene encoding a surface protein from the sexual stages of Plasmodium berghei. *Mol Biochem Parasitol,* 59**,** 263-75.

PROUD, C. G. (2005) eIF2 and the control of cell physiology. *Semin Cell Dev Biol,* 16**,** 3-12.

QIU, H., DONG, J., HU, C., FRANCKLYN, C. S. & HINNEBUSCH, A. G. (2001) The tRNA-binding moiety in GCN2 contains a dimerization domain that interacts with the kinase domain and is required for tRNA binding and kinase activation. *Embo J,* 20**,** 1425-38.

RAFIE-KOLPIN, M., CHEFALO, P. J., HUSSAIN, Z., HAHN, J., UMA, S., MATTS, R. L. & CHEN, J. J. (2000) Two heme-binding domains of heme-regulated eukaryotic initiation factor-2alpha kinase. N terminus and kinase insertion. *J Biol Chem,* 275**,** 5171-8.

RAFIE-KOLPIN, M., HAN, A. P. & CHEN, J. J. (2003) Autophosphorylation of threonine 485 in the activation loop is essential for attaining eIF2alpha kinase activity of HRI. *Biochemistry,* 42**,** 6536-44.

RANGANATHAN, A. C., OJHA, S., KOURTIDIS, A., CONKLIN, D. S. & AGUIRRE-GHISO, J. A. (2008) Dual function of pancreatic endoplasmic reticulum kinase in tumor cell growth arrest and survival. *Cancer Res,* 68**,** 3260-8.

RBM Roll Back Malaria Programme: Economic costs of malaria.

REDPATH, N. T. & PROUD, C. G. (1990) Activity of protein phosphatases against initiation factor-2 and elongation factor-2. *Biochem J,* 272**,** 175-80.

REININGER, L., BILLKER, O., TEWARI, R., MUKHOPADHYAY, A., FENNELL, C., DORIN-SEMBLAT, D., DOERIG, C., GOLDRING, D., HARMSE, L., RANFORD-CARTWRIGHT, L., PACKER, J. & DOERIG, C. (2005) A NIMA-related protein kinase is essential for completion of the sexual cycle of malaria parasites. *J Biol Chem,* 280**,** 31957-64.

RIDLEY, R. G. (2002a) Introduction. Antimalarial drug resistance: ramifications, explanations and challenges. *Microbes Infect,* 4**,** 155-6.

RIDLEY, R. G. (2002b) Medical need, scientific opportunity and the drive for antimalarial drugs. *Nature,* 415**,** 686-93.

ROBINSON, M. J. & COBB, M. H. (1997) Mitogen-activated protein kinase pathways. *Curr Opin Cell Biol,* 9**,** 180-6.

RUTKOWSKI, D. T. & KAUFMAN, R. J. (2004) A trip to the ER: coping with stress. *Trends Cell Biol,* 14**,** 20-8.

SACHS, J. & MALANEY, P. (2002) The economic and social burden of malaria. *Nature,* 415**,** 680-5.

SAMBROOK, R. *Molecular Cloning, a laboratory manual,* Cold Spring Harbor Laboratory Press.

SAWASAKI, T., GOUDA, M. D., KAWASAKI, T., TSUBOI, T., TOZAWA, Y., TAKAI, K. & ENDO, Y. (2005) The wheat germ cell-free expression system: methods for high-throughput materialization of genetic information. *Methods Mol Biol,* 310**,** 131-44.

SCHNEWEIS, S., MAIER, W. A. & SEITZ, H. M. (1991) Haemolysis of infected erythrocytes--a trigger for formation of Plasmodium falciparum gametocytes? *Parasitol Res,* 77**,** 458-60.

SHOCK, J. L., FISCHER, K. F. & DERISI, J. L. (2007) Whole-genome analysis of mRNA decay in Plasmodium falciparum reveals a global lengthening of mRNA half-life during the intra-erythrocytic development cycle. *Genome Biol,* 8**,** R134.

SIDHU, A. B., VALDERRAMOS, S. G. & FIDOCK, D. A. (2005) pfmdr1 mutations contribute to quinine resistance and enhance mefloquine and artemisinin sensitivity in Plasmodium falciparum. *Mol Microbiol,* 57**,** 913-26.

SILVESTRINI, F., BOZDECH, Z., LANFRANCOTTI, A., DI GIULIO, E., BULTRINI, E., PICCI, L., DERISI, J. L., PIZZI, E. & ALANO, P. (2005) Genome-wide identification of genes upregulated at the onset of gametocytogenesis in Plasmodium falciparum. *Mol Biochem Parasitol,* 143**,** 100-10.

SMALLEY, M. E. & BROWN, J. (1981) Plasmodium falciparum gametocytogenesis stimulated by lymphocytes and serum from infected Gambian children. *Trans R Soc Trop Med Hyg,* 75**,** 316-7.

SMITH, T. G., LOURENCO, P., CARTER, R., WALLIKER, D. & RANFORD-CARTWRIGHT, L. C. (2000) Commitment to sexual differentiation in the human malaria parasite, Plasmodium falciparum. *Parasitology,* 121 (Pt 2)**,** 127-33.

SNOW, R. W., GUERRA, C. A., NOOR, A. M., MYINT, H. Y. & HAY, S. I. (2005) The global distribution of clinical episodes of Plasmodium falciparum malaria. *Nature,* 434**,** 214-7.

SONENBERG N, H. J., MATHEWS MB (2000) *Translational Control of Gene Expression,* Cold Spring Harbor Laboratory Press.

STUDIER, F. W. (2005) Protein production by auto-induction in high density shaking cultures. *Protein Expr Purif,* 41**,** 207-34.

SUDHAKAR, A., RAMACHANDRAN, A., GHOSH, S., HASNAIN, S. E., KAUFMAN, R. J. & RAMAIAH, K. V. (2000) Phosphorylation of serine 51 in initiation factor 2 alpha (eIF2 alpha) promotes complex formation between eIF2 alpha(P) and eIF2B and causes inhibition in the guanine nucleotide exchange activity of eIF2B. *Biochemistry,* 39**,** 12929-38.

SUDO, A., KATO, K., KOBAYASHI, K., TOHYA, Y. & AKASHI, H. (2008) Susceptibility of Plasmodium falciparum cyclic AMP-dependent protein kinase and its mammalian homologue to the inhibitors. *Mol Biochem Parasitol,* 160**,** 138-42.

SULLIVAN, W. J., JR., NARASIMHAN, J., BHATTI, M. M. & WEK, R. C. (2004) Parasite-specific eIF2 (eukaryotic initiation factor-2) kinase required for stress-induced translation control. *Biochem J,* 380**,** 523-31.

SUROLIA, N. & PADMANABAN, G. (1991) Chloroquine inhibits heme-dependent protein synthesis in Plasmodium falciparum. *Proc Natl Acad Sci U S A,* 88**,** 4786-90.

TAYLOR, S. S., KNIGHTON, D. R., ZHENG, J., TEN EYCK, L. F. & SOWADSKI, J. M. (1992) Structural framework for the protein kinase family. *Annu Rev Cell Biol,* 8**,** 429-62.

TAYLOR, S. S., RADZIO-ANDZELM, E. & HUNTER, T. (1995) How do protein kinases discriminate between serine/threonine and tyrosine? Structural insights from the insulin receptor protein-tyrosine kinase. *Faseb J,* 9**,** 1255-66.

THOMPSON, J. D., HIGGINS, D. G. & GIBSON, T. J. (1994) CLUSTAL W: improving the sensitivity of progressive multiple sequence alignment through sequence weighting, position-specific gap penalties and weight matrix choice. *Nucleic Acids Res,* 22**,** 4673-80.

TRAGER, W. & JENSEN, J. B. (1976) Human malaria parasites in continuous culture. *Science,* 193**,** 673-5.

UMA, S., HARTSON, S. D., CHEN, J. J. & MATTS, R. L. (1997) Hsp90 is obligatory for the heme-regulated eIF-2alpha kinase to acquire and maintain an activable conformation. *J Biol Chem,* 272**,** 11648-56.

UMA, S., THULASIRAMAN, V. & MATTS, R. L. (1999) Dual role for Hsc70 in the biogenesis and regulation of the heme-regulated kinase of the alpha subunit of eukaryotic translation initiation factor 2. *Mol Cell Biol,* 19**,** 5861-71.

UMLAS, J. & FALLON, J. N. (1971) New thick-film technique for malaria diagnosis. Use of saponin stromatolytic solution for lysis. *Am J Trop Med Hyg,* 20**,** 527-9.

UNG, T. L., CAO, C., LU, J., OZATO, K. & DEVER, T. E. (2001) Heterologous dimerization domains functionally substitute for the double-stranded RNA binding domains of the kinase PKR. *Embo J,* 20**,** 3728-37.

VATTEM, K. M., STASCHKE, K. A. & WEK, R. C. (2001) Mechanism of activation of the double-stranded-RNA-dependent protein kinase, PKR: role of dimerization and cellular localization in the stimulation of PKR phosphorylation of eukaryotic initiation factor-2 (eIF2). *Eur J Biochem,* 268**,** 3674-84.

WALTHER, B. & WALTHER, M. (2007) What does it take to control malaria? *Ann Trop Med Parasitol,* 101**,** 657-72.

WARD, P., EQUINET, L., PACKER, J. & DOERIG, C. (2004) Protein kinases of the human malaria parasite Plasmodium falciparum: the kinome of a divergent eukaryote. *BMC Genomics,* 5**,** 79.

WATERS, A. P. (2008) Genome-informed contributions to malaria therapies: feeding somewhere down the (pipe)line. *Cell Host Microbe,* 3**,** 280-3.

WEINMANN, H. & METTERNICH, R. (2005) Drug discovery process for kinase inhibitors. *Chembiochem,* 6**,** 455-9.

WEISS, L. M. & KIM, K. (2000) The development and biology of bradyzoites of Toxoplasma gondii. *Front Biosci,* 5**,** D391-405.

WEK, R. C., JACKSON, B. M. & HINNEBUSCH, A. G. (1989) Juxtaposition of domains homologous to protein kinases and histidyl-tRNA synthetases in GCN2 protein suggests a mechanism for coupling GCN4 expression to amino acid availability. *Proc Natl Acad Sci U S A,* 86**,** 4579-83.

WEK, R. C., JIANG, H. Y. & ANTHONY, T. G. (2006) Coping with stress: eIF2 kinases and translational control. *Biochem Soc Trans,* 34**,** 7-11.

WEK, S. A., ZHU, S. & WEK, R. C. (1995) The histidyl-tRNA synthetase-related sequence in the eIF-2 alpha protein kinase GCN2 interacts with tRNA and

is required for activation in response to starvation for different amino acids. *Mol Cell Biol,* 15**,** 4497-506.

WHO (2007) Malaria factsheet.

WILKES, J., DOERIG, C. (2008) The protein-phosphatome of the human malaria parasite Plasmodium falciparum. *BMC Genomics,* In press.

WIRTH, D. F. (2002) Biological revelations. *Nature,* 419**,** 495-6.

YOUNG, J. A., JOHNSON, J. R., BENNER, C., YAN, S. F., CHEN, K., LE ROCH, K. G., ZHOU, Y. & WINZELER, E. A. (2008) In silico discovery of transcription regulatory elements in Plasmodium falciparum. *BMC Genomics,* 9**,** 70.

ZHANG, F., ROMANO, P. R., NAGAMURA-INOUE, T., TIAN, B., DEVER, T. E., MATHEWS, M. B., OZATO, K. & HINNEBUSCH, A. G. (2001) Binding of double-stranded RNA to protein kinase PKR is required for dimerization and promotes critical autophosphorylation events in the activation loop. *J Biol Chem,* 276**,** 24946-58.